Closing the nuclear fuel cycle

Potential of the Gas Cooled Fast Reactor (GCFR)

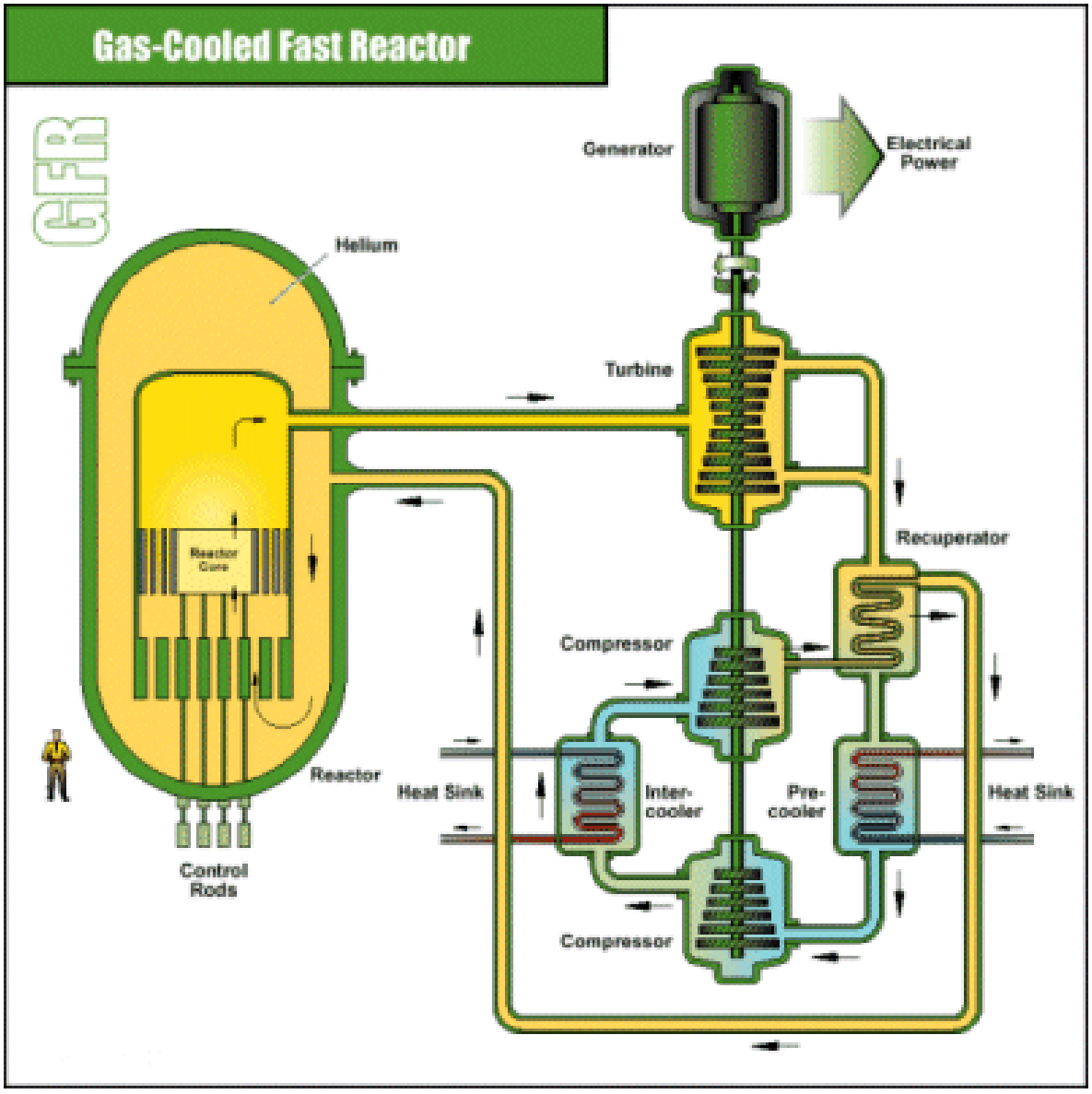

Godart van Gendt
Physics of Nuclear Reactors (PNR)
Department of R3 – Faculty TNW
TU Delft

Supervisors: Dr. ir. W.F.G. van Rooijen
Dr. ir. J.L. Kloosterman
Prof. dr. ir. T.H.J.J. van der Hagen

ABSTRACT

The fuel composition of the Generation IV 600 MWth 'efficient' Gas Cooled Fast Reactor (GCFR) that realizes zero breeding gain without using fertile blankets is determined. The analysis includes all the stages of the nuclear fuel cycle, including irradiation, reprocessing and fuel fabrication. The time-dependent multiplication factor, reactor safety parameters, and decay heat production for different fuel compositions are simulated using the deterministic SCALE 4.4 code. The depletion equation and the 1-D transport equation are solved for multiple timesteps during reactor irradiation.

It is seen that adding a small percentage of minor actinides (MA) to a mixture of uranium- and plutonium carbide favors the creation of a closed fuel cycle with zero breeding gain. Furthermore, addition of MA increases the burnup potential of the fuel, extending its feasible irradiation time from 40 to 90 MWd / kg, due to the transmutation of ^{237}Np to fissionable ^{238}Pu and ^{241}Am to fissionable ^{242}Am. Mixing MA negatively affects safety parameters by decreasing the delayed neutron fraction, decreasing the negative Doppler feedback and increasing the positive reactivity introduced when the reactor is depressurized. However, the magnitude of the delayed neutron fraction is comparable to existing fast reactors.

Worths of individual isotopes are introduced as a value of their contribution to the core reactivity. Throughout the fuel cycle, the time-dependence of the isotopic and total worth of the fuel is determined. Zero breeding gain is achieved when the initial total worth of the fuel stays constant for multiple cycle burnup.

The effect of different reprocessing strategies on the closed fuel cycle is shown. Research confirms that when there are no reprocessing losses, depleted uranium can be used during the recycling step to replace fission products and obtain a new critical fuel composition. If there are substantial (>1%) HM losses during reprocessing, additional MA can be added to compensate for fissile losses.

Assuming a 1% reprocessing loss, the time that the waste of the GCFR must be stored before it reaches the reference radiotoxicity of uranium ore is reduced by a factor 14 (50.000 years from 700.000 years). The GCFR can reduce the volume of HM waste produced per unit of energy by a factor ~300 when compared to conventional thermal reactors. Although it is concluded that the GCFR can contribute to reducing the MA inventory, to burn all MA produced by thermal reactors additional dedicated burner reactors will be needed.

The decay heat production of the irradiated fast reactor fuel is compared to the existing ANS 5.1 standard used for thermal reactors. The ANS model underestimates the decay heat produced by the fast reactor spent fuel. Parameters are formulated for the decay heat production using an exponential decay model similar to the ANS model. These parameters more accurately estimate the decay heat production during the first hours of decay. It is seen that the decay heat production immediately after shutdown is dependent on the burntime. The maximum decay heat production is not at the end-of-burnup.

TABLE OF CONTENTS

1 Fast Reactors – closing the fuel cycle

"The world's population is expected to expand from about 6 billion people to 10 billion people by the year 2050, all striving for a better quality of life. As the Earth's population grows, so will the demand for energy and the benefits that it brings"[1]

Nuclear technology supplies around 16% of current worldwide electricity demand, and will continue to provide for an important part of the future energy mix. The technology provides opportunities for an economical and large scale decrease of CO_2 emissions. In addition, energy security and energy independence are stimuli for further expansion of nuclear technology. Alternative sustainable technologies will not be rapidly available in sufficient supply to significantly replace current fossil fuel powered plants. Although efficient use of energy could possibly decrease or stabilize demand in developed countries, increasing demand in developing economies such as China and India will more than compensate for this decrease.

Although it is clear that application of current nuclear technology is necessary, a further development of the technology for future application can further improve safety, nuclear sustainability and proliferation resistance, while keeping costs market competitive. This thesis studies the possibilities of drastically limiting nuclear waste production by using fast reactor technology, specifically the gas cooled fast reactor (GCFR). Fast reactor technology has the potential to limit both the volume and lifetime of waste produced, and thus improve nuclear sustainability.

The goal of this thesis is to determine the fuel composition of the GCFR with power 600 MWth that realizes a goal of zero breeding gain. The design specifications of the GCFR 600 MWth, and the isotopic compositions of the minor actinide and plutonium vectors, are the boundary conditions of the performed research. Reactor and safety parameters of the possible fuel compositions are determined. The effects of implementing different recycling strategies are studied. Decay heat curves are calculated for the first hours after reactor shutdown.

1.1 Generation IV – challenging nuclear power towards sustainability

Currently, so called second generation nuclear reactors provide for 16% of the total worldwide electricity demand. The first commercial third generation reactors are being built in Finland (EPR), Japan and Taiwan (ABWR's). When the existing 440 nuclear reactors that make up the reactor park must be replaced, either 'Generation III' or 'Generation IV' technology could be implemented. Research emphasis is presently placed upon Generation IV reactors with goals to further improve nuclear sustainability, safety, economics, and proliferation resistance. The research on these reactors is performed with the combined efforts of the international nuclear scientific community.

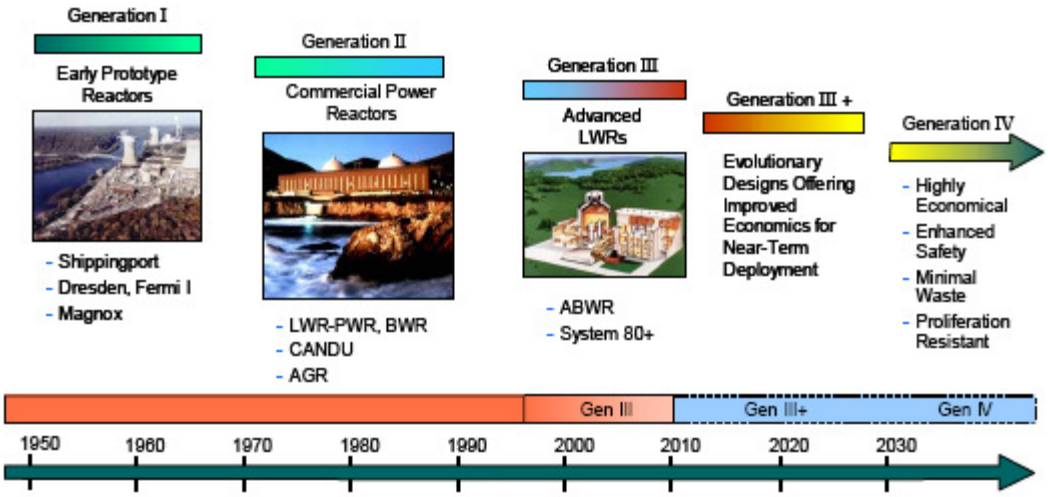

Figure 1: Four generations of nuclear reactors over time[2]

In general, nuclear reactor types can be distinguished from each other by looking at the neutron spectrum and the coolant used. Reactors with a fast spectrum have relatively more neutrons at high energies compared to reactors with a thermal spectrum. The relatively greater amount of neutrons at lower energies within thermal reactors is due to the more frequent collisions with moderating material.

Six nuclear reactor designs have been put forward by the Generation IV Forum. The innovative Gas Cooled Fast Reactor (GCFR) is one of the three fast reactor designs. Up to 2006, all fast reactors have been liquid metal fast (breeder) reactors cooled by liquid sodium. Prototype fast reactors cooled by other liquid metals (such as mercury, lead and NaK) have also been built.

1.2 Nuclear fuel cycle - the open, reprocessing and closed fuel cycle

Currently, the nuclear fuel cycle uses only a small fraction of the total nuclear fuel. Thermal reactors produce power mainly by fissioning of fissile nuclides. Fissile fuels in thermal reactors include ^{235}U and ^{239}Pu. These nuclides can fission after absorption of low-energy neutrons. In thermal reactor fuel, fissile enrichment of fresh fuel is limited to around 5% of the total reactor loading. Prior to irradiation, only fissile ^{235}U and fertile ^{238}U are present in the fuel. During irradiation, the fertile ^{238}U can capture a neutron and decay to fissile ^{239}Pu. At the end of irradiation, a significant percentage of the reactor power is produced by fissioning ^{239}Pu. After irradiation, the irradiated nuclear fuel is either directly transported and prepared for permanent storage (an ‘open cycle’), or it is sent to a reprocessing plant (the ‘reprocessing cycle’).

Different countries have decided to implement different fuel cycle strategies. The United States have chosen to implement the open fuel cycle due to possible proliferation dangers of reprocessing. Among others, France, Japan, the United Kingdom and the Netherlands have opted for reprocessing the irradiated fuel and recycling the uranium and plutonium. Although the reprocessing costs incurred are not compensated by the fissile fuel gains, the choice to reprocess and recycle limits nuclear waste production by making better use of the nuclear fuel, and thus limiting the potential environmental impact of nuclear waste.

In the reprocessing fuel cycle, uranium and plutonium, about 96% of the spent fuel, are separated using the PUREX (Plutonium Uranium REduction and eXtraction) process. The minor actinides (see Box I), are not extracted and remain as waste products. They follow the path of the fission products and are stored in a glass matrix. The plutonium, as an oxide, is then mixed with depleted uranium left over from an enrichment plant to form fresh mixed oxide fuel. The new fuel is called 'MOx (Mixed Oxide) fuel'. A single recycling of plutonium increases the energy derived from the original uranium by some 17%.

Current thermal reactors can be designed to operate on MOx fuel assemblies. In general, however, only 1/3rd of the thermal reactor cores are loaded with MOx fuel. During multiple cycles, further neutrons are captured resulting in parasitic higher plutonium isotopes (e.g. ^{240}Pu, ^{241}Pu) After about two recycles, parasitic absorption in higher plutonium isotopes limits the plutonium recycling potential of thermal reactors. Thus, after recycling twice, new reprocessed plutonium is needed for the MOx assemblies.

Fully closing the fuel cycle

When implementing the PUREX reprocessing strategy, part of the irradiated fuel (minor actinides such as Np, Am, Cm) is kept in the waste stream. Compared to current light-water reactors, fast reactors have the potential to fully close the fuel cycle for all heavy metals. All uranium, plutonium and actinide isotopes can fission in a fast spectrum. To keep the fuel at the same density for multiple cycles, and thus keep the total Heavy Metal (HM) mass loaded equal, the fission products that are removed must be replaced. Reprocessing and subsequent recycling in a fast reactor fuel cycle can thus be called an integral (closed) fuel cycle.

Box I: Depleted Uranium (DU) and Minor Actinides (MA)

In the research performed, both DU and MA are used as replacements for the removed fission products.

Depleted Uranium

To be used in conventional thermal nuclear reactors, uranium must be enriched from 0.7% to 3%. This is performed by either a gas diffusion process or by the more sophisticated ultracentrifugal technique. The enriched product is manipulated further to produce UO_2 pellets for the reactor fuel. The tails, so called depleted uranium (DU), are stored for possible further use. There are large stockpiles of DU which can be used in fast reactors.

Minor Actinides

Minor Actinides are all elements heavier than uranium and plutonium, but including neptunium. MA are produced in thermal reactors through multiple capture reactions and subsequent decay in the uranium and plutonium isotopes. During PUREX reprocessing, MA are separated from the uranium and plutonium. If the current nuclear fuel cycle practice is continued, the MA will be prepared for long-term storage after reprocessing. Research is being performed to burn MA in so-called Accelerator Driven Systems (ADS). Their focus is on burning (fissioning) nuclear wastes as efficiently as possible. There would be significant costs involved to burn MA in an ADS. For this reason, commercial power reactors that could produce power and limit or even decrease MA stockpiles are most welcome.

After the uranium, plutonium and minor actinides are removed from the spent fuel, the remaining waste (fission products) becomes relatively harmless in hundreds of years instead of hundred thousands of years for spent fuel storage. Since the plutonium is not separated from the spent fuel, the reprocessing cost of integral reprocessing are lower than PUREX reprocessing.[3] However, there are increases in the costs of fuel fabrication due to higher shielding demands in the presence of minor actinides.

1.3 Neutron economy of thermal vs. fast reactors

Neutrons interact with the fuel in a reactor core. Neutron interactions within the fuel include capture, fission, elastic- and inelastic scattering. After each fission, multiple neutrons are produced. The number of neutrons produced in a fission reaction increases with the energy of the incoming neutron. Neutrons can also be lost due to leakage from the reactor core. To achieve a fission chain reaction, the neutron production and absorption must balance. When these contributions balance, the reactor is called critical.

The probability that a neutron undergoes an interaction with a nuclide is expressed as a 'cross section' (σ) [cm^2]. Cross sections vary for different interactions, nuclides and incident neutron energies. Larger cross sections indicate a greater possibility for an interaction. With increasing neutron energy, both fission and capture cross sections decrease. In other words, the probability of a fission or capture interaction decreases. The leakage of neutrons in a fast reactor increases. To compensate for these decreases, fast reactors are loaded with a higher percentage of fissile material compared to thermal reactors.

As can be seen in figure 2, fast neutrons with energies of 1 MeV or higher have a greater possibility of causing fission to occur. It is especially important to note the drastic decrease of the capture-to-fission cross section ratio of the fertile isotopes: ^{238}U, ^{240}Pu and ^{242}Pu. At energies above 1 MeV, all isotopes have a greater chance to fission than to capture a neutron.

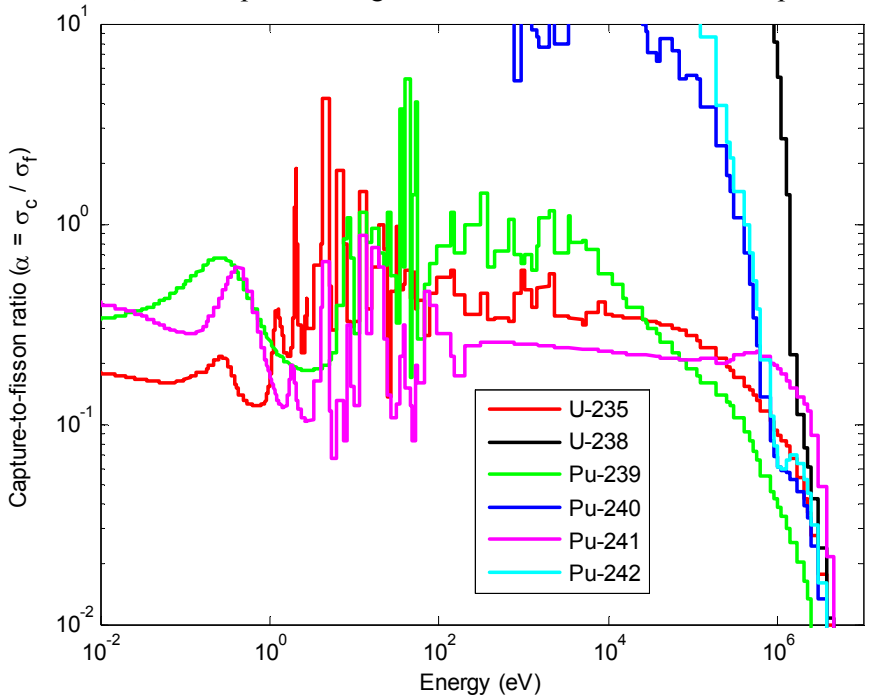

Figure 2: Decreasing capture-to-fission cross section ratio with increasing neutron energies. Fast energies range from 100 keV to multiple MeV. [4]

The η factor, Conversion Ratio (CR) and Breeding Gain (BG)

The reproduction factor η is a factor relating the number of neutrons produced per fission (ν), the fission- and absorption cross sections (σ_f and σ_a). The absorption cross section is equal to the sum of the capture cross section and the fission cross section: $\sigma_a = \sigma_f + \sigma_c$

Reproduction factor: $\eta = \frac{\nu\sigma_f}{\sigma_a}$

Figure 3 compares the reproduction factor η for different isotopes as a function of energy. In a thermal reactor, the energy of neutrons are mainly between 0.1-1 eV, and the η is around 2. Fast reactors have a greater proportion of high neutron energies. The reproduction factor can increase to 2.5-3.5.

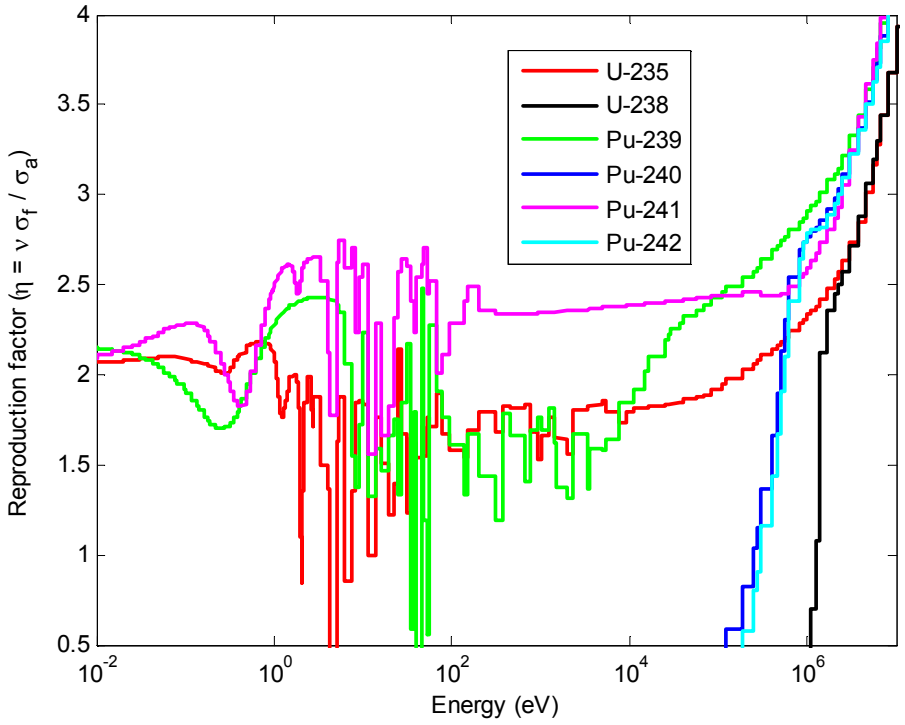

Figure 3: Increasing reproduction factor for high neutron energies [5]

In the GCFR, the neutron economy is such that during irradiation enough neutrons remain after each fission reaction to allow for a capture in a fertile nuclide such as ^{238}U. Often, a fertile nuclide becomes fissile after capture. This is called 'conversion' of fertile to fissile nuclides. During reactor operation, ^{238}U can capture a neutron and form fissile ^{239}Pu via β-decay:

$$^{238}U(n,\gamma)^{239}U \xrightarrow[23\,\mathrm{min}]{\beta^-} {}^{239}Np \xrightarrow[2.3\,days]{\beta^-} {}^{239}Pu$$

In all reactors, one neutron of all neutrons produced per fission is needed to keep the chain reaction going. Another neutron is either parasitically captured by non-fissile nuclides or lost by leakage from the reactor core. In fast reactors, although the leakage from the core is greater than a thermal reactor, the increased reproduction factor allows excess neutrons to be used for breeding fissile fuel (also called conversion of fertile fuel).

To further favor a higher reproduction factor, a higher plutonium mass-fraction it utilized in fast reactor fuel. Where most thermal reactor fuel is loaded with no initial plutonium, fast reactor fuel is loaded with plutonium mass-fractions of 20% or higher. As can be seen in figure 3, the η of Pu-isotopes is greater than for the U-isotopes. Thus, the breeding potential of fast reactor fuel is further increased.

Breeding excess plutonium in fast reactors was for a time believed to be the solution for depleting uranium supplies. However, as demand for nuclear energy slowed and as more low-cost uranium became available, the main driving force for breeder reactors disappeared.

New designs have looked at the possibility to keep the amount of fissile material in a reactor constant throughout the irradiation. In this case, no addition of extra fissile material would be necessary during fuel manufacturing. The amount of fissile material produced compared to the fissile material destroyed is described by the conversion ratio:

$$\text{Conversion Ratio} = \frac{\text{fissile material produced}}{\text{fissile material destroyed}} \qquad \textbf{1. 1}$$

The breeding gain is closely related to the conversion ratio. One of the widely used definitions for breeding gain is: [6]

$$\text{Breeding Gain} = \text{Conversion Ratio} - 1. \qquad \textbf{1. 2}$$

For both parameters, it is important to specify which stages of the nuclear fuel cycle are taken into consideration. In this thesis, it is shown that for an accurate determinaton of breeding gain, the integral cycle (irradiation, storage and reprocessing) must be encompassed in the definition. A breeding gain of zero would express that the amount of fissile material stays constant over multiple integral cycles.

1.4 Goals & design of the 'efficient' GCFR 600 MWth

The goals of the 'efficient' GCFR are intrinsically related to the goals of Generation IV reactors. In this section, the goals of the GCFR are presented. The design of the 'efficient' GCFR 600 MWth is shown. The advantages of gas coolant are discussed.

The goals of the GCFR include creating a more sustainable, proliferation resistant, safe and economic nuclear reactor. See table 1 for a discussion of these goals.

Goals of the GCFR	
Sustainability	The design of the GCFR must achieve near zero breeding gain. It thus has the potential to truly close the nuclear fuel cycle. During the recycling step, depleted uranium and minor actinides separated from thermal reactor spent fuel can be used as replacement for the fission products. Apart from minimizing its own nuclear waste production, it can also reduce long-lived minor actinide stockpiles.
Proliferation resistance	The breeding gain of zero must be achieved without use of fertile blankets. Blanket material is a potential source of weapon-grade plutonium. The reprocessing technology must manage uranium, plutonium and minor actinides simultaneously. As uranium and plutonium are not separated, an important objection to the current reprocessing practice is removed. [7] In addition, the reprocessed isotopic composition of plutonium, and the presence of minor actinides, provide for additional nonproliferation characteristics.[8] When the irradiated fuel is reprocessed on-site, the integral fuel cycle of a fast reactor offers the advantage of minimizing the transport of nuclear materials to and from the nuclear site, thus providing an intrinsic reduction of opportunities of diversion or theft of weapons-usable material. [9]
Safety	Maximizing removal of decay heat by natural convection has been put forward as one of the goals of the GCFR. The cooling system is composed of diversified and redundant He loops designed to be operated in natural circulation. Natural circulation is favored by the upward flow of coolant under nominal conditions. To maximize safety, a relatively low power density (compared to former fast reactor systems) has been chosen. The large fraction of Helium coolant in the reactor limits the core pressure drop. Back-up pressure is established by a secondary containment around the primary circuit. The requirement for the whole system is a failure occurrence less than 10^{-7} event/year with all initiators taken into account.
Economics	The proposed direct cycle power conversion and the high outlet temperatures allow for high thermal efficiency. The high temperature opens the range of applications to high value heat production for industrial processes, including hydrogen production by thermochemical water cracking. [10] To reduce fuel cycle costs, the goal is to maximize energy production within a minimal period of time. However, safety considerations limit the power density. The specific power (W / g HM) of the GCFR is low when compared to other reactors (intrinsically related to the power density). Higher fuel costs are incurred since the investment in (fissile) fuel must be made before the produced power can be sold.

Table 1: **Goals of the GCFR – Generation IV status**

Design of the 'efficient' GCFR 600 MWth

There are a number of competing designs for the GCFR. Differences include the fuel design and the unit power of the reactor. The exact design specifications of the 'efficient' GCFR were formulated in 2004 by CEA.[11] The specifications detail the design of both the 'efficient' and the 'robust' 600 MWth GCFR. The designs differ significantly as to the percentage of structural materials in the core. The research of this thesis has been performed for the most ambitious fuel design, the "efficient" GCFR fuel design with a direct cycle power conversion system.

Reactor core design parameters			
Unit power	600 MWth	Height	1.95 m
Average power density	103 MW/m^3	Diameter	1.95 m
He average pressure	70 bar	Ratio - fuel / struct / cool	35 / 10 / 55
Fuel element type	Plate		
Subassemblies & Fuel composition			
Plates per S/A	21	Volume % SiC	30%
Fuel element number per rhombus	7	Volume % (U,Pu,MA)C	70%
Fissile S/A's in the core	112	Pu (v%)	16%
Specific power	~40 W/g HM	Theoretical density	13.6 g/cm^3
Volume GCFR core	~5.8 m^3	SiC density	3.16 g/cm^3
Fuel mass	~16 ton	Fuel density	85-88% t.d.
Temperatures			
$T_{core,in}$	480 °C	Max fuel temp	< 1200 °C
$T_{core,out}$	850 °C	Max cladding temp	< 1000 °C
Fuel	990 °C	Coolant	665 °C
Cladding	665 °C	Reflector	565 °C

Table 2: GCFR reactor core design parameters

Power density and coolant

The 600 MWth GCFR has a power density of 103 MWth / m^3. Prior to the reference design of CEA, it was concluded that earlier power densities of pioneering generations of GCFR's - all targeting power densities in the range 230-300 MW/m^3 – would have to be modified if the proposed safety goals of the Gen IV GCFR were to be met. [12] The lowered power density still requires a large cooling capacity, thus the volume fraction of coolant is maximized: the fuel / structures/ coolant ratio is 35% / 10% / 55%. Gaseous coolant at high average helium pressure of 70 bar is needed to provide sufficient cooling capacity.

Fuel design, core and subassemblies

The GCFR is characterized by a very high fuel vs. structural material ratio: 70% (U,Pu,MA)C - 30% SiC. Studies at CEA have shown that dense carbide fuels could achieve the high fuel content in the core required to achieve fissile self-generation. This is especially relevant as the fissile fraction in the fuel is limited; earlier research has shown that higher fissile fractions will limit fissile self-generation capacity. Dispersed fuel is used as a first barrier against fission product release. [13]

In table 3, the initial fuel composition for different mixtures of U, Pu, and MA studied are shown. In addition, the isotopic vectors of each component is shown. As can be seen, minor actinides that are mixed to the fuel replace uranium. The initial plutonium content remains constant for all compositions.

Fuel composition and vectors			
Volume fractions 84% U, 16% Pu, 0% MA 79% U, 16% Pu, 5% MA 74% U, 16% Pu, 10% MA			
Uranium		**Minor Actinides**	
U-235	0.70%	Np-237	16.86%
U-238	99.30%	Am-241	60.64%
Plutonium		Am-242m	0.23%
Pu-238	2.70%	Am-243	15.69%
Pu-239	56.00%	Cm-242	0.02%
Pu-240	25.90%	Cm-243	0.07%
Pu-241	7.40%	Cm-244	5.14%
Pu-242	7.30%	Cm-245	1.25%
Am-241	0.70%	Cm-246	0.10%

Table 3: Fuel composition and isotopic vectors of components of HM fuel

A distinguishing aspect of the GCFR core design of CEA when compared to the vast majority of other (innovative) nuclear reactor designs is the fuel sub-assembly (S/A) with fuel elements in the form of plates. Implementation is in a homogeneous reactor core, refraining from the use of fertile blankets. The subassemblies are hexagonal, containing a plate bundle with three plate sub-bundles, each forming a regular rhombus. The plates are clad with SiC. The reflector is made of Zr_3Si_2 / SiC / He: 70% / 10% / 20%. For an illustration of a sub-assembly, see figure 4 (next page).

The actual density of the fabricated fuel in the core is smaller than its theoretical density. After fuel fabrication, small gaps (regions of void) remain. The theoretical density (t.d.) of the fuel plates ranges from 85% to 88% of the actual fuel density. A higher theoretical density increases the fuel loading in the core. As the power remains the same, the power per unit mass (also called the specific power with units [W / g]) decreases. For the GCFR with a t.d. of 88%, the specific power equals 37 W / g.

As mentioned, the GCFR has a high initial plutonium enrichment compared to thermal reactors. Since α-decay of plutonium and minor actinides produces significant amounts of helium, the pressure in the fuel will build-up during irradiation. A smaller theoretical density will result in a smaller pressure build-up in the fuel, as there is a greater volume available for the fission and decay gases that are released.

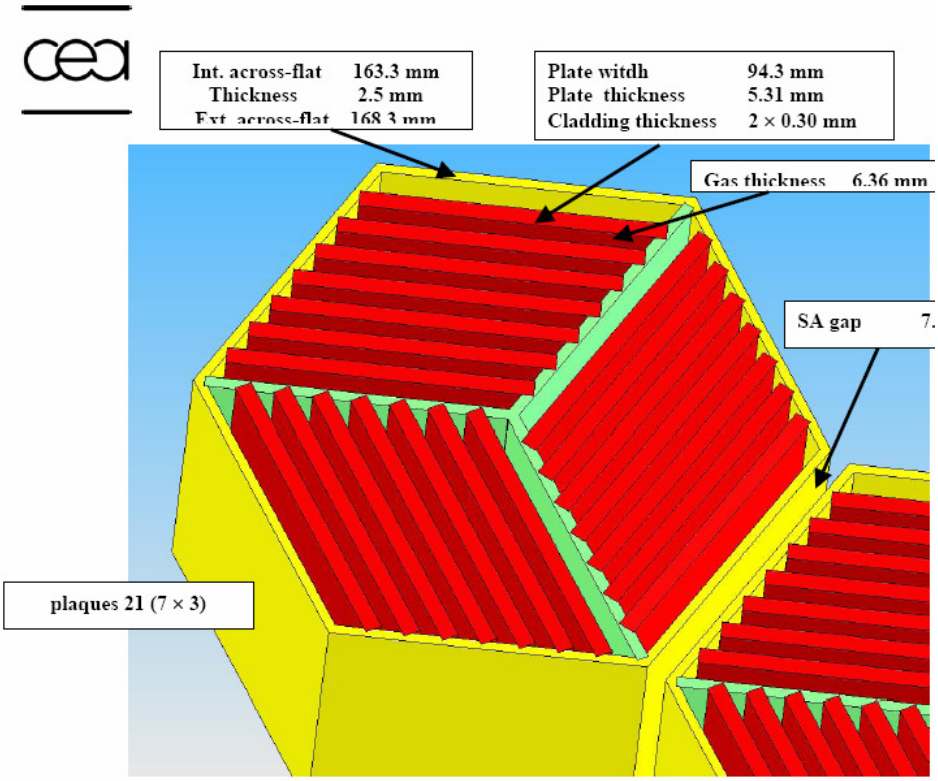

Figure 4: Subassembly of the "efficient" GCFR [14]

1.5 Advantages and disadvantages of gas coolant

The advantages of gas as a coolant in a fast reactor include its maintenance ease, safety, hard spectrum, single phase at all operating temperatures, and the potential high efficiency of the direct Brayton cycle. Disadvantages include its low density, and the resulting need for high pressures. An overview is presented in table 4.

Advantages	
Maintenance	Gas coolant offers maintenance advantages compared to other coolants. Coolant metals, such as lead-bismuth, sodium and mercury, are opaque. Thus, it is much more difficult to visually spot defects of the fuel assembly or control elements. In addition, the coolants are solids at room-temperature. Maintenance and sub-assembly changes must be performed at high temperatures.
Safety	Helium gas is chemically inert. It does not interact with the nuclear fuel, thus allowing for direct cycle power conversion system without radiation contamination. A major disadvantage of sodium coolant compared to gas coolant is its flammability when in accidental contact with water or steam of the secondary loop.

Spectrum	Interaction between neutrons and coolant is minimized when using helium. There is very limited moderation, further hardening the neutron spectrum, thus making zero breeding gain feasible.
Single phase	There is no phase change of the coolant. Thus, the danger of positive voiding reactivity effects is smaller when compared to sodium or lead cooled reactors.
High efficiency	The high thermal efficiency afforded by the high temperature helium coolant and a direct Brayton cycle results in a more effective utilization of the nuclear fuels and thus lower amounts of waste per unit of energy generated.[15]
Disadvantages	
Low density resulting in high system pressures necessary to remove (decay) heat	Due to the low density of helium compared to metal coolants, the gas must be kept at a very high pressure in order for the heat to be removed from the reactor core. A much more expensive and tested vessel must be created for these high pressures. In contrast, metal coolants kept at ambient pressures allow for sufficient heat removal. Back-up gas at high pressures must be present in case emergency cooling is needed to keep the coolant pressure at an acceptable level and remove decay heat from the core.

Table 4: Advantages and disadvantages of using gas coolant

1.6 Objective of the thesis and scope

In the following chapters, the nuclear fuel cycle of the GCFR is analyzed in detail. The results of the calculations help to determine the fuel composition that succeeds in creating a closed fuel cycle. As Generation IV designs should tackle both sustainabilty and safety, the safety parameters for the different fuel compositions and their decay heat production are studied. The objectives of this thesis are:

- To investigate and explain the time-dependent multiplication factor of the GCFR for different fuel compositions. To calculate and compare the safety parameters of the reactor for these compositions.
- To quantify changes in breeding gain, allowing for a time-dependent isotopic breakdown of the breeding gain measure.
- To compare different reprocessing strategies and their effect on the closed fuel cycle. To determine the fuel composition of the GCFR with power 600 MWth that realizes a goal of zero breeding gain. To quantify the effects of the GCFR on limiting nuclear waste production.
- To compare the decay heat production of the irradiated fast reactor fuel to the existing standards used for thermal reactors. To investigate the reasons for possible differences and formulate parameters that more accurately estimate the decay heat produced.

The boundary conditions of the performed research are the:

- design specifications of the 'efficient' GCFR 600 MWth.
- isotopic compositions of the minor actinide and plutonium vectors (Table 3).

In Chapter 2, relevant nuclear reactor theory is reviewed. The code used to calculate burnup and reactor parameters is presented. A model for calculating the breeding gain for multiple cycle burnups using isotopic worths is introduced. In Chapter 3, a single cycle burnup is simulated for different percentages of minor actinides initially added to the fuel. Chapter 4 utilizes the model for isotopic worths to analyze the reactivity and breeding gain of the reactor for multiple cycle burnups. The effects of storage and different reprocessing scenarios are discussed. Chapter 5 analyzes the decay heat production after shutdown.

2 Reactor neutronic analysis and fuel cycle theory

Reactor neutronics calculations allow for a detailed analysis of the changing nuclear fuel composition, safety parameters and reactor criticality. Code systems are used to solve the depletion and the neutron transport equations. Extensive libraries exist with nuclear data for all relevant isotopes, including the energy and temperature dependence of their cross sections, (delayed) neutron production, half-lives and decay energies.

In this chapter, depletion analysis theory and the burnup code are presented. Time-dependent reactor core (safety) parameters, including k-effective, β-effective, void- and fuel temperature coefficients, are discussed. A model for the fissionability of the reactor is given. This model will be used in the next chapters to quantify the breeding gain and estimate reactivity changes in the GCFR for single and multiple cycle burnups. After shutdown of a reactor core, the irradiated fuel produces decay heat. The standard that is used to calculate decay heat in thermal reactors for different fuel compositions is presented.

2.1 Depletion analysis – calculating flux, k_{eff} and burnup

Nuclide depletion is dependent on the neutron interaction cross sections, neutron flux density (φ), and the nuclide densities in a reactor core. The fission, absorption and capture cross sections used in the depletion formula are the so called 'average cross sections'. Average cross sections are a function of the integral of the energy dependent cross section and the energy-dependent flux over the entire energy range, divided by the integral over the energy-dependent flux.

A constant power throughout the irradiation is assumed. During each subinterval of a depletion step, the flux is taken to be constant. The flux is calculated using the known power of the GCFR: 600 MWth. The initial densities in the reactor core are calculated using the GCFR fuel- and geometrical specifications. The depletion formula is solved to calculate the new atomic densities before going to the next depletion step:

$$= \quad 1 \quad + \quad 2 \quad + \quad 3 \quad + \quad 4 \quad + 5 \quad + \quad 6$$

$$\frac{dN_i}{dt} = -N_i\sigma_a\varphi - \lambda_i N_i + \sum_{j\neq i}\lambda_{j\to i}N_j + \sum_{k\neq i}\sigma_{c,k\to i}\varphi N_k + Q_i + \sum_{l\neq i} y_{l\to i}\sigma_{f,l}\varphi$$

with:

$N_i\sigma_a\varphi$ = Absorption in nuclide with index 'i'

$\lambda_i N_i$ = Decay of nuclide 'i' **2. 1**

$\sum_{j\neq i}\lambda_{j\to i}N_j$ = Decay of nuclide 'j' to nuclide 'i'

$\sum_{k\neq i}\sigma_{c,k\to i}\varphi N_k$ = Capture rate nuclide 'k' to nuclide 'i'

Q_i = External source

$\sum_{l\neq i} y_{l\to i}\sigma_{f,l}\varphi$ = Fission yield of nuclide 'l' to nuclide 'i'

The terms on the right hand side of the equation represent:

1) loss by neutron absorption, with a spectrum averaged microscopic absorption cross section which includes fission and capture;
2) nuclide decay;
3) production by radioactive decay of a nuclide.
4) production by neutron capture with a spectrum averaged microscopic capture cross section;
5) an external source;
6) production term for fission products, where the value of the fission product yield 'y' is dependent on both the fissioning isotope and the energy of the neutron causing fission (in a multiple energy-group calculation).

Flux calculation

The fission rate is defined as the macroscopic fission cross section (Σ_f) multiplied by the flux (φ). The thermal power is calculated by multiplying the fission rate by the energy released per fission. Since the thermal power is known, we can normalize the flux to a value which results in a power of 600 MWth:

$$P = E_{\text{Released per Fission}} \Sigma_f \varphi V$$

where: V = volume of reactor core **2. 2**

P = power

After the depletion calculation, the new nuclide densities are given as an input for the next depletion step.

The mathematical description of the neutron distribution is based on the neutron transport equation. The equation tracks the change in the number of neutrons due to sources, scattering, leakage and other interactions within a control volume. The control volume can be the entire reactor, or just a very small part of the reactor. The number of neutrons at time t in control volume element dV, with energy between E and E + dE, which moves in a solid-angle $d\Omega$ around the direction $\vec{\Omega}$ is expressed as $n(\vec{r}, E, \vec{\Omega}, t)dVdEd\Omega$. The flux is directly proportional to the neutron density: $\varphi(\vec{r}, E, \vec{\Omega}, t) = n(\vec{r}, E, \vec{\Omega}, t)\upsilon$, with: υ = velocity of neutron [m/sec].

The neutron transport equation is defined as [16]:

$$\frac{1}{\upsilon}\frac{\partial \varphi}{\partial t} = \underbrace{S(\vec{r}, E, \vec{\Omega}, t)}_{1} + \underbrace{\int_{4\pi}\int_{0}^{\infty} \Sigma_s(\vec{r}, E' \to E, \vec{\Omega}' \to \vec{\Omega})\varphi(\vec{r}, E, \vec{\Omega}, t)dE'd\Omega'}_{2} \qquad \textbf{2. 3}$$

$$\underbrace{-\vec{\Omega}\cdot\vec{\nabla}\varphi(\vec{r}, E, \vec{\Omega}, t)}_{3} \underbrace{-\Sigma_t(\vec{r}, E)\varphi(\vec{r}, E, \vec{\Omega}, t)}_{4}$$

The term on the left hand side of transport equation is equal to the change of the number of neutrons over time within the control volume. The terms on the right hand side of the equation represent:

1) neutron source term(s), representing for example fission
2) neutron scatter term, where neutrons scatter from other energies (E') and directions (Ω') to the relevant energy (E) and direction (Ω)
3) neutron leakage from the reactor core
4) all neutron interactions (e.g. neutron absorption)

The multiplication factor, also called k-effective (k_{eff}), is the ratio of the total production of fission neutrons to the total loss of neutrons by absorption and leakage. The time-dependent behavior of a neutron population in a reactor core will depend on the ratio between on one hand the production term, and on the other hand the absorption and leakage terms. The one-group, one-dimensional diffusion equation is used to introduce k_{eff}. The equation does not take into account delayed neutrons. The effect of delayed neutrons is discussed in the next section on safety parameters.

The reactor is critical when production of neutrons is equal to loss. In that case, the time rate of change of the flux equals zero. The one-group, one-dimensional diffusion equation for a critical reactor is given below.[17]

$$\frac{\partial}{\partial x} D(x) \frac{\partial}{\partial x} \varphi(x) + \nu\Sigma_f(x)\varphi(x) - \Sigma_a(x)\varphi(x) = \frac{1}{\upsilon} \frac{\partial \varphi}{\partial t} = 0 \qquad \textbf{2. 4}$$

with:

D = Diffusion coefficient

υ = Neutron velocity

For a non-critical reactor, a measure is introduced for the 'off-balance'. The left-hand-side of the diffusion equation is altered so that it is not necessary to solve the time-dependent diffusion equation. The steady-state equation (2.5) is obtained by adjusting the fission source term, making the system critical by a (fictive) change in neutron production per fission.[18] Mathematically this results in an eigenvalue equation with eigenvalue k:

$$\frac{\partial}{\partial x} D(x) \frac{\partial}{\partial x} \varphi(x) + \frac{\nu}{k}\Sigma_f(x)\varphi(x) - \Sigma_a(x)\varphi(x) = 0 \qquad \textbf{2. 5}$$

By adjusting the source term – multiplying the source by 1 / k – an important physical meaning is given to k – the 'multiplication factor'. It represents the ratio of neutron production by fissions to the total neutron loss by leakage and absorption (see also eq. 2.7).

If it is assumed that the macroscopic cross sections are space independent, the reactor is assumed to be 'homogeneous'. For a homogeneous system, the one-dimensional diffusion equation can be written as:

$$\nabla^2\varphi(x) + B^2\varphi(x) = 0$$

with:

$$B^2 = \frac{\nu\Sigma_f / k - \Sigma_a}{D} \qquad \textbf{2. 6}$$

D = diffusion coefficient

B = B_g = geometrical buckling factor

Finally, the above expression can be solved for the multiplication constant, which can be written split into a contribution for an infinitely large reactor k_∞, and a term including the leakage (utilizing the geometrical buckling factor):

$$k_{eff} = \frac{\nu\Sigma_f}{\Sigma_a + DB_g^2} = k_\infty \frac{1}{1 + B_g^2 L^2} \text{ where } k_\infty = \frac{\nu\Sigma_f}{\Sigma_a},\ L = \sqrt{\frac{D}{\Sigma_a}}$$

with: **2. 7**

L = diffusion length

In neutronic calculations, the k_{eff} of the GCFR is calculated for each simulated depletion step. As long as k_{eff} of the reactor exceeds one, the reactor can be operated critically. Supercriticality must be compensated by insertion of control rods in the core. It is preferred to have a reactor operating close to criticality, without large reactivity changes, as this is most favorable for ease of reactor operation.

When studying the time-dependence of the neutron population in a reactor, the multiplication factor is often expressed as a 'reactivity'. Reactivity (ρ) is a measure indicating the deviation of the core multiplication factor from unity, and is defined as:

$$\rho = \frac{k_{eff} - 1}{k_{eff}} \quad \textbf{2. 8}$$

Burnup

Burnup gives an indication of the amount of fuel that is fissioned relative to the initial amount of fuel present. Burnup can be expressed in the amount of energy that is produced by a specified mass of reactor fuel. It can also be expressed as a percentage of heavy metal (HM) atoms that is fissioned during irradiation relative to the total number of initial atoms (Fissions per Initial Metal Atom – FIMA). In the studies performed, the maximum burnup is around 10% FIMA over 2500 days irradiation. This is equivalent to around 90 MWd / kg.

The burnup at the boundaries of the reactor core is lower compared to the burnup in the centre of the core. This is due to the higher flux in the centre as compared to the outer region. As it is favorable to have a flat flux profile, fuel management in thermal reactors dictates placing higher enriched assemblies with higher reactivities at the boundaries of the reactor. Such an arrangement flattens the flux in the core. However, as a near zero breeding gain is accomplished in the GCFR, the change in the reactivity of different subassemblies in the GCFR varies much less compared to thermal reactors. The research performed implements homogeneous fuel loading.

2.2 Reactor dynamics and safety parameters

Using the reactivity as defined in the previous section, the diffusion equation can be written as:

$$\frac{1}{\upsilon\nu\Sigma_f}\frac{d\varphi}{dt} = \rho\varphi \quad \text{or} \quad \frac{d\varphi}{dt} = \frac{\rho}{\Lambda}\varphi, \text{ and thus } \varphi = \varphi_0 \exp(\frac{\rho}{\Lambda}t)$$

with: **2. 9**

Λ=neutron generation time

For fast reactors, the generation time can be as small as 10^{-7} to 10^{-6} seconds. Thus, small deviations from criticality (e.g. k_{eff} = 1.001) causes the flux and power to increase exponentially. Luckily, around 1% of the total number of neutrons are not emitted immediately after fission, but

are released by the fission products after a certain time delay. Although the ratio of delayed neutrons to prompt neutrons is small (for fissioning ^{235}U, only 0,64% of the total number of fission neutrons are delayed) they are very important for controlling the nuclear chain reaction.

The delayed neutrons are emitted up to several minutes after the fission process. A 'precursor', is a fission product that undergoes β-decay forming a daughter nucleus. The daughter nucleus can have a higher excitation energy than its neutron-separation energy. This results in the daughter emitting a neutron.

The three parameters that are discussed in this section are used within reactor safety analysis. The delayed neutron fraction is expressed by the measure β_{eff}. β_{eff} gives an indication of the controllability of the reactor. The void- and temperature coefficients are measures for the effect of loss of coolant or temperature excursions on the multiplication constant.

2.2.1 Delayed neutrons and the kinetics equations

As indicated, not all of the neutrons are promptly emitted. In this section, β_{eff} and the kinetics equations are introduced. β is defined as the ratio of delayed neutron production to the total yield of fission neutrons (prompt and delayed) emitted per fission. Since the average energy of prompt neutrons is greater than the energy of delayed neutrons, the probability that delayed neutrons leak from the reactor core is smaller than prompt neutrons. Delayed neutrons thus have a greater importance than prompt neutrons to the chain reaction. The β_{eff} is calculated taking the importance of delayed neutrons into account, and can be up to 15% larger than β.

The delayed neutrons are typically split into six different delay groups. Each delayed neutron group has a typical half-life $T_{1/2,i}$ (decay constant λ_i). Using the fractions of delayed neutrons produced per group, the average time between fission and the eventual release of the delayed neutrons of group i can be determined.

The effective generation time is dependent on the multiplication constant, the delayed neutron fractions and decay constants of each delayed neutron group.

$$\Lambda_{eff} = \frac{1}{k_{eff}} \sum_i \frac{\beta_i}{\lambda_i} + \Lambda_{prompt} \approx \frac{1}{k_{eff}} \sum_i \frac{\beta_i}{\lambda_i} \qquad \textbf{2. 10}$$

The delayed neutrons cause the effective neutron generation time to increase (e.g. from 10^{-7} to 0.1 seconds). As can be seen in equation (2.9), an increased generation time decreases the rate with which the neutron flux and thus the power of the reactor increases when reactivity increases.

The total fraction of delayed neutrons varies from nuclide to nuclide. Two simple 'rules of thumb' are relevant for delayed neutron production. The delayed-neutron yield:
- increases with the mass-number (A), for the same atomic number (Z)
- decreases with increasing atomic number (Z).[19]

Using the above rules, it can be concluded that the delayed neutron fraction in fast reactors will be smaller than the fraction in thermal reactors. When mixing MA in the fuel as a replacement for uranium, it is to be expected that the β_{eff} decreases. Using one of the above rules of thumb: the fissioning isotopes are more often plutonium (Z=94), while in thermal reactors uranium is fissioned (Z=92).

To calculate the change in neutron population after a reactivity change, the emittance of delayed neutrons must be taken into consideration. The kinetic equations are derived by changing the original diffusion equation to take into account a decrease in prompt neutrons and production of

delayed neutrons by precursors. The first equation calculates the change in neutron population, while the second group of six equations calculates the change of the precursor concentration per group. When the reactor is critical and the number of neutrons in the reactor is stationary, the decay rate of precursors is equal to their production.

$$\frac{dn}{dt} = \frac{\rho - \beta}{\Lambda} n(t) + \sum_i \lambda_i C_i(t)$$

$$\frac{dC_i}{dt} = \frac{\beta}{\Lambda} n(t) - \lambda_i C_i(t) \qquad \text{i} = 1,..,6$$

with : **2. 11**

$C_i(t)$ = precursor concentration of group$_i$

$\sum_i \lambda_i C_i(t)$ = rate of delayed neutrons emitted by precursors of group$_i$

When reactivity is inserted, the number of neutrons increases by an initial prompt jump (a factor β / (β-ρ)), after which the population continues to rise. The slope with which the population increases depends on the magnitude of the reactivity change. The 'stable reactor period' is proportional to the difference between β and ρ. Thus, if β becomes almost equal to ρ, the stable reactor period becomes very small. In the equation below, the flux as a function of time after a reactivity insertion is given for a suitable one-group delayed neutron fraction and half-life.

$$\varphi(t) = \varphi_0 \left\{ \frac{\beta}{\beta - \rho} e^{\frac{\rho\lambda}{\beta - \rho} t} - \frac{\rho}{\beta - \rho} e^{-\frac{\beta - \rho}{\Lambda} t} \right\}$$

with: **2. 12**

λ=half-life of delayed neutrons of one-group approximation

The prompt jump and the stable reactor period can be found in the first exponential term. The second term in the brackets does not affect the magnitude of the jump or the stable reactor period. The prompt-jump-approximation (PJA) ignores the effect of the second term. Due to the small generation time in fast reactors, the PJA suffices to approximate the time-dependent flux after a reactivity insertion.

When the reactivity change is equal to the delayed neutron fraction, the reactor is called supercritical. After such a large reactivity insertion, the stable reactor period (normally 10-100 seconds) decreases rapidly to 10^{-3} to 10^{-5} seconds, dependending on the generation time.

Due to the smaller β in fast reactors, the absolute deviation from reactor criticality must be smaller compared to reactors with a larger β to obtain the same stable reactor period. By calculating reactivity in units $, equal to the ratio of the reactivity and the total effective delayed neutron fraction, it is possible to better compare changes in reactivity in a thermal reactor core to changes in a fast reactor core. It is defined as:

$$\rho(\$) = \frac{\rho}{\beta_{eff}} \qquad \textbf{2. 13}$$

A reactivity of $1 corresponds to a prompt-critical reactor. When β_{eff} decreases, a specified 'reactivity' is reached after a smaller change of the reactivity.

2.2.2 Calculation of the Void & Fuel Temperature Coefficients

Void coefficient
In general, reducing the amount of coolant in the core reduces moderation, and thus increases the average energy of neutrons (harder spectrum). The harder spectrum decreases resonance absorption, and increases the number of neutrons per fission, resulting in positive reactivity effects. The positive reactivity effects are usually not fully compensated by an increased leakage effect.

The void coefficient (VC) is a measure of the change in the reactivity of the reactor after a depressurization, also called 'loss of coolant accident' (LOCA). Under normal conditions, the helium in the GCFR is at 70 bars. 'Voiding' of helium results in a pressure drop from the nominal pressure. The change in the multiplication factor (k_{eff}) is normalized with the multiplication factor calculated at nominal pressure and divided by the absolute change in pressure:

$$\alpha_v = \frac{1}{k_0}\frac{\Delta k}{|\Delta P_c|} \qquad \textbf{2. 14}$$

and is expressed in pcm / bar.

$$\Delta k = k_{(\%\text{ of nominal})} - k_{70bar}$$
$$k_{70bar} = k_0$$

Fuel temperature coefficient
The fuel temperature coefficient (FTC) is a measure for the change in the reactivity of the reactor after a fuel temperature excursion. An increase in temperature leads to Doppler-broadening of resonances, thus increasing resonance absorption. In fast reactors, not only the absorption rate but also the fission rate is affected by Doppler-broadening. Since the Doppler effect is a fast feedback mechanism, and considering the shorter prompt neutron lifetime of a fast core as compared to thermal cores, the negative sign of the Doppler coefficient is extremely important. It provides for essential negative feedback.

Compared to thermal reactors, the relatively high percentage of plutonium (16% of HM atoms) present in the reactor fuel and the relatively hard neutron spectrum are important reasons why the Doppler coefficient in fast reactors is smaller. When the temperature of the fuel rises, the most significant resonance absorption increase is due to Doppler-broadening of the resonance of ^{238}U. With more plutonium, there is less absorption in ^{238}U, and a smaller negative reactivity change.

The FTC is given by:

$$\alpha_f = \frac{1}{k_0}\frac{\Delta k}{\Delta T} \qquad \textbf{2. 135}$$

and is expressed in pcm / K.

$$\Delta k = k_{T+\Delta T} - k_T$$
$$k_T = k_0$$

2.3 Simulation of reactor burnup – code BURN1D

Analysis of the changing fuel composition is performed by solving the depletion equation using a quasistatic approach. The depletion equation and the 1-D transport equation are solved for multiple timesteps until the end of the irradiation is reached. The length of each time step is selected to be small enough to assume that neutron spectrum changes can be ignored. As a 1-D calculation is performed only the radial reflector is modelled. The validy of the 1-D simulation is discussed in Appendix A, where the results of 1-D and 3-D calculations are compared.

A depletion code has the qualitative structure as indicated in figure 5.

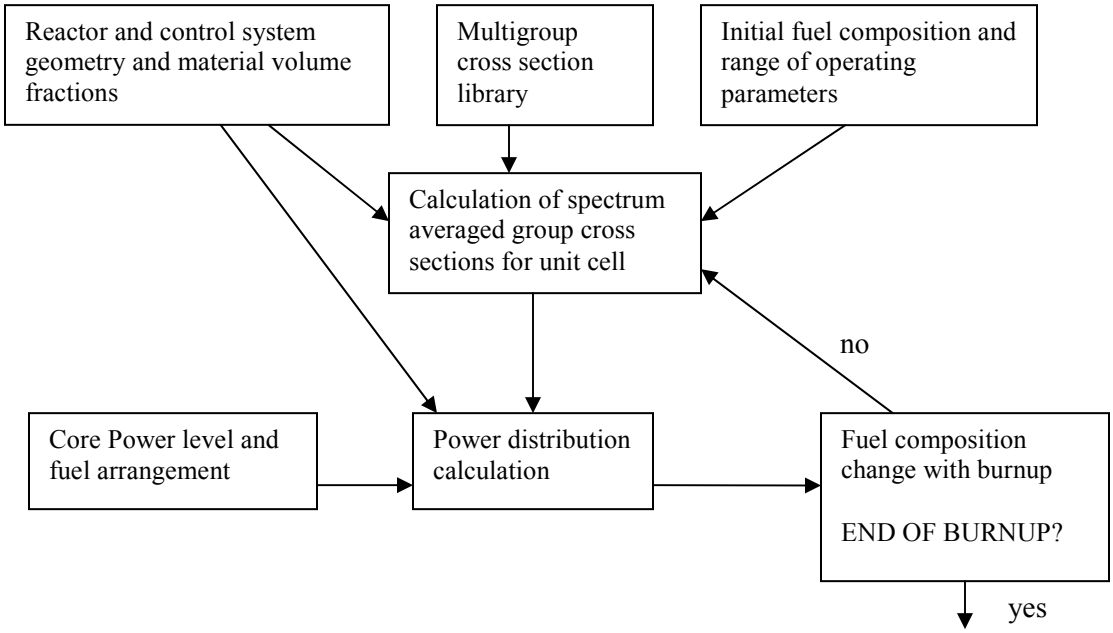

Figure 5:General lay-out of a multigroup depletion code.[20]

2.3.1 Unit cell

A unit cell characterizes the shape and volume ratio of recurring fuel elements. The unit cell of the GCFR models an individual plate surrounded by cladding and moderator in a 1-D description. The fuel elements are modelled as an infinite array of symmetrical slabs. This model can be implemented for the desired ratio of fuel / cladding / coolant. The ratio determines the widths of the components of the unit cell. As mentioned in section 1.3, the ratio's of the fuel / structure / coolant in the GCFR is 35% / 10% / 55% respectively. A sketch of the unit cell is shown in figure 6.

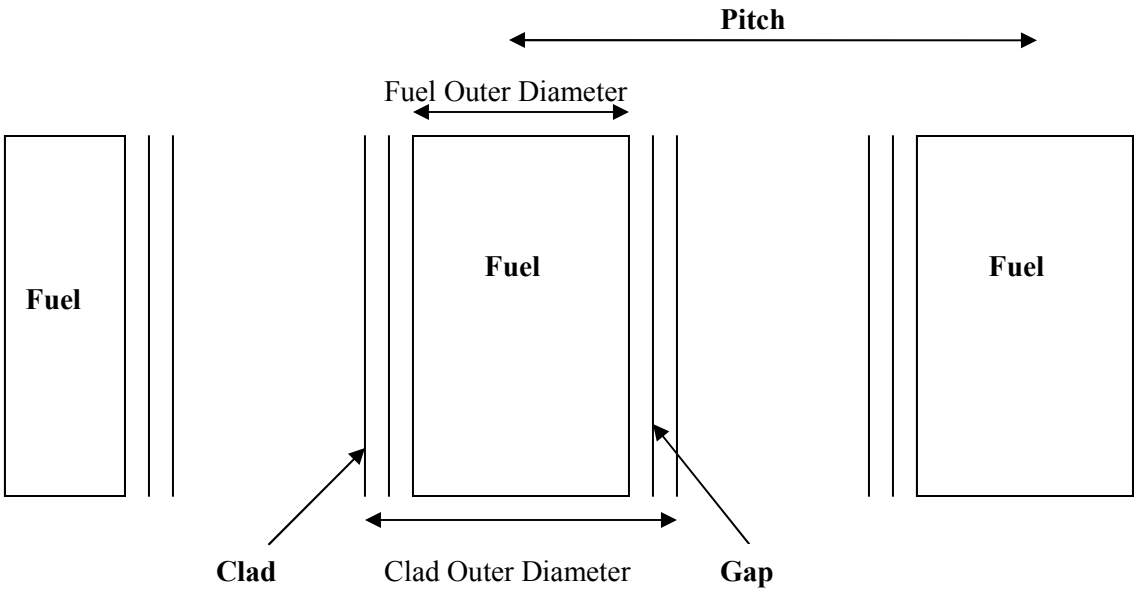

Figure 6: Symmetric-slab unit cell used to simulate the GCFR, indicating fuel, cladding and coolant regions. In the calculations, the gap between the fuel and the cladding is disregarded. The pitch is defined as the distance from fuel centre-to-centre. Exact dimensions of the unit cell of the GCFR are given in Appendix A.

As the reflector has not been defined accurately in the GCFR design specification, it is modelled as an infinite homogeneous mixture.

2.3.2 Program description and flow chart

In this section, the BURN1D code is described. The PERL script BURN1D is used to couple several SCALE 4.4[21] modules together to calculate the average cross sections in the unit cells and the reactor parameters of the GCFR during burnup. The depletion code ORIGEN-S [22] [23]has been used to calculate the change of nuclide densities during burnup and decay. An AMPX master library is used with a 175-group VITAMIN-J energy structure for fast reactor applications.

The code solves the 1-D transport equation, taking account only the radial dimension of the cylindrical reactor core. Thus, only the radial reflector of the GCFR can be accounted for, and not the two axial reflectors at the top and bottom of the reactor core. An axial dependence is partly simulated through a buckling factor for the axial direction.

The GCFR is split into three separate zones of approximately the same volume and equal number of sub-assemblies (S/A's). Both a 'zone-weighted' and a 'cell-weighted' calculation are performed to calculate the average microscopic cross sections of the unit cells in the four different zones (3 fuel zones, 1 reflector zone) and the depletion of the nuclide densities in the reactor core.

Cell weighting homogenizes the cross sections in a heterogeneous unit cell. Cell weighted cross sections preserve the reaction rates which occur in a representative unit cell of the reactor. The unique cell weighted cross sections of the unit cells are merged (using WAX). This merged library characterizes the entire core, and is used for a calculation of the total flux over the reactor. Zone weighting in a unit cell defines the flux in the fuel, structures and coolant separately.

Cross section processing takes into consideration the temperature and the geometry of the components of the unit cell, as well as the nuclide densities.

Before being able to do the depletion calculation, the flux must be normalized so that the total power of the reactor equals 600 MWth. The normalization is done in the 'cell-weighted' part of the flow chart in a procedure called 'flux to power'. Macroscopic zone weighted cross sections are used. Constant power per zone is used for the depletion calculation. The general formula relating power and flux, presented in section 2.1, is specified per zone:

$$P_Z = E_{\text{Released per Fission}} \Sigma_f^z \varphi_Z V_Z$$

The power per zone is taken together with the average isotopic cross sections per zone and is input in the depletion code (ORIGEN-S) to calculate new initial densities. A flow chart of the depletion calculation can be found in figure 7.

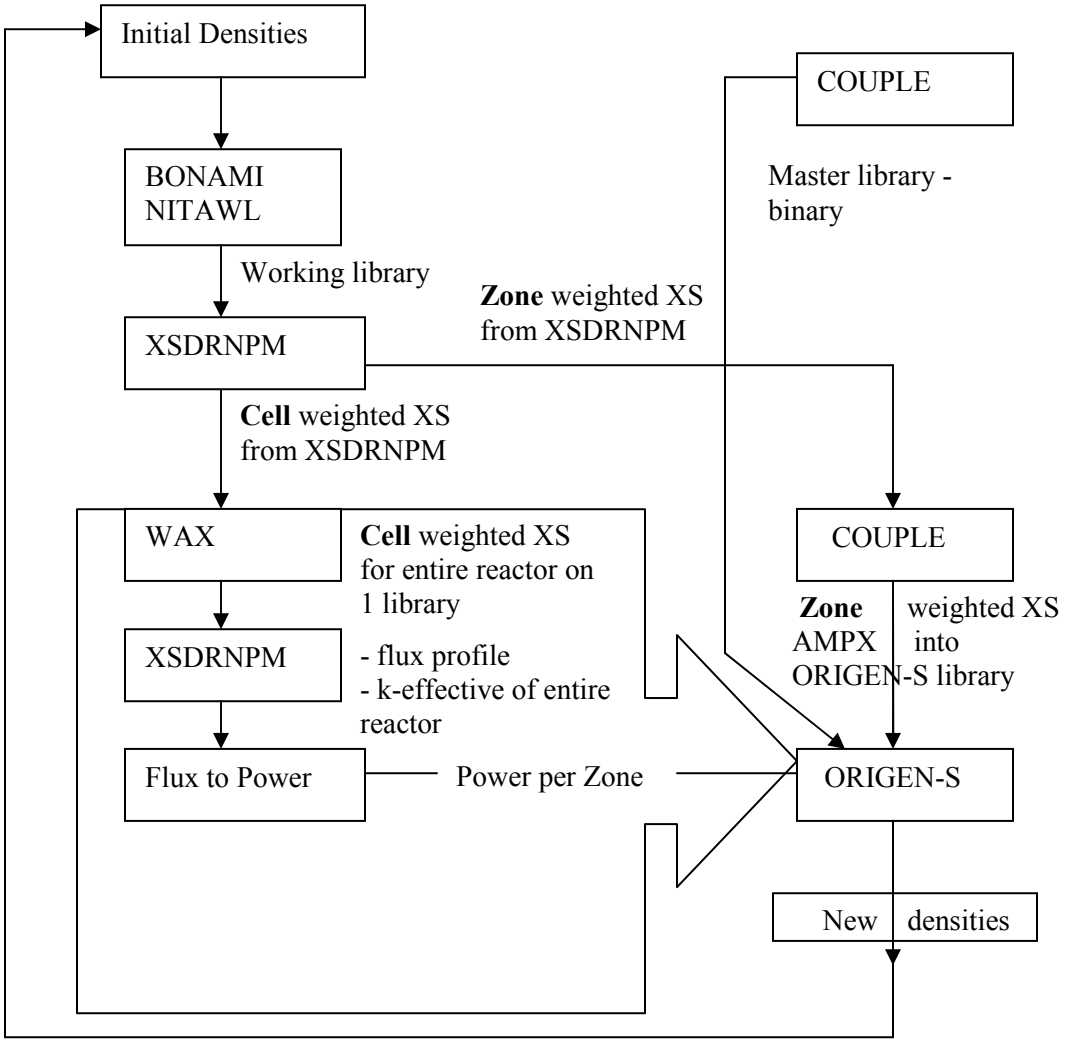

Figure 7: Flow chart of depletion code BURN1D, using the SCALE 4.4 system. NITAWL, BONAMI and XSDRNPM create a problem dependent cross section library. XSDRNPM solves the one-dimensional transport equation, calculates the multiplication constant and the new flux profile. The flux profile and the new densities are used in the next step.

2.4 Defining zero breeding gain

The formulation for breeding gain that is given in Chapter 1 couples the breeding gain to the conversion ratio. The conversion ratio depends on the fissile fuel produced and destroyed. This former formulation focuses upon changes in fissile fuel concentration throughout irradiation. Although it is possible to track the buildup of fissile isotopes during irradiation, a number of fissile isotopes do not remain in the fuel after interim storage due to their short half-lives. To accurately analyze breeding gain, all stages, including irradiation, decay and fuel fabrication must be taken into account. The entire cycle from from the beginning of irradiation to the end of fuel fabrication is called the 'integral cycle'.

Since a breeding gain of zero cannot be verified by looking solely at the depletion of reactor fuel during irradiation, a different definition for breeding gain is introduced that is better applicable to the integral fuel cycle of the GCFR.

2.4.1 Arguments for a new definition for breeding gain

When performing simple breeding gain calculations, it often suffices to focus on changes of the atomic density of the fissile isotopes. If the atomic density of the fissile fuel remains the same throughout irradiation, the conversion ratio is equal to 100% while the breeding gain is equal to zero. Although individual nuclides can be more fissile than others, this is ignored in simple breeding gain calculations. A more complex breeding gain measure should consider these isotopic variations.

In thermal reactors, a limited number of fissile atoms (^{235}U and ^{239}Pu) are the main contributors to fission neutron production. The atomic density of higher plutonium and MA isotopes in a thermal reactor is small. A number of these nuclides are parasitic, and thus decrease reactivity. The fissile isotopes of irradiated fuel of thermal reactors have long half-lives, thus their density in the fuel stays constant during decay.

In contrast, the GCFR is loaded with a significant Pu and MA vector. Many isotopes contribute to the fission neutron production. In addition, a number of the fissile nuclides present at the end of irradiation have short life-times, and thus show significant decay when in interim storage. A more accurate breeding gain measure is introduced that takes into account the differences between thermal and fast reactors.

2.4.2 Definition of an Integral Cycle Breeding Gain

For each isotope, a microscopic worth is calculated that is dependent on the number of neutrons per fission, and the fission- and absorption cross sections. The microscopic worth of an isotope (w_i) is defined as:[24]

$$w_i = (\nu\sigma_f - \sigma_a)_i \qquad \textbf{2. 16}$$

σ_f = microscopic fission cross-section

σ_a = microscopic absorption cross-section

ν = average number of neutrons produced per fission

If the microscopic worth of an isotope is positive, on average more fission neutrons are produced than are absorbed. A negative worth of an isotope indicates that more neutrons are absorbed than are produced by fission. It will be shown in the next chapter that the microscopic worth has a slight time-dependence. When analyzing breeding gain it is easier to work with a single

microscopic worth for all neutron energies. This worth is calculated by collapsing the 175-group cross sections into an equivalent one-group cross section.

The total macroscopic worth of the reactor fuel is dependent on the density of the different isotopes present in the fuel. The time-dependent macroscopic worth of an isotope is defined as:

$$W_i(t) = n_i(t)(\nu\sigma_f - \sigma_a)_i$$

$W_i =$ macroscopic worth **2. 17**

$n_i =$ isotopic density

When adding up the macroscopic worths of HM atoms, fission products (f.p.'s), and reactor structures, the total fissionability of a reactor is determined. The time dependent total fissionability of the reactor is defined as:

$$\text{Fiss(t)} = \sum_i n_i(t) w_i \quad \textbf{2. 148}$$

The total fissionability of the reactor can be compared with the true reactivity of a reactor core as calculated using the neutron transport equation. In addition, the change of fissionability over an irradiation cycle can be compared to the change of reactivity of the reactor:

$$\Delta fiss_{\text{irradiation}} = \sum_i (n_i w_i(EOB) - n_i w_i(BOB)) \quad \textbf{2. 19}$$

It will be shown that fissionability compares well with the true reactivity of the reactor, even though the fissionability disregards geometrical aspects of reactor criticality. In addition to comparing the change of fissionability to reactivity during irradiation, research is performed analyzing the changing fissionability over the integral cycle. If the fissionability of reactor at beginning-of-burnup of the first cycle (BOB-1) is equal to the fissionability at the beginning of the second cycle (BOB-2), the total worth of all HM components have remained the same throughout the integral cycle. Zero breeding gain is thus defined as: constant HM worth over an integral cycle.

In this thesis, each time worths are discussed, the term will describe 'macroscopic worths'. Each discussion of microscopic worths will emphasize 'microscopic'.

2.4.3 Microscopic worth of recycling vectors

As mentioned, both DU and MA are used for recycling purposes. The different isotopic fractions of both vectors have been shown in Chaper 1. When the isotopic fractions and the microscopic cross sections are known, the microscopic worth of recycling vectors can be determined:

$$w_{DU} = \sum_{DU_i} fract_{DU_i} \sigma(BOB)_{DU_i}$$
$$w_{MA} = \sum_{MA_i} fract_{MA_i} \sigma(BOB)_{MA_i} \quad \textbf{2. 20}$$

The microscopic cross sections used to calculate the worth of the recycling vectors are determined at the BOB. These recycling worths can be used to compare the individual HM worths to the worths of recycling vectors. To calculate the effect of adding DU or MA to the existing reactor fuel, the microscopic worth of the recycling vector is used in combination with the amount added. The atomic density of the reactor fuel is kept the same for multiple irradiations.

2.5 Modelling of Decay Heat Production

Throughout reactor operation, fission- and decay power combined result in the total thermal power rating of the reactor. Decay power is only a small fraction of the total nominal power. After the fission reaction has stopped, the spontaneous decay of fission products and minor actinides continues to produce residual heat, so called decay heat. Under normal circumstances, cooling systems can easily remove the Decay Heat Production (DHP). However, when reactor thermalhydraulic systems malfunction, the power produced by DHP is sufficient to melt the fuel elements in a reactor core. An accurate knowledge of the DHP is necessary to design adequate back-up systems to mitigate such risks.

To estimate DHP for different reactor fuel compositions, standards have been created for thermal reactors that allow for an accurate prediction of DHP for numerous hours and days after reactor shutdown. Each standard has a set of parameters linked to multiple time dependent decreasing exponential terms that accurately describe the decreasing DHP curve. The ANS model, for example, assumes that all fission products of the four fissionable nuclides can be grouped into 23 groups, each decaying with their own time constant λ_k with an amplitude a_k.[25]

Current standards are accurate for irradiated thermal reactor fuel. These standards focus solely on the DHP by fission products from major fissionable nuclides. A number of the more exotic fissionable nuclides that fission in the GCFR (such as ^{242}Am) are not taken into account. Accurate calculations of the decay heat curves of innovative fuel compositions must be calculated by solving coupled nuclear decay equations using ORIGEN-S. The coupled decay equations are equal to the depletion equations for zero flux.

Although a standard for fast reactors does not yet exist, the model which is used for the ANS standard - multiple time-dependent decreasing exponential terms - is applicable to modelling DHP curves in fast reactors. The fission products in spent fast reactor fuel decay in the same manner as fission products in spent thermal reactor fuel. The diversity of HM atoms that fission are cause for a different distribution of decaying fission products. In the research performed, the thermal reactor standard ANS5.1 has been compared with the calculated DHP.

2.5.1 Short review of the ANS model

The ANS5.1 standard prescribes DHP for fissionable nuclides present in LWR's (^{235}U, ^{238}U, ^{239}Pu, ^{241}Pu)[26]. The standard is based upon the evaluated nuclear data file (ENDF/B-IV). It gives a bandwidth of uncertainty for the different reactor operating histories for different decay times. The standard does not prescribe the spatial distribution of the energy deposition, nor does it describe DHP from activation products in reactor materials. It is assumed that, during operation, the energy release per fission is independent of time.

The ANS model is described by the following equation:

$$f_i(t) = (\sum_{k=1}^{K} a_k \exp(-\lambda_k t))_i$$

$f_i(t)$ = decay heat power after fission pulse

from fissionable nuclide$_i$ [MeV / sec / fission]

a_k = amplitudal constant [MeV / sec / fission] **2. 21**

λ_k = decay constant [1/sec]

t = decay time [s]

K = number of exponential terms [-] : 23 exponents in ANS

Total DHP curves are calculated by weighing the estimated contributions of the different fissioning isotopes to the power production of the reactor. In thermal reactors, ^{235}U and ^{239}Pu would have the greatest weighting factors. Total decay power is a weighted sum of the individual contributions of the fission products of the fissionable isotopes:

$$f(t) = \sum_i f_i(t) \quad \textbf{2. 22}$$

In figure 8, the different isotopic functions of the ANS model are shown. The fission products of ^{235}U and ^{238}U are significantly bigger contributors to DHP compared to the fission products of ^{239}Pu and ^{241}Pu during the first 1000 seconds after reactor shutdown. The difference is greatest during the first 10 seconds after shutdown. As the heat produced during these first seconds often determines the limiting transients, the lower decay heat production of ^{239}Pu and ^{241}Pu can be seen as an advantage of using plutonium as a fuel.

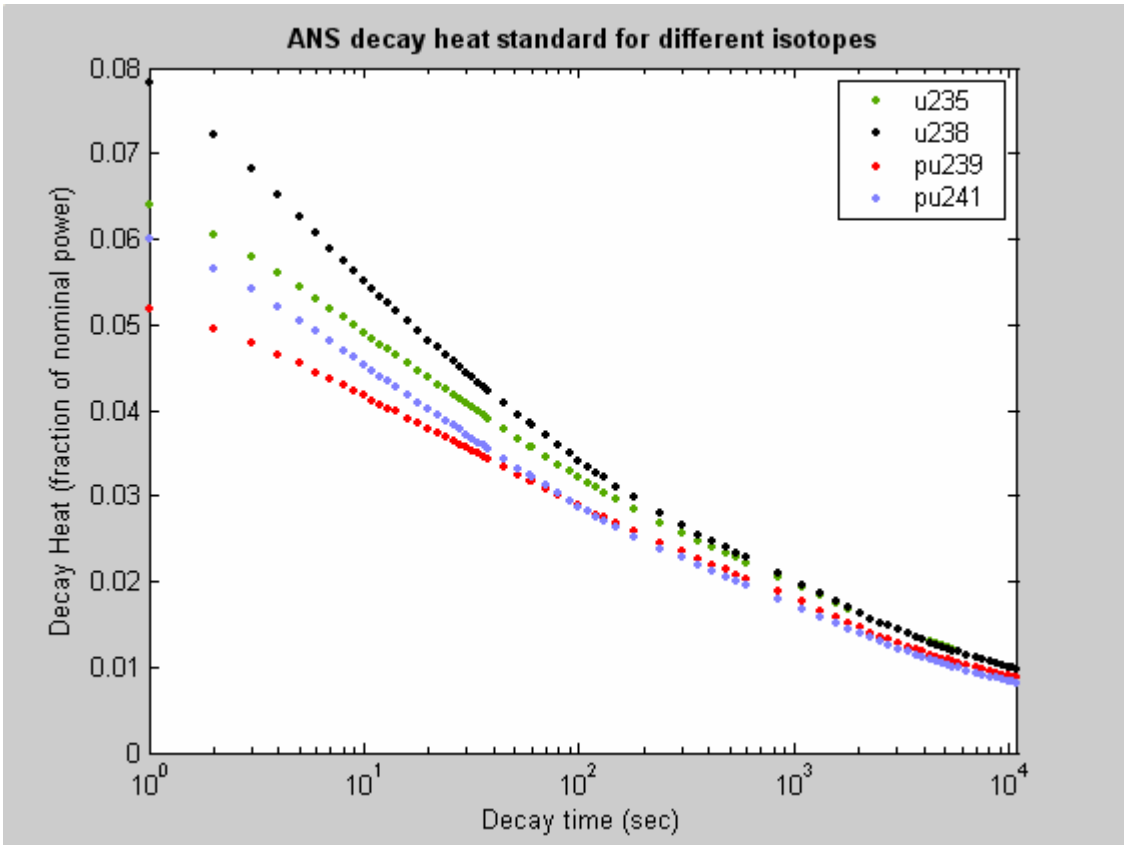

Figure 8: During the first minute, there are significant differences in the contribution of the fission products of different isotopes to the DHP.

In Chapter 5, an estimate of the DHP of the GCFR using the ANS model is made using a theoretical 'power mixture' of fissioning isotopes of 20% fast fissions in ^{238}U, 40% fissions in ^{239}Pu and 40% fissions in ^{241}Pu.[27] The weighted sum of different isotopic contributions will be compared to the actual DHP. Parameters for an exponential model describing the DHP curves of the GCFR are proposed for different fuel compositions.

3 Mixing Minor Actinides for single cycle irradiations

The GCFR is designed to have zero breeding gain for a (U,Pu)C fuel. In this chapter, the effect of the addition of Minor Actinides (MA) to the reactor fuel is investigated, including the effect on reactivity and on safety parameters. Fissionability as a measure for reactivity has been introduced in the previous chapter. It is used to analyze the changing composition and isotopic cross sections of the reactor. The changing microscopic worths of different components of the fuel are given.

It is found that addition of MA to the fuel decreases the reactivity swing during irradiation. The safety parameters of the GCFR are comparable with earlier fast reactors. The amount of MA in the reactor decreases during irradiation. The GCFR thus has the additional capacity to burn a limited amount of MA. The breakdown of the change of HM worth into components shows that the change of MA worth dominates. The fission gas that is produced is calculated for different compositions.

3.1 Neutronic calculations for a single irradiation

The depletion- and transport equation are solved for the GCFR core with different MA fuel compositions. The time-dependent percentage of MA in the core due to isotopic depletion is presented. Furthermore, the effect of adding MA to the reactor fuel on the reactivity swing and the safety parameters are studied.

3.1.1 Burning MA in the GCFR

Although the breeding gain is close to zero, the densities of both fissile and fertile isotopes change significantly during irradiation. The total burnup of HM is around 9.5% FIMA. Results in table 5 show that the following burnups per isotope (for the fuel composition with 5% MA) relative to Beginning of Burnup (BOB) are reached.

5% MA composition	Density change	Average atom% in fuel	Contribution to burnup
U-238	11%	78%	8.40%
Pu-239	-1%	9%	-0.10%
Pu-240	-10%	4%	-0.40%
Pu-241	38%	1%	0.40%
Pu-242	-4%	1%	-0.10%
Am-241	45%	3%	1.20%
Total burnup			**9.40%**

Table 5: The average isotopic percentage in the fuel and the burnup of each significant isotope from BOB to EOB are shown. These nuclides make-up almost 97% of the total fuel. A negative density change indicates increasing atomic density. For example, the atomic density of ^{240}Pu increases during irradiation. Isotopes making up less than 1% of the total fuel throughout the irradiation have not been taken into consideration.

As has been mentioned in Chapter 1, fast neutrons above 1 MeV have a greater probability upon collision with a nuclide to cause fission rather than be captured. When irradiating the fuel containing no initial MA, it was seen that the total MA percentage during irradiation remained below 2% of the total fuel. For this reason, it was decided to investigate whether it would be possible to destroy extra MA.

The representative MA vector of reprocessed fuel of LWR's as predicted for 2016 has been used in this research. The isotopic composition of the MA vector has been displayed in Chapter 1. After irradiation of the fuel mixture originally containing 5% MA, only 3.8% remains at EOB (Δ=1.2%). Thus, more than 260 kg's of MA are destroyed. For the 10% MA mixture, 6.7% remains at EOB (Δ=3.3% - 650 kg destroyed). If mixing higher percentages of MA (~10%) is possible, the potential for MA burning would grow.[28]

3.2 Reduced reactivity swing with added MA

In thermal reactors, most of the excess reactivity that is present at the beginning-of-burnup is needed to compensate for the decreasing reactivity during irradiation due to fissile fuel depletion and build-up of fission products. In reactors with near zero breeding gain, the increase or decrease in the amount of fissile fuel is limited. In addition, the capture cross sections of fission products are smaller in the fast spectrum compared to a thermal spectrum (e.g. ^{135}Xe, thermal: >100.000 barns, fast: <1 barn). Thus, the reactivity swing is expected to be smaller in a fast reactor.

In most reactor types, excess reactivity at the beginning-of-burnup (BOB) is compensated by absorption in standard control rods or using burnable poisons (see section 3.4). In this case, the neutrons do not contribute to breeding of new fissile fuel. It will be seen that MA make more effective use of the excess fission neutrons than the conventional absorbers.

The composition of MA is initially dominated by ^{237}Np and ^{241}Am. These isotopes have a large absorption cross section. After neutron capture, these isotopes transmute to fissile materials: ^{237}Np to ^{238}Pu and ^{241}Am to ^{242}Am. When instead of absorption in control rods, neutrons are absorbed in ^{237}Np and ^{241}Am and thus transmuted to fissile ^{238}Pu and ^{242}Am, the added MA behave similarly to other fertile fuels and increases the breeding potential of the fuel.

Using the BURN1D code, the reactivity is determined for the different fuel compositions (see figure 9). The reactivity swing – defined as the difference of the reactivity between BOB and end-of-burnup (EOB) – decreases with addition of MA. An advantage of the smaller swing includes the smaller worth of control rods necessary for core reactivity control. Transmutation of MA, for an initial compositions of 6% MA, results in an increase of the reactivity during irradiation.

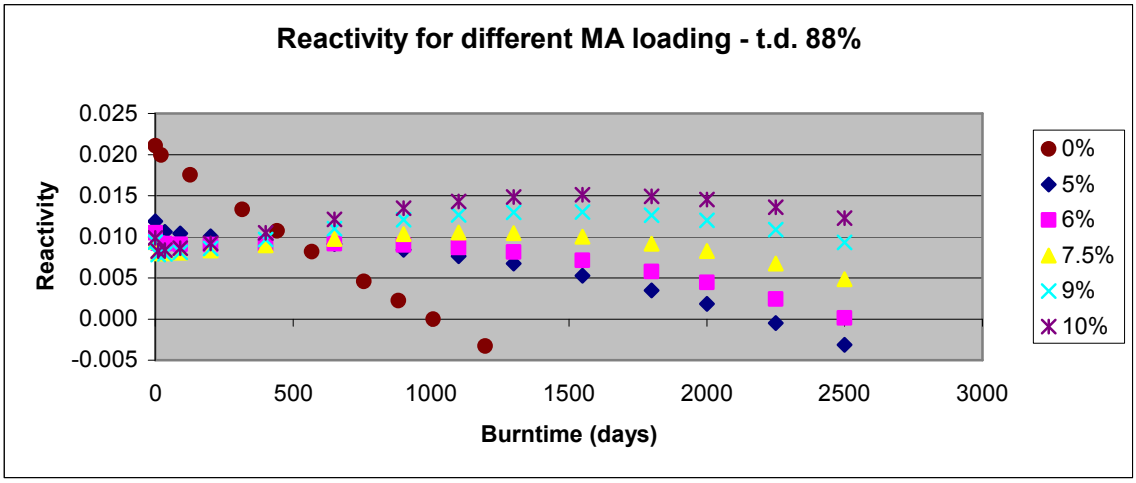

Figure 9: The reactivity for different MA loadings. The reactivity swing decreases for increased MA loading. For a MA loading above 6%, the reactivity increases during the irradiation - a positive reactivity swing.

The possible duration of the irradiation is lengthened due to the improved breeding potential of the GCFR mixed with MA.[29] As better use is made of the reactor fuel, the cycle (at full power) can be lengthened from 1000 days to 2500 days (see figure 9, compare the x-intercept for the 0% and the 6% MA curves). This increases burnup of the fuel from less than 40 MWd / kg to 90 MWd / kg. A detailed analysis and explanation of the shape of the reactivity curve during irradiation is included in section 3.4.

3.3 Effect of MA on safety parameters

The advantages of using extra MA in the fuel, namely increased burnup and decreased reactivity swing, are attractive. This section focuses upon the safety characteristics of the reactor fuel. It is of vital importance that the safety parameters do not deteriorate unacceptably. As mentioned in section 2.2.1, the fission products of MA produce less delayed neutrons than the fission products of the uranium it replaces. The resonance broadening which occurs during a temperature excursion is on average smaller for fuel with MA mixing.

3.3.1 β-effective

The VAREX code [30] calculates the β_{eff} of the fuel mixture. Addition of MA to the fuel decreases β_{eff}, shortens the stable reactor period, and thus negatively influences reactor controllability. In figure 10, it is shown that the β_{eff} at BOB decreases from 0.40% to 0.34% when increasing the MA loading from 0% to 10%. During burnup, the β_{eff} decreases on average by 0.02% (relative change up to 6%).

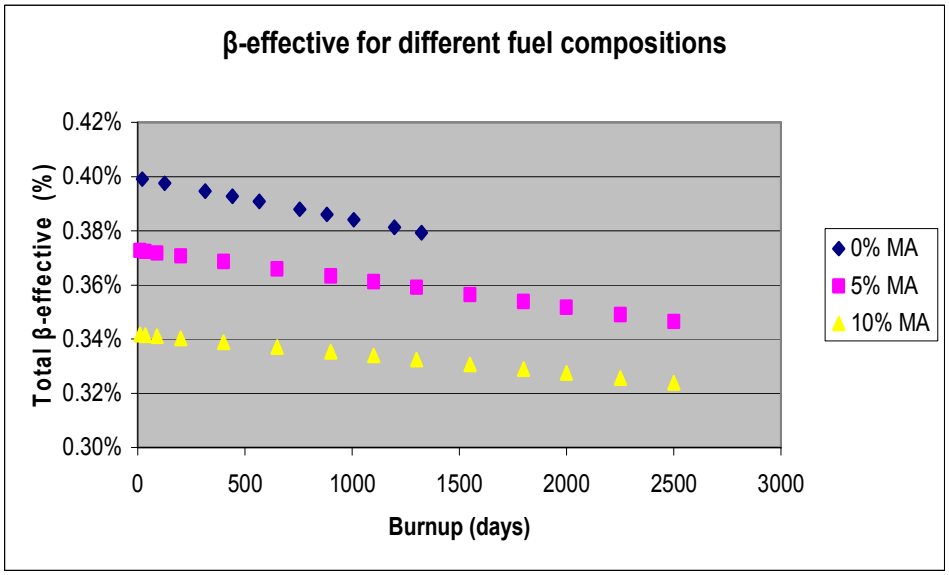

Figure 10: **Decreasing β-effective for higher MA loadings. The decrease is ~ 15% when the loading of MA is increased from 0% to 10%.**

As can be seen in table 6 below, the β_{eff} of the GCFR is comparable to the β_{eff} of sodium cooled fast reactors (MONJU, SUPERPHENIX) that have been built in the past. However, the β_{eff} is at the lower end of the range.

Reactor name	Country	β_{eff}
SEFOR	UK	0.32%
PFR	UK	0.34%
MONJU	Japan	0.36%
SUPERPHENIX	France	0.40%
JOYO	Japan	0.45%
FERMI	USA	0.70%

Table 6: **β-effective of existing and past fast reactor designs**

In the GCFR, the fission products of several fissionable nuclides contribute to the delayed neutron source. The total delayed neutron source is the sum of all isotopic contributions. As shown in figure 11, the contribution to total β_{eff} is dominated by the uranium and plutonium elements present in the reactor fuel (96% of β_{eff}). The isotopes ^{238}U, ^{239}Pu and ^{241}Pu are the greatest contributors to the β_{eff} of the fuel.

The contributions of these isotopes compared to other uranium and plutonium isotopes is shown in Table 7. When mixing MA to the fuel and replacing uranium, the β_{eff} decreases. As mentioned in section 2.2, as a rule of thumb isotopes with a higher number of protons in the nucleus (Z) have smaller β_i's. The MA contribute less to β_{eff} than the ^{238}U which they replace. Furthermore, due to the changing composition of the fissioning fuel during operation the β_{eff} decreases. This shows that the distribution of the fissions in the fuel changes slightly from fissions in HM with a relatively high β_{eff} to a lower β_{eff}.

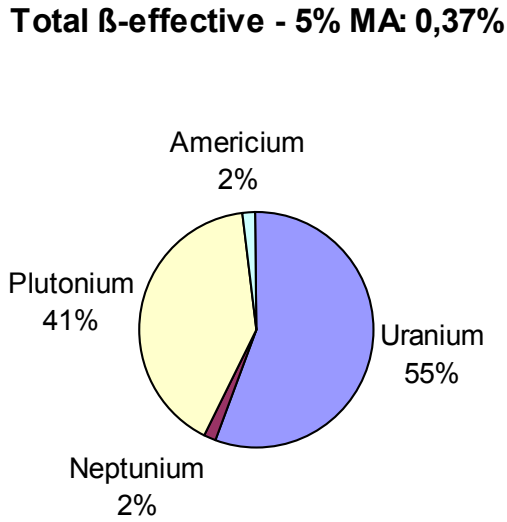

Figure 11: β_{eff} after 35 days burnup for 5% MA mixed in fuel. The distribution of contributions to β_{eff} does not change significantly during burnup.

Isotopic contribution to β_{eff}	
Uranium	
U-235	7%
U-238	93%
Plutonium	
Pu-238	2%
Pu-239	57%
Pu-240	9%
Pu-241	28%
Pu-242	4%

Table 7: Isotopic contribution of both uranium and plutonium to the β_{eff}. The uranium and plutonium are the greatest contributors to the β_{eff}.

The time-dependent β_{eff} can now be used to calculate the reactivity ($). In figure 12, the reactivity of the reactor fuel without MA and at a lower theoretical density is compared with the fuel composition with 5% and 10% MA. Once again, the reactivity swing, defined as the difference in reactivity between BOB and EOB, is smaller for the fuel with MA. For a reactor with 5% MA, the reactivity swing is only only $3. Increasing the MA to 10% decreases the reactivity swing to less than $3. Without MA, the reactivity swing is $6 and the feasible irradiation time is much shorter.

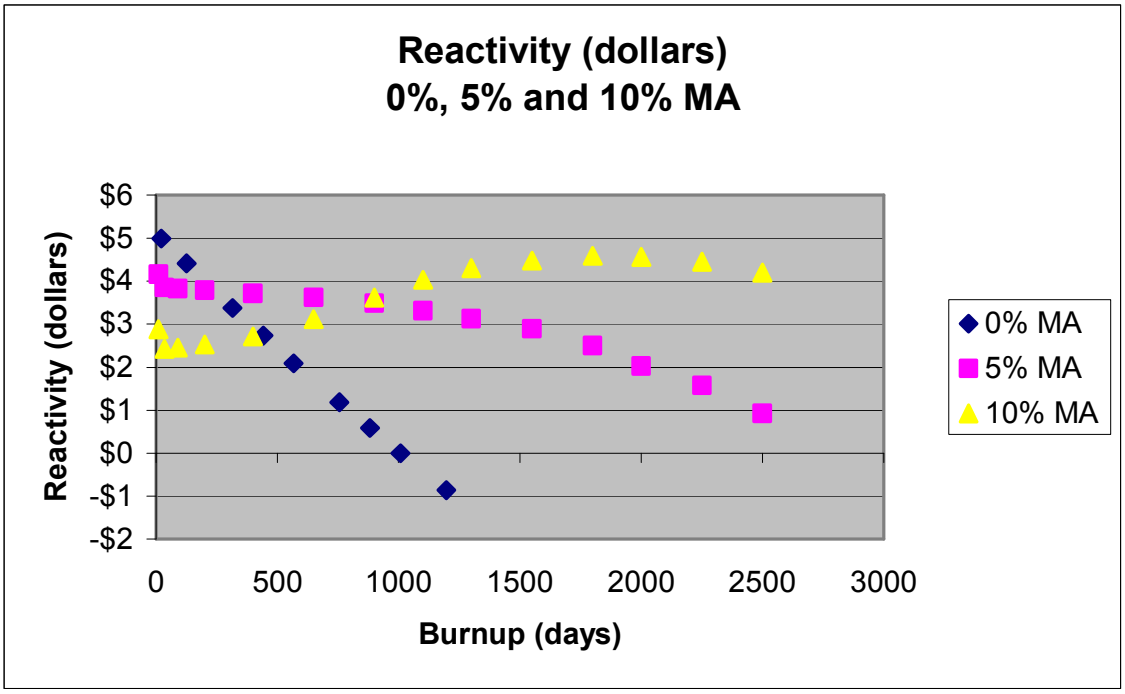

Figure 12: **Reducing the reactivity swing by adding MA to the fuel. The net reactivity incrases by $1 during the irradiation period for the 10% MA mixture. The reference fuel is at 85% t.d., while the other mixtures are at 88% t.d. The slope of the 0% MA fuel with 88% t.d. is less negative (reactivity ~ $0 at 1300 days for 88% t.d. and $0 at 1000 days for 85% t.d.).**

Although it looks like the reactivity loss for the fuel without MA is large, compared to modern PWR reactors it is still small. For example, the reactivity swing of an EPR using MOx fuel has been calculated to be around $24 when it is irradiated to 4% FIMA over three years.[31] The reactivity swing is small compared to thermal reactors due to the near zero breeding gain in the reactor.

3.3.2 Void- and Fuel Temperature Coefficient

Research performed on the void coefficient of the GCFR has shown that it is positive. The void coefficients for the fuel without initial MA at 88% t.d. ranges between 4.1 – 4.4 pcm / bar.

Void coefficient - pcm / bar		
MA%	Average	Range
0%	4.23	4.1 to 4.4
5%	5.29	5.1 to 5.5
10%	6.41	6.3 to 6.5

Table 8: Void coefficient for different MA mixtures, 88% t.d. The coefficient increases slightly during burnup. The void coefficient of the 85% t.d. – 0% MA – equals 3.4 pcm / bar (relative to 4.2 for the 88% t.d.). Thus, it is seen that the void coefficient increases with t.d.

To investigate whether voiding of the coolant at the end of burnup will cause a greater reactivity excursion, the helium pressure was set to different fractions (1%-50%) of nominal pressure of 70 bar.

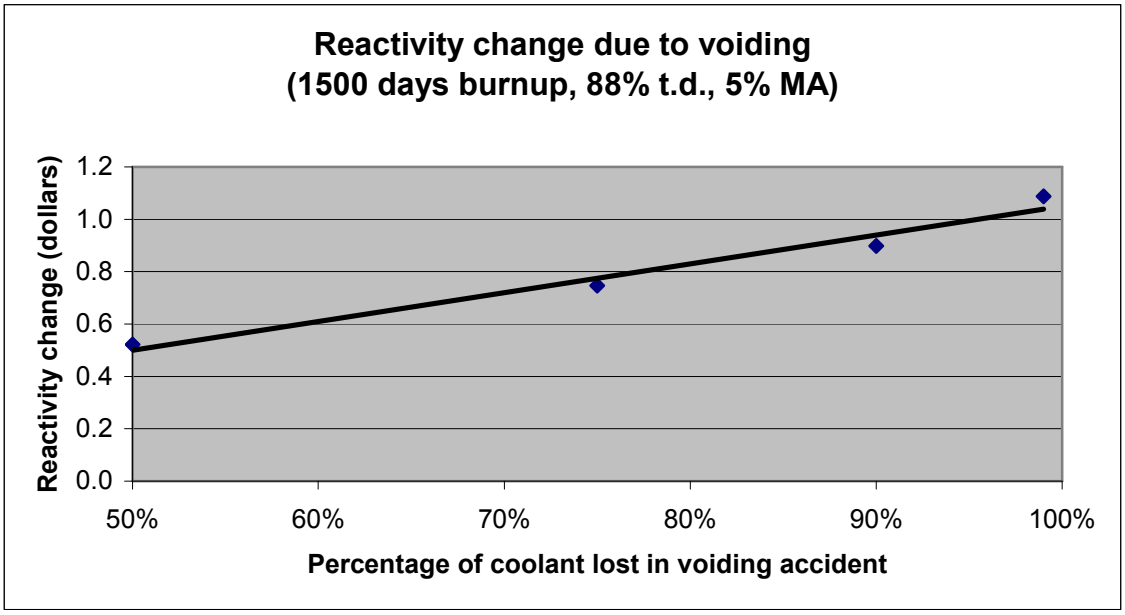

Figure 13: As the percentage of the void increases from 50% to 100%, the reactivity change increases from $0.5 to $1.0.

As is expected, the reactivity effect of voiding increases when greater amounts of coolant is lost. (see figure 13) However, the effect is limited to $0.50 for 50% of voiding. The reactivity change is around $1.00 for maximum coolant losses.

Fuel temperature coefficient (FTC)
In the calculations of the fuel temperature coefficient, the fuel was increased by 100 K. The change in the multiplication factor is normalized with the k-effective calculated at the reference temperature and divided by the total change in temperature.

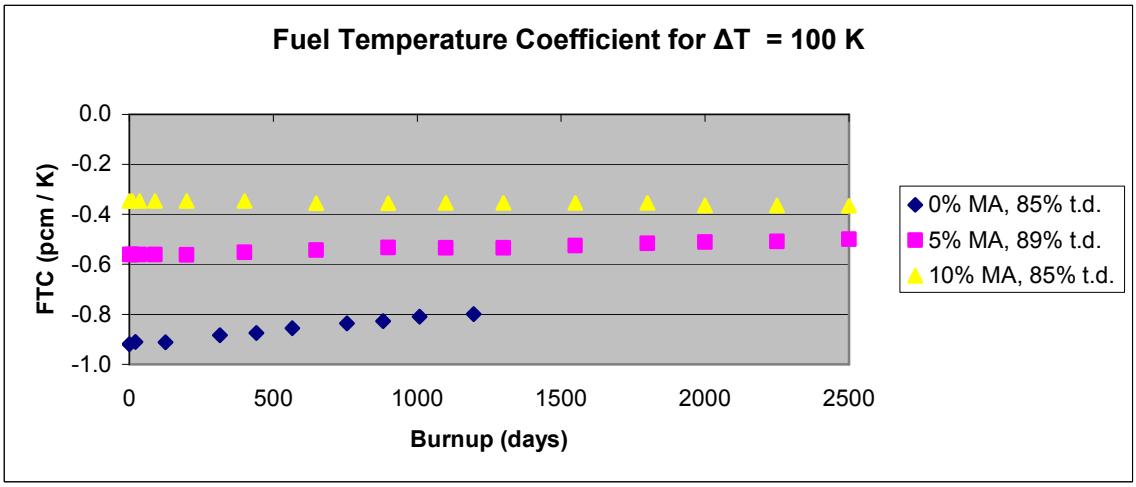

Figure 14: The negative reactivity Doppler feedback decreases with increasing MA contents.

In the GCFR, the reactivity feedback upon a 100 K temperature increase is negative throughout the irradiation (see figure 14). The negative feedback decreases with increasing MA in the fuel. This is due to the extra absorption of ^{237}Np and ^{241}Am, decreasing the flux in the resonance energy range, and thus decreasing resonance absorption.[32] Adding MA to the fuel hardens the spectrum.

MA%	pcm / K	β	Δρ / 100 K
0%	-0.91 to -0.80	~0.39%	-$0.21
5%	-0.56 to -0.50	~0.37%	-$0.15
10%	-0.37 to -0.34	~0.33%	-$0.10

Table 9: Conversion pcm / K to Δρ / 100 K

In the table 9, the FTC [pcm / K] is expressed as an equivalent reactivity change per 100 K [$]. A FTC of -0.34 pcm / K is equivalent to a reactivity change of $0.10 afte a fuel temperature step change of 100 K. The negativity reactivity decreases by ~50% when the MA percentage increases from 0% to 10%.

3.4 Analysis of changing fissionability during irradiation

The goal of the time-dependent analysis of isotopic worths is to explain the reactivity changes during burnup of the GCFR for different loadings of MA. The analysis is broken down into different components allowing for specification of categories of isotopes. As was shown, for higher percentages of MA, the reactivity of the reactor increases during irradiation.

In the research performed, the focus has been on the fuel composition with a loading of 5% MA. It will be shown that the fuel composition with a higher MA loading (e.g. 10% MA) does not allow for zero breeding gain given the assumptions that reprocessing losses can be disregarded and the theoretical density is kept the same.

The use of burnable poisons is an example of a technique in thermal reactor cores to limit the reactivity swing during burnup. Burnable poisons have a large absorption cross section. The resulting isotope, after an absorption of a neutron, often has a much smaller cross section. Thus, the effect is to limit reactivity at the beginning of an irradiation when the fissile concentration is highest and the fission product concentration is lowest. As the concentration of the poison decreases, so does its effect on the reactivity. Burnable poisons limit the negative reactivity that must be introduced by control rods to achieve a critical reactor.

A positive reactivity swing could indicate that specific isotopes become fissile after a capture. As the effect of fission products on the reactivity of fast reactors is limited, the reactivity can increase. The research confirms that MA initially capture neutrons, after which the resultant products are fissile.

In this section, the microscopic and macroscopic worths are analyzed. The model of isotopic worths, introduced in the previous chapter, is implemented. The analysis of changing worths of the different components of the reactor fuel allows for the explanation of the reactivity changes. In addition, the fissionability (total worth) of the reactor is given for different fuel compositions.

3.4.1 Changing microscopic worth of isotopes during irradiation

As presented in the previous chapter, the microscopic worth of each isotope is dependent on the total number of neutrons per fission, the one-group microscopic fission cross section, and the one-group microscopic absorption cross section. As the cross section of an isotope is dependent on the fuel composition and the resultant neutron spectrum over the reactor, there are small changes of the microscopic worth during irradiation.

The microscopic worth one-group cross sections are calculated in each separate reactor zone. The individual absorption or fission cross section of the reactor has been calculated by weighing the cross sections with the zonal volume, and dividing by the total volume of the reactor. Each spatial zone is thus given an equal weight, regardless of its position in the reactor (e.g. centre vs. boundaries).

In figure 15, isotopes with a negative microscopic worth (^{238}U, ^{241}Am, ^{243}Am, ^{237}Np) are shown. It is important to note that the total microscopic worth of all isotopes decreases during irradiation.

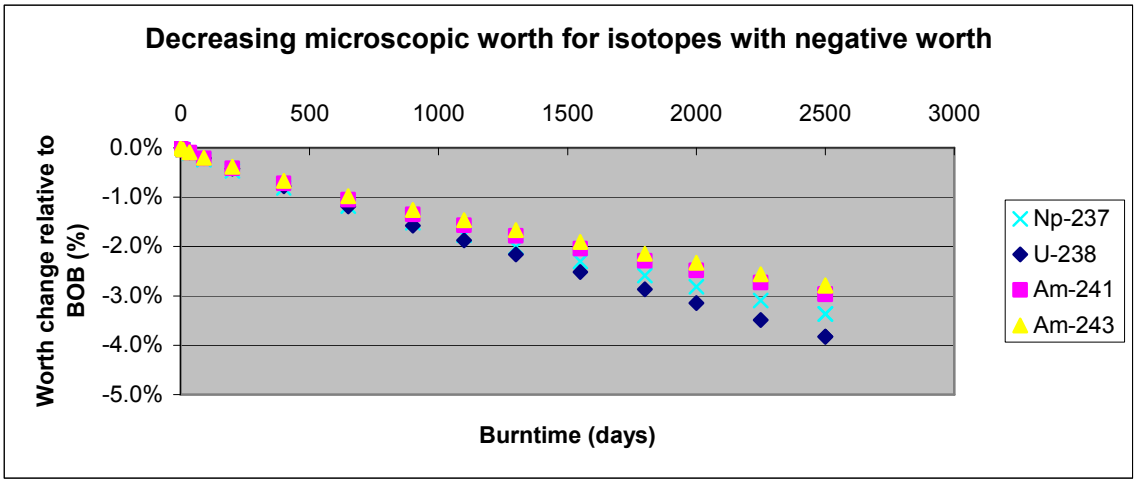

Figure 15: **Change of the microscopic worth of different isotopes during irradiation. All isotopes in the figure are negative contributors to the fuel worth. The analysis is performed for a mixture starting with 5% MA.**

Increasing the percentage of MA added to the fuel increases the negative change in the microscopic worth of the isotopes. As an example, the change of the worth of ^{238}U in a fuel with 5% and 10% MA relative to the worth at the BOB is shown in figure 16. The relative change of MA during irradiation increases for higher initial loading percentages (Δ=1.2% for 5% and Δ=3.3% for 10%). Spectrum changes would be expected to be greater (e.g. more MA results in a harder neutron spectrum), resulting in larger changes of the microscopic worth.

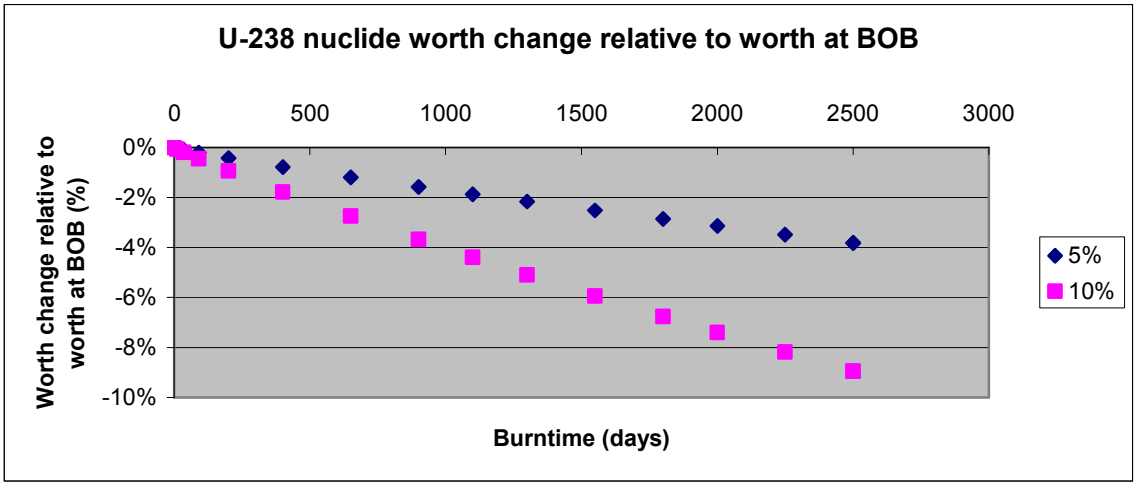

Figure 16: Comparison of the changing ^{238}U worth for mixtures with increasing MA composition.

The microscopic worth decreases because the fission term ($\nu\sigma_f$) decreases and the absorption term (σ_a) increases during irradiation. The microscopic fission term decreases because the spectrum becomes softer as MA are burnt.

The analysis of the different contributions to the microscopic worth ($\nu\sigma_f$ and σ_a) allows us to conclude the following:

- The individual cross sections change less during irradiation than would be expected from the figures. The microscopic absorption cross sections change is ~1.5%. The fission cross section is ~1%;
- Since $\nu\sigma_f$ decreases while σ_a increases, the changes are cumulative (worth = $\nu\sigma_f$ *minus* σ_a). The net microscopic worth of the isotope is smaller than the individual cross sections. The change of the microscopic worth is relatively 3% - 4% for the fuel composition with an initial MA loading of 5%.

3.4.2 Average microscopic worth of fuel vectors

In the numerical analysis of the fissionability of the reactor, the exact microscopic worth of each isotope at each step in the irradiation is used. For rough estimation of the fissionability, it is sufficient to use the average microscopic worth of each isotope. However, it will be shown that it is necessary to calculate these microscopic worths for each separate mixture.

In table 10 (next page), the average microscopic worths of isotopes that make up the natural Uranium, the Plutonium vector in the year 2016 (Pu-2016) and the Minor Actinide (MA) vectors have been displayed. Each worth has been weighted with the percentage of each isotope in the vector. The resultant weights of the natural Uranium, Pu-2016 and MA vectors are calculated.

$$\text{Microscopic vector worth} = \sum_i \text{atom}_i(\%) * \sigma_i \qquad \textbf{3. 1}$$

Isotope	Microworth	w%	Weight	Isotope	Microworth	w%	Weight
Natural U				**MA**			
U-235	2.33	0.70%	0.02				
U-238	-0.20	99.30%	-0.20	Np-237	-0.99	16.86%	-0.17
			-0.18	Am-241	-1.08	60.62%	-0.66
Pu-2016				Am-242	1.06	0.24%	0.00
Pu-238	2.04	2.70%	0.05	Am-243	-1.09	15.70%	-0.17
Pu-239	3.05	56.00%	1.71	Cm-242	1.36	0.02%	0.00
Pu-240	0.29	25.90%	0.08	Cm-243	8.03	0.07%	0.01
Pu-241	4.70	7.40%	0.35	Cm-244	0.64	5.14%	0.03
Pu-242	0.14	7.30%	0.01	Cm-245	6.91	1.26%	0.09
Am-241	-1.08	0.70%	-0.01	Cm-246	0.37	0.10%	0.00
			2.19				**-0.87**

Table 10: **Worths of the different isotopes that can be used in the recycling strategy. Microscopic 'cross sections' averaged for fuel composition with 5% MA over the entire irradiation cycle.**

Although ^{238}U has a small negative microscopic worth (-0.20) compared to the positive worth of ^{235}U (2.33), it dominates the worth of the general uranium vector. The plutonium isotopes ^{238}Pu, ^{239}Pu, and ^{241}Pu are progressively more fissile (2.04, 3.05 and 4.70). ^{241}Am and ^{243}Am contribute negatively while ^{242}Am contributes positively to the microscopic vector worth. ^{243}Cm and ^{245}Cm are the most fissile isotopes. Their atomic densities, however, are small.

3.4.3 Analysis of core fissionability

It was hypothesized that certain MA-isotopes initially act as absorbers (predominantly ^{237}Np, ^{241}Am, ^{243}Am). After undergoing transmutation they become fissionable fuel. This hypothesis is supported by figure 17 (next page) which shows the fissionability of the reactor for initial MA loadings relative to the fissionability of the 0% HM fuel at BOB.

The total macroscopic fissionability decreases over time for the 0% MA composition, while the fissionability increases for 10% MA. Where the fissionability of the fuel without MA decreases monotonously over 20% during irradiation, that of the 10% loading increases by 10% relative to its fissionability at BOB. Defining the fissionability swing in the same manner as the reactivity swing, it is thus seen that the fissionability swing is negative for 0% MA, and becomes positive for the 10% MA composition. As will be seen, in order to create a zero breeding gain for multiple integral cycles, it is favorable that the total fissionability of the reactor decreases during burnup.

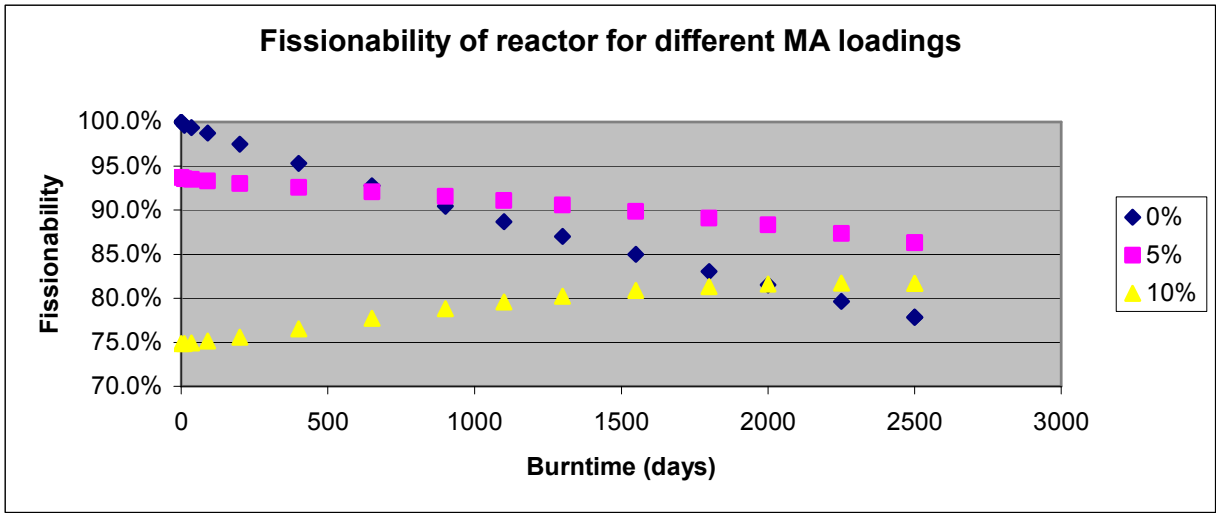

Figure 17: **The initial fissionability of the reactor decreases with increasing MA load. It is seen that the negative slope of the fissionability becomes less steep from 0% to 5%, and becomes positive for 10% MA loading. The fissionability increases as the fuel is irradiated, indicating that the original MA present in the fuel contribute positively when transmuted. Note that the fuel compositions all have a theoretical density of 88%. The negative slope of the 0% curve is smaller than in the figure 9.**

The initial fissionability of the reactor without MA loading is greater than the fissionability of the reactor initially loaded with 5% and 10%. However , for the 5% loading, the fissionability is greater than the 0% load after 900 days. For the 10% loading, the fissionability is greater than the 0% load after 2000 days.

Using the average microscopic worth of the different HM isotopes determined for the 5% mixture, the initial fissionability is calculated for different compositions (see table 11). The initial fissionability that is calculated is compared to the actual fissionability as was simulated for the different mixtures.

Composition	Estimated from figure	Calculated using average w_i's
84% U, 16% Pu	100%	100%
79% U, 16% Pu, 5% MA	94%	83%
74% U, 16% Pu, 5% MA	75%	65%

Table 11: **The fissionability for different fuel compositions relative to the fissionability of the reference composition (0% MA) is compared to the fissionability calculated using the average microscopic worths for the 5% MA mixture.**

Table 11 shows that it is incorrect to use the reference average microcopic worths for the 5% fuel composition to calculate the fissionability for other initial compositions of fuel. For example, where the fissionability of the 5% MA mixed fuel composition is only 6% less than the fuel composition with 0% MA (see figure 17), the average microscopic worths would predict it to be 17% less (see table 11). It must be concluded that for each mixture, separate calculations of the average microscopic worths are necessary to use the weights as a more accurate predictor of the initial fissionability of a reactor mixture.

3.5 Comparing reactivity and fissionability for single cycle burnup

Figure 18 compares fissionability to reactivity for the 5% MA composition. Linear interpolation of the reactivity curve results in a calculated zero reactivity during the first cycle at exactly 2200 days. The fissionability that was calculated at 2200 days was set to zero by subtracting the value of fissionability at 2200 days. The resulting curve for fissionability follows the curve for reactivity.

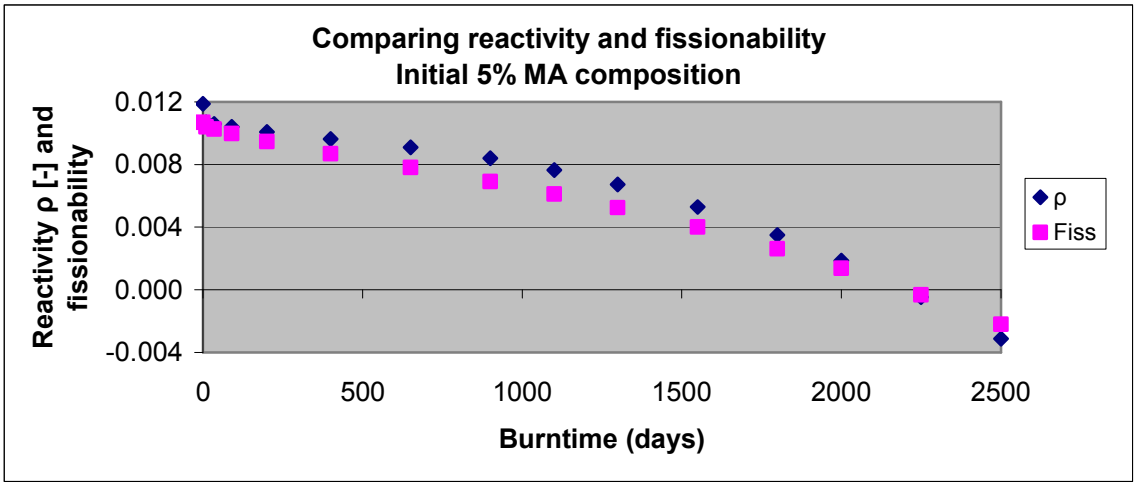

Figure 18: Comparing reactivity and fissionability for single cyle burnup for an initial fuel mixture of 5% MA and a theoretical density of 88%.

3.6 Breakdown of fissionability into different components

More insight is given when the different components of the total fissionability are analyzed. The fissionability of the reactor with 5% MA loading has been analyzed using the following components:

1) positive HM, negative HM, fission products effects
2) Minor Actinide (MA), uranium (U), and plutonium (Pu) effects, thus only looking at the HM.

The effects of structures on the changing fissionability is minimal. They are disregarded from the analysis.

3.6.1 Effects of positive- and negative HM, fission products

During irradiation, the fissionability of the reactor decreases. The figure below illustrates that the increasing concentration of the fission products is the major contributor to the decrease of the fissionability. As was mentioned, in general fission products in a fast spectrum are much less influential to the reactivity compared to a thermal spectrum. Due to the relatively small change in HM worth during the irradiation cycle (almost zero breeding gain), the contribution of the fission products to the changing fissionability is significant.

$$\Delta\text{fiss}\ (\%) = \frac{fiss(t) - fiss(BOB)}{fiss(BOB)} \qquad \textbf{3. 2}$$

A number of HM that have a negative microscopic worth (^{237}Np, ^{241}Am, ^{243}Am) decrease in concentration during irradiation. Throughout the burnup, these isotopes capture a neutron, and become fissionable fuel. In figure 19, this effect is seen by the increasing slope of the 'negative HM' curve. This indicates that the negative contribution to the worth becomes smaller during irradiation.

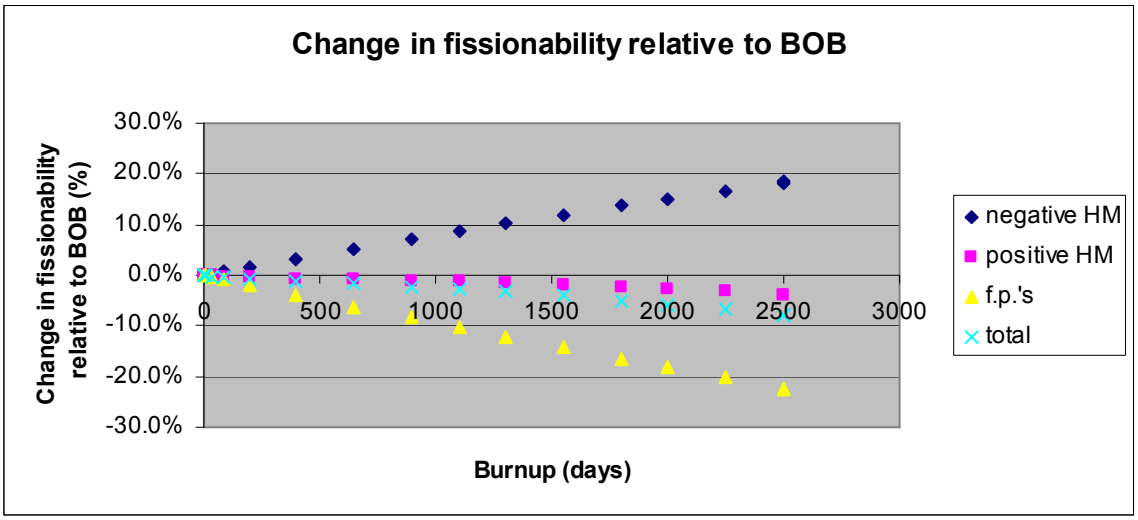

Figure 19: Changed total fissionabililty compared to BOB. As can be seen, the fission products contribute as much to decrease in fissionability as the decreasing concentration of the negative HM. The net effect is that the total fissionability decreases by 8% for the 5% MA mixture during irradiation.

The negative HM contributions to the macroscopic worth are dominated by the isotopes shown in table 12. The contributions of negative HM's with less than 1% effect throughout the irradiation have been ignored. The relative contribution of ^{238}U increases during irradiation. The increase of the ^{238}U contribution is caused by the burnup of the MA during the irradiation. For example, the small burnup of ^{238}U (~11%) compares to the greater burnup of ^{241}Am (~45%).

Nuclide	BOB	EOB
U-238	75%	82%
Np-237	4%	3%
Am-241	17%	11%
Am-243	4%	4%

Table 12: **Changing negative HM contributions over an irradiation**

A closer analysis of the positive HM shows that during irradiation the net contribution of the positive HM to the worth decreases by a small amount (see figure 19). The positive contributors to the worth consist of plutonium, higher actinides and fissile uranium. Specific absorbing MA that capture a neutron and become fissionable contribute to the 'positive HM' curve (see the effect of neutron capture in ^{237}Np on the ^{238}Pu curve – figure 20).

In figure 20, the change of the worth of plutonium isotopes is expressed as a percentage of the total fissionability.

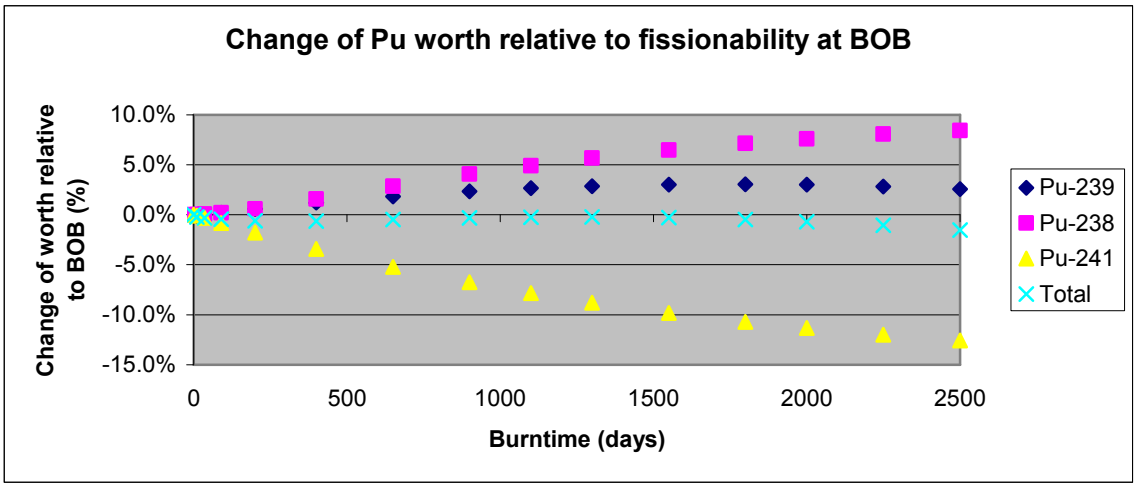

Figure 20: **Changing plutonium isotopes as a percentage of total fissionability. The Pu-worth decreases by 0.5%. The decrease of the Pu-worth would be much greater if ^{237}Np would not have been added. It can be clearly seen that ^{238}Pu is produced by neutron capture in ^{237}Np: its contribution to the total fissionability increases by 10%.**

Conclusions for the changing worth analyzed using the categories positive, negative and fission product contributions to the total HM worth for the fuel mixture originally consisting of 5% MA are:

- the decreasing negative worth (e.g. through MA capture in ^{237}Np) almost balances the increasing parasitic effect of the fission products;
- the positive worth changes slightly;
- the total worth (HM and f.p.'s) during burnup decreases.

3.6.2 Change in HM worth dominated by changing MA worth

The worths can also be analyzed using plutonium, uranium and minor actinides as separate categories. The total worth of the HM is equal to the sum of the worths of the uranium, plutonium and MA. In this section, it is shown that a small decrease of the Pu worth is compensated by a similarly small increase of the U worth. The largest change to the worth is due to the decrease of the MA concentration due to the burnup of MA.

The worth of the plutonium decreases by only 1.55% relative to the total initial fissionability. As the microscopic worth of the ^{238}U is negative, the macroscopic worth of uranium increases due to its burnup. As mentioned, the ^{235}U macroscopic worth decreases. The net result is an increase of the worth of uranium in the reactor (table 13).

The slight increase of uranium compensates the decrease of plutonium. Thus, the net change of the HM worth is dependent on the change of MA worth. Figure 21 shows the change of the worth of the HM during the burnup relative to the total HM worth at the BOB.

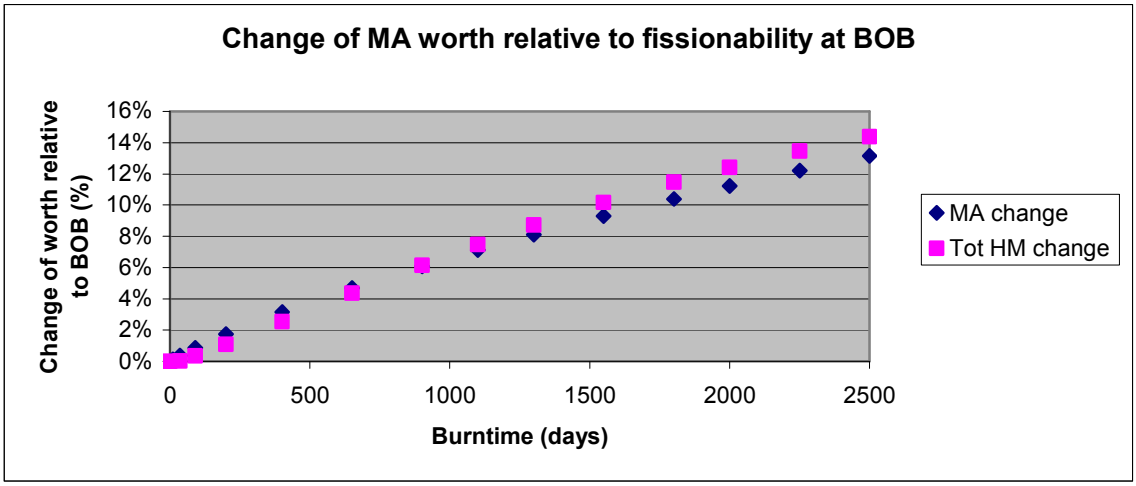

Figure 21: **The changing MA worth closely follows the changing HM worth. Both worths are expressed relative to the fissionability at BOB.**

The total HM worth increases by 14% relative to the initial total fissionability of HM. This increase is almost exclusively due to the increased contribution of MA to the fissionability. The change of the MA isotopic worth is predominantly due to the burnup of ^{241}Am. Other isotopes that contribute are ^{237}Np, ^{243}Am, and the Cm isotopes.

In table 13, a short summary is given of the effect of burnup of the HM isotopes relative to the total fissionability at BOB. The Minor Actinide worth increases, the uranium worth increases, and the plutonium worth decreases.

In the next chapter, recycling studies are performed for the fuel mixture originally containing 5% MA. It will be shown that the dependence on the changing MA worth continues when reprocessing and irradiating multiple times.

Change of worth during burnup							
MA		**Uranium**		**Plutonium**		**Total HM**	
Np-237	1.91%	U-235	-4.30%	Pu-238	8.43%	Uranium	2.45%
Am-241	8.66%	U-238	6.75%	Pu-239	2.58%	Plutonium	-1.55%
Am-243	1.23%			Pu-241	-12.56%	MA	13.16%
Cm	1.39%						
Total MA	13.16%	*Total U*	2.45%	*Total Pu*	-1.55%		14.06%

Table 13: Summarizing changes of macroscopic worth for different components of total HM worth as a percentage of total fissionability.

3.7 Fission gas build-up for different MA mixtures

Although we have studied the effect of addition of MA on the reactivity of the GCFR, there are other important effects related to fuel fabrication and fuel burnup. In this section, the build-up of fission gas in the fuel is studied.

It has been mentioned that an advantage of the gaps in the fuel (a theoretical density of fuel ~88%) is to limit the pressure increase during burnup. Throughout irradiation fisson gas is produced by α-decay of MA and by formation of gaseous fission products (xenon and krypton). During fuel storage (treated in detail in the next chapter), there is continued α-decay of MA.

In figure 22, the increasing atomic density of helium is shown during burnup and decay. The rate at which the atomic density increases is dependent on the original MA fraction present in the fuel. Higher MA fractions result in a faster increase of the atomic density.

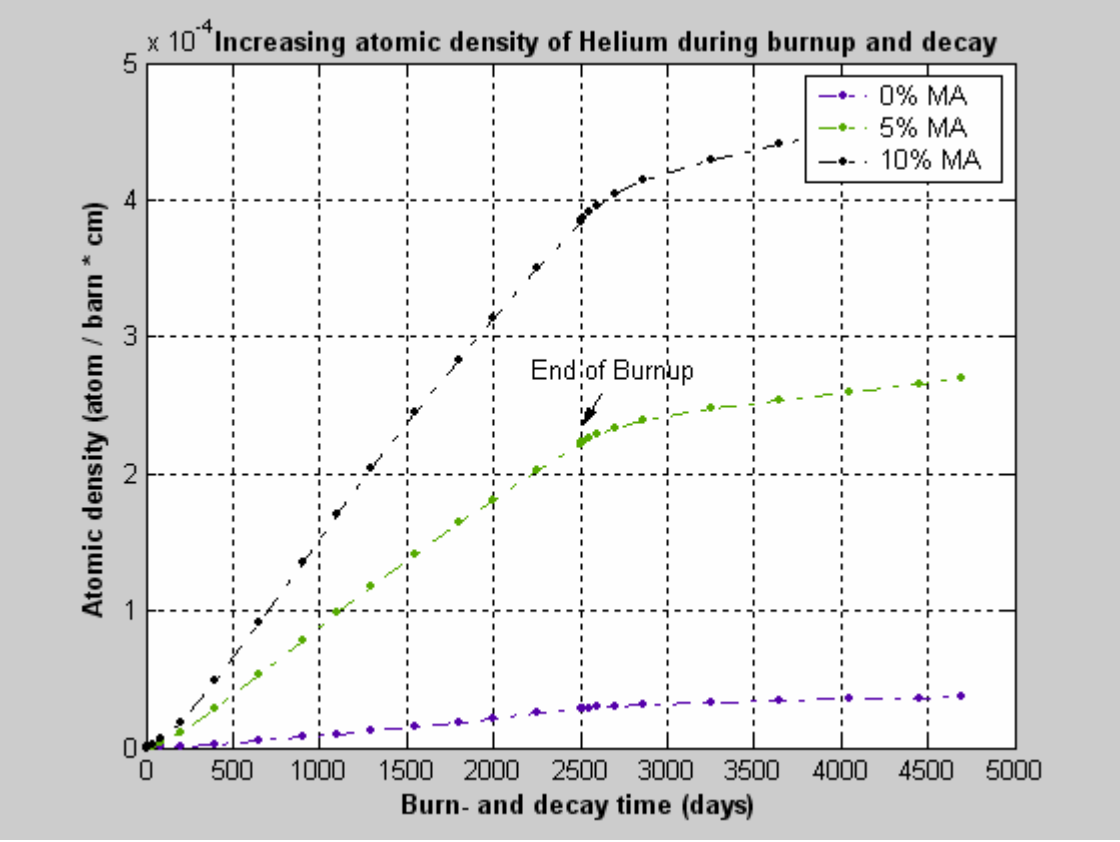

Figure 22: **Increasing atomic density of helium during burnup and decay (storage) of the fuel. The increase in atomic density is equal to a factor 3 for the 5% MA mixture relative to the reference fuel without MA, and a factor 5 for the 10% MA mixture.**

As can also be seen, the rate of increase of atomic density is greater during burnup than during fuel storage. It can be concluded that the production, and consequent decay, of short-lived MA during burnup is larger than the constant decay of MA with longer life-times during storage. As the amount of MA in the fuel at EOB increases for higher original MA loadings, the slope during storage is greater for higher initial MA loadings.

The burnup of the fuel remains constant for different fuel compositions. Thus the atomic density of the gaseous f.p.'s remains almost the same. The slight changes with changing MA composition would be due to a changing production of gaseous f.p.'s when MA fission. With increasing MA loading, the total amount of xenon and krypton decreases relative to the total amount of gas production. Helium increases from 33% for the 0% MA mixture to 86% for the 10% MA mixture (both relative to the total fission gas including xenon and krypton - see table 14).

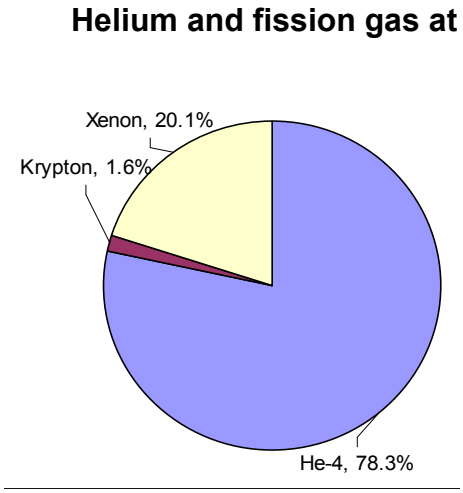

Figure 23: **Fraction of helium, krypton and xenon present after burnup of 2500 days and decay of 6 years for an initial composition of 5% MA.**

Effect of increasing MA on He production		
	Helium (% of total)	Factor increase
0% MA	33.1%	1.0
5% MA	78.3%	3.1
10% MA	86.2%	4.9

Table 14: **The atomic density of helium relative to the total amount of fission gas increases for higher MA loadings. The atomic density of He at EOD increases by a factor 5 when increasing MA from 0% to 10%.**

In first estimation, assuming that there is no increase in the leakage of fission gas during burnup and decay, the increase of atomic density would be directly proportional to the increase in the pressure of the fission gas in the fuel. Table 14 shows that the atomic density of He at EOD increases by a factor 5 when increasing MA from 0% to 10%. The decision to add increasing amounts of MA should, thus, not only be dependent upon criticality calculations, but also upon the strength of the carbide fuel at higher gas pressure.

3.8 Conclusions

- The GCFR has the potential to burn MA. Higher initial loadings result in greater MA burning potential. However, mixing MA negatively affects safety parameters by decreasing the delayed neutron fraction. In addition, β_{eff} decreases by ~ 6% over 2500 days irradiation.
- The initial excess positive reactivity necessary to achieve long periods of irradiation is small (around $4). For MA loading greater than 6%, the reactivity swing becomes positive. Addition of smaller amounts of MA already has a favorable effect, lengthening burnup potential in the fuel by extending the irradiation time (1300 days to 2500 days, from 40 MWd / kg to 90 MWd / kg). This is due to the transmutation of ^{237}Np to fissionable ^{238}Pu and ^{241}Am to fissionable ^{242}Am.
- Voiding of the coolant results in a positive reactivity introduction, while an increase in the fuel temperature by 100 K introduces negative feedback. Around $0.50 is inserted for 50% voiding. The fuel temperature coefficient is negative, ranging varying between -0.91 to -0.80 pcm / K for a mixture without MA, and -0.37 to -0.34 for an initial mix with 10% MA.
- Taking the sum of all isotopic average microscopic one-group cross sections multiplied by their atomic densities is equal to the total fissionability of the reactor. The change of the fissionability during irradiation closely follows the change of reactivity.
- The fissionability of the fuel decreases during irradiation for an initial 0% or 5% loading. Increasing the MA loading in the fuel decreases initial fissionability. The fissionability of compositions with higher MA loading (e.g. 10%) increases during burnup.
- The microscopic cross sections cannot be used to calculate the potential criticality of other reactor compositions since the absorption- and fission microscopic cross sections change significantly for different mixtures.
- The total change in fissionability is predominantly determined by the changing MA composition in the fuel during irradiation.
- Addition of MA significantly influences the build-up of fission gas during fuel burnup and storage. The production of helium through α-decay is much greater than the production of the fission gas krypton and xenon. Increasing the loading of MA to 10% could increase the internal pressure of the fission gas in the fuel by a factor 5.

4 Analysis of Breeding Gain for multiple cycles

After irradiation, the fast reactor fuel is temporarily stored before reprocessing the irradiated fuel and manufacturing the HM into new fuel plates. The storage prior to further handling leads to a decrease in decay heat production (see Chapter 5). The decay of short-lived fissile isotopes in the irradiated fuel causes the HM worth to decrease. To keep the same HM density at the start of irradiation, MA and DU are added to the fuel to replace the fission products. The previous chapter has shown that both MA and DU have a negative worth. As long as the removal of fission products compensates the negative worth added by the addition of MA and DU, it is possible to fully recycle the HM fuel for multiple cycle irradiation, thus closing the fuel cycle.

In this chapter, the effects on the HM worth of density changes during decay, reprocessing, recycling and fuel fabrication are presented. Different recycling strategies and the potential for nuclear waste reduction are studied for multiple cycle irradiation.

4.1 HM worth during fuel decay, reprocessing and recycling

In the research performed, a six year interval is taken between burnups to allow for a decrease in decay heat production, reprocessing and reactor fuel fabrication. During these six years, short-lived HM isotopes fully decay.

When recycling with DU, the total worth of the HM fuel increases from End of Decay (EOD) to the beginning of the next irradiation since removing the fission products during the reprocessing step more than compensates the decrease of HM worth during decay and the addition of DU during recycling. Table 15 displays these changes for the different contributions to the fissionability for the following three phenomena:

1) Decay: decrease in HM worth due to ^{241}Pu -> ^{241}Am decay;
2) Reprocessing: increasing worth due to removal of fission products;
3) Recycling: decreasing worth due to addition of DU to keep the fuel at the same HM density.

Component	BOB	EOB	EOD[1]	Reprocessing[2]	Recycling – Manufacturing[3]
Negative HM	0.0%	18.4%	17.2%	17.2%	9.7%
Positive HM	0.0%	-4.0%	-9.6%	-9.6%	-9.4%
Fission Products	0.0%	-22.3%	-22.3%	0.0%	0.0%
Total worth	*0.0%*	*-7.9%*	*-13.3%*	*9.0%*	*0.3%*

Table 15: **Change in worth of HM during burnup, decay, reprocessing and fuel manufacturing. The changes are given relative to the fissionability at BOB. For example, the fuel is 13.3% less fissionable at EOD compared to BOB. The numbers [1], [2] and [3] refer to the above three phenomena.**

Aspect [1]: The macroscopic worth of the HM decreases during decay. This is due to an increase in the atomic densities of the HM that have a negative influence on the worth (^{237}Np, ^{241}Am, ^{243}Am), and a decreases in the HM that have a positive influence on the worth (^{241}Pu).

As was indicated in chapter 3, the positive microscopic worth of ^{241}Pu (4.70) is much greater than the negative microscopic worth of ^{241}Am (-1.08). This explains the greater effect of ^{241}Pu decay compared to the increase of ^{241}Am. As can be seen in the table, the contribution of the negative HM (mainly ^{241}Am) decreases from 18.4% to 17.2%, while the contribution of positive HM

(mainly ^{241}Pu) decreases from -4.0% to -9.6%.Two smaller contributors to the decreasing positive worth are ^{242}Cm and ^{244}Cm.

Increasing or decreasing the decay time influences the amount of ^{241}Pu that decays to ^{241}Am. When comparing the worth after three years and six years decay time, it is seen that the macroscopic worth decreases to 3% and 6%, respectively, relative to the worth of the HM at EOB. The feasibility of shortening the storage times by half has not been studied. It can be concluded that the HM worth must increase during irradiation, to compensate for the decrease during storage, in order for a closed fuel cycle to be achieved.

Aspect [2]: Removing fission products compensates for the decreasing worth of HM during decay. Removal of the fission products increases the worth from -13.3% to 9.0% relative to the total fissionability at BOB. Thus, the reprocessed fuel has a higher total worth compared to BOB.

Aspect [3]: After reprocessing, additional DU and MA are added prior to fuel fabrication to keep the theoretical density of the fuel the same. The amount of HM added must be equal to the change in atomic density. The type of metals added (DU or MA) determines the net change of the worth of the HM from EOD to BOB. The exact change is also influenced by possible reprocessing losses (e.g. 1% of HM). In the table, the worth of the HM decreases from 9% to 0.3% relative to BOB. Thus, the total worth of the HM increases slightly from BOB-1 to BOB-2. With the new fuel, another cycle can be initiated.

4.2 Comparing reactivity, fissionability and safety parameters for multiple cycles

As shown in the previous chapter, the fissionability is a good measure for the reactivity. After equating reactivity and fissionability at 2200 days, figure 24 shows that the calculated fissionability becomes a less accurate measure for the reactivity for multiple cycles. The simple fit underestimates the actual reactivity in the second and third run.

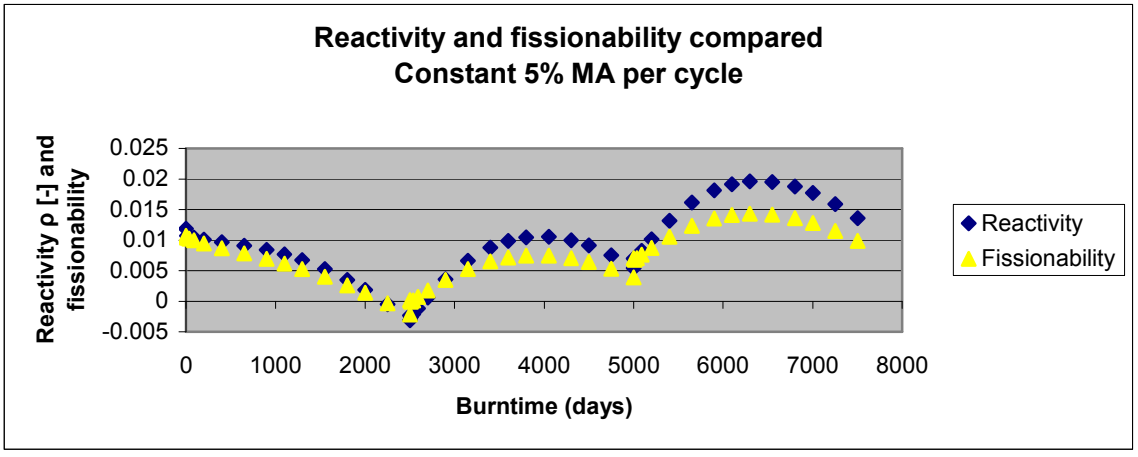

Figure 24: Comparison of reactivity and fissionability of reactor fuel during multiple irradiations.

The shape of the reactivity and fissionability curves for multiple cycle burnup is very similar. Thus, if the fissionability of the core at BOB and EOB are equal, it can be expected that the reactivity is equal as well.

The void- and fuel temperature coefficients have been calculated for the second and third cycle recycling with only depleted uranium or to keep the MA loading constant (see section 4.3). The results are shown in table 16. In both cases, the VC changes very little. When recycling to keep the MA loading constant, a slight change in the time-dependence of the VC is shown. While the VC increases during first cycle burnup, it decreases during the second cycle.

When recycling utilizing only depleted uranium, the FTC becomes more negative for multiple cycle burnup as the percentage of uranium in the fuel increases. The FTC does not change for multiple burnups with constant initial MA loadings.

FTC and VC analyzed for multiple cycles and different recycling strategies			
Decreasing FTC – DU only		Changing VC – Constant MA%	
Cycle	FTC (pcm / K) at BOB	Cycle	Range (pcm / bar)
1st	-0.56	1st	5.1 to 5.4
2nd	-0.69	2nd	5.7 to 5.6
3rd	-0.75		

Table 16: Changing void- and fuel temperature coefficients for multiple cycles.

4.3 Effect of different recycling strategies on reactivity and fissionability

As noted in Chapter 2, MA and DU are used as recycling vectors when manufacturing new fuel for a subsequent irradiation. The three recycling strategies that are studied are:

1) addition of DU only
2) addition of mixture of DU and MA, keeping MA% constant
3) addition of mixture of DU and MA, keeping total HM worth constant

In this section, the recycling vectors of DU and MA, as well as the simulated reactivity and the calculated fissionability for each of the three recycling strategies are shown. The reactivity and fissionability for the constant MA% strategy are compared. The different isotopic contributions to the reactor fissionability are discussed in detail.

The recycling vector of depleted uranium is shown in table 17. In addition, the microscopic worths of the MA vector and fission products are shown. The average microscopic worth of the fission products is calculated by dividing the total macroscopic worth of the fission products at EOB by their total nuclide density. The total fission product density is equal to twice the change of the HM density. Both the MA vector and the average fission product microscopic worth have a greater negative worth compared to the DU vector.

Isotope	Microworth	DU	Net
U-235	2.33	0.25%	0.01
U-238	-0.20	99.75%	-0.20
			-0.19
MA	(see Ch. 3)		-0.87
f .p.'s			-0.57

Table 17: Microscopic worth of depleted uranium (DU), MA and fission products (f.p.'s). The microscopic worth is the average of the microscopic worths for the 5% MA composition.

In the calculations that follow, it is assumed that there are no reprocessing losses. Comments on the effect of this assumption will be given in section 4.3.3.

4.3.1 Reactivity and fissionability for multiple cycles

In figure 25, the reactivity of the reactor is shown for the first cycle and two subsequent cycles for the three different recycling strategies. In general, it is seen that the reactivity for multiple irradiations for a closed cycle stays within a small reactivity bandwidth. When keeping the MA percentage constant, the reactivity increases per cycle. More reactivity control would be needed for the second and third cycle. The increase in reactivity is due to the increased worth of the MA and PU vectors during multiple burnups (see 4.3.2).

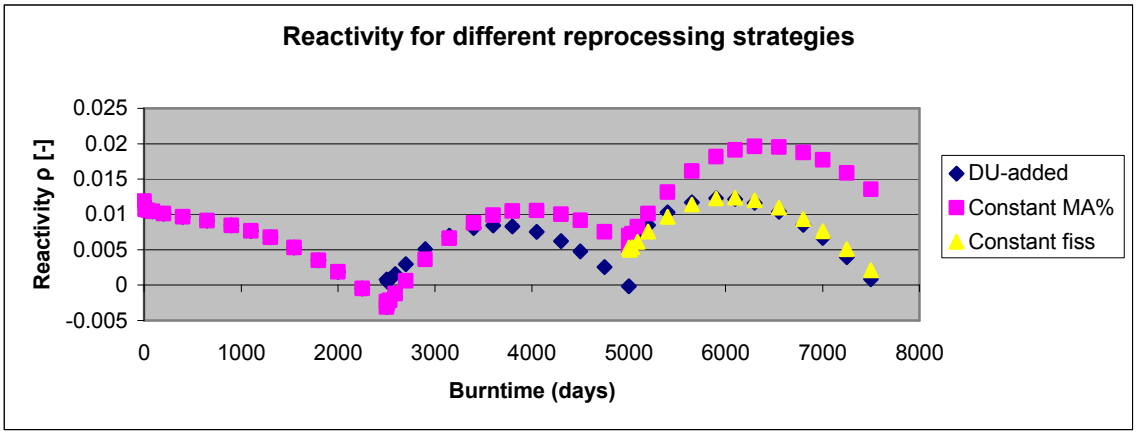

Figure 25: Reactivity as calculated with SCALE for three recycling scenarios.

Recycling with DU displays the best 'closed fuel cycle' reactivity pattern, as the reactivity for multiple cycles changes little. The above results favor recycling with DU.

The calculated fissionability is shown in figure 26. In general, the fissionability of the reactor fuel during multiple irradiations stays within a bandwidth of 15% of the initial fissionability.

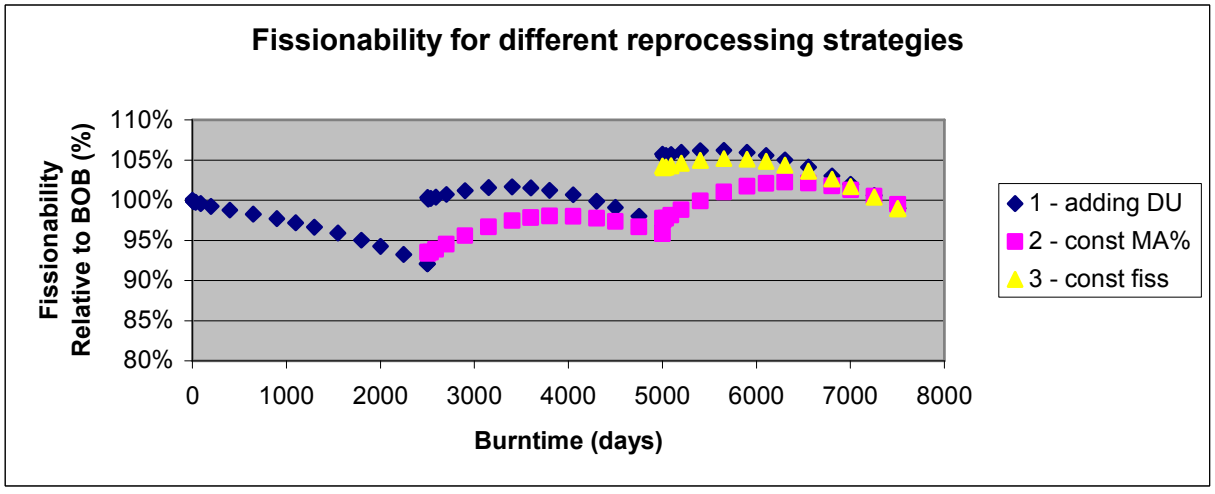

Figure 26: The fissionability during burnup is an approximate measure for the reactivity of the reactor. The fissionabilility is shown relative to BOB-1.

In the multiple recycling calculations, the exact microscopic worth of the recycled isotopes (DU, MA) at the BOB have been used instead of the average microscopic worth during the previous irradiation. As the recycling vectors will be added to fresh fuel, it is hypothesized that the exact worths at BOB would be more representative for their worths during recycling.

4.3.2 Analysis for three different recycling strategies

The results of the analysis of the three recycling strategies are shown below. Figure 27 shows the percentage of MA in the fuel during the three stages of the integral cycle: irradiation, decay and 'reprocessing and recycling'. The last stage is taken together – forming the new fuel – and is denoted as BOB-2 and BOB-3.

Addition of DU only

Replacing fission products by DU allows for an increase of the initial fissionability from EOB to BOB-2. The increase is seen in the figures displaying the reactivity and fissionability. The fissionability increases from 92% to 100% (both relative to BOB-1). As Minor Actinides are destroyed during irradiation, and *only* depleted uranium is added when manufacturing new fuel, the percentage of MA in the fuel decreases for each cycle (see figure 27 illustrating MA% over time).

Constant MA%

When keeping the MA percentage in the fuel constant for multiple cycles, the increase of HM worth displayed between EOB and BOB vanishes. However, there remains a very small increase of the HM worth. Although the percentage of MA in the fuel stays constant for multiple burnups, the composition of the MA vector changes during burnup. Table 18 shows the different initial MA vector for three cycles.

Comparing MA worth for multiple cycles			
	Percentage of total MA in reactor fuel		
	BOB1	BOB2	BOB3
Np-237	16.50%	15.70%	15.40%
Am-241	61.70%	57.60%	54.60%
Am-243	15.30%	16.40%	17.30%
Cm-243	0.10%	0.20%	0.20%
Cm-244	5.00%	8.10%	9.90%
Cm-245	1.20%	1.60%	2.00%
Cm-246	0.10%	0.30%	0.50%
Microworth	**-0.87**	**-0.78**	**-0.71**

Table 18: **Compare MA worth for multiple cycles.**

As can be seen in table 18, the presence of ^{244}Cm and ^{245}Cm isotopes in the MA vector increases, while the presence of ^{241}Am decreases. The worths of these isotopes are, respectively, 0.64, 6.91, and -0.99. The negative worth of the MA vector at the start of the third burnup is ~20% less than the worth at the start of the first burnup. The change of the MA vector partly explains the increasing fissionability for multiple cycles. The change in the plutonium vector is discussed in the section 4.4.

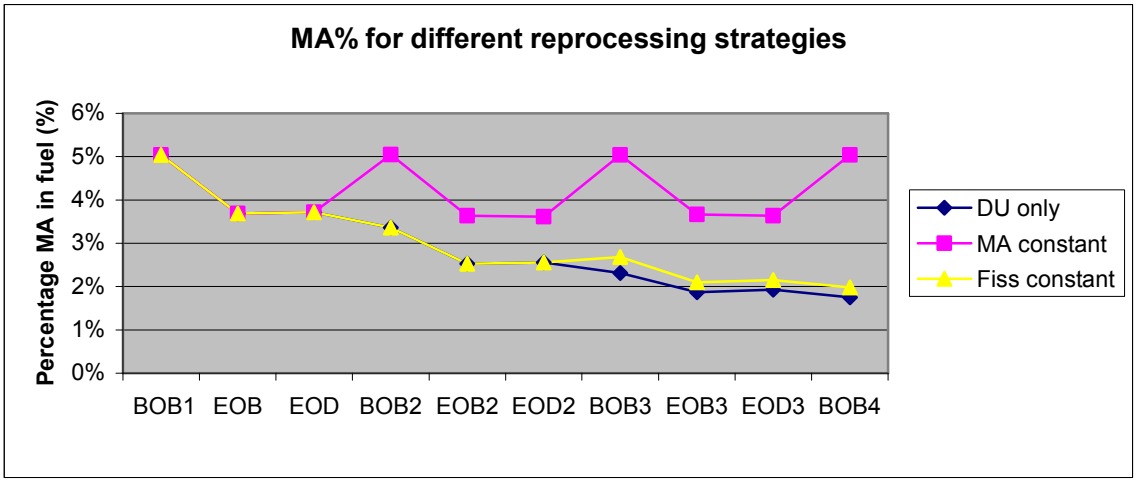

Figure 27: Total MA% in the fuel composition during multiple irradiations for the three different recycling strategies.

Adding DU and MA, keeping constant fissionability

To keep the fissionability the same over multiple burnups, both MA and DU are added. The boundary conditions are to keep the total HM worth as well as the nuclide density constant for multiple cycles. The necessary equations are:

$$\Delta n_{DU} + \Delta n_{MA} = \Delta n$$
$$w_{DU} * \Delta n_{DU} + w_{MA} * \Delta n_{MA} = \Delta W$$

where:

$n_i = \text{nuclide density}_i$

$w_i = \text{microscopic worth}_i$

$\Delta W = \text{change total HM Worth}$

Unknowns:

1) Amount of MA to be added (atom / barn * cm)
2) Amount of DU to be added (atom / barn * cm)

Knowns:

1) Microscopic worth of DU vector
2) Microscopic worth of MA vector
3) Change of total HM Worth
4) Change of HM atomic density

4. 1

When the above formulas are algebraically solved, the following relationship is obtained:

$$\Delta n_{MA} = \frac{\Delta W - w_{DU}\Delta n}{w_{MA} - w_{DU}}$$
$$\Delta n_{DU} = \Delta n - \Delta n_{MA}$$

4. 2

An analysis has been made from BOB-3 (after recycling with DU only) to BOB-4 (beginning of the third cycle). This choice was made as the shape of the total fissionability and reactivity curves become similar for the second and third burnup. To keep the fissionability the same, very little extra MA could be added. Recycling allows an addition of a mixture of 5% MA and 95% DU.

As shown in figure 28, the calculation of a recycling strategy keeping fissionability constant is inaccurate. The recycling microscopic worths (w_{MA} and w_{DU}) change too much over multiple cycles to calculate accurate new compositions with constant fissionability. In figure 28, the fissionability increases from 100% to 104%.

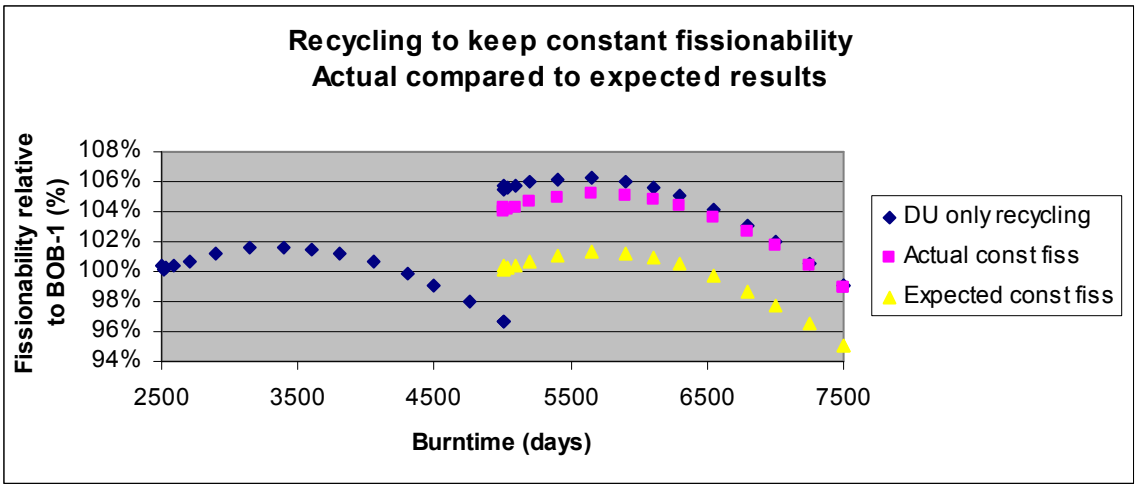

Figure 28: **The resulting composition after recycling to keep the fissionability constant does not achieve constant fissionability. Constant fissionability is calculated for the third cycle after recycling with DU only in the second cycle.**

As was concluded in section 3.3 when analyzing the fissionability of the reactor for different compositions, using the recycling microscopic worths of a specific composition to predict the fissionability of new mixtures is shown to be problematic. Reasons for the difference include the fuel composition changes over multiple cycles and the accompanying flux changes. Both factors influence the calculated total fissionability of the reactor.

4.3.3 Effect of reprocessing losses

As mentioned, the assumption was made that there are no reprocessing losses. Currently, industrial reprocessing efficiencies up to 99% are seen as realistic. The PUREX process could possibly separate uranium and plutonium from the spent fuel with an efficiency up to 99.9%.[33]

Since around 80% of the 1% loss consists of fertile uranium, this HM loss can be replaced by DU without introducing extra negative worth. A total of 20% of 1% (thus 0.2% - around 30 kg) of material that contributes positively to the total HM worth is lost. These include fissile nuclides lost during reprocessing. In order to make-up for these losses, it may be necessary to add more MA to the fuel so that the reactor is kept critical.

As is seen in figure 26, each subsequent cycle with a constant MA loading of 5% becomes more fissionable. As shown (table 18), the MA worth becomes less negative for each cycle, increasing 20% from the first to the third cycle. Addition of MA (instead of plutonium) to compensate fissile losses would be a more sustainable alternative to achieve the closed fuel cycle. Another option which can be investigated is changing the theoretical density of the fuel to increase or decrease fissionability. Lower t.d. decreases fissionability, and vice versa.

4.4 Breakdown of fissionability into components for multiple cycles

In the previous chapter, the analysis of the different components of the HM macroscopic worth clearly shows that the macroscopic worth of the positive components (predominantly ^{235}U and Pu) decrease and negative components (predominantly MA) increase during irradiation. In addition, the increasing negative worth due to decay and recycling between EOB and BOB has been discussed. Finally, the increasing total fissionability of the reactor for multiple burnups has been presented (see figure 26). In this section, it will be shown that the increase for multiple cycle burnup is predominantly due to the increasing worth of the MA isotopes. It is emphasized that referrals to worth in this section are to macroscopic worths.

As concluded in the previous chapter, the change of the worth of the HM component during a single irradiation can be almost fully explained by the changing worth of the MA. In figure 29, multiple reprocessing are shown for 'DU only' recycling. The conclusion regarding HM and MA worth can be seen once more, as the curve of the changing worth of the total HM follows the changing worth of the MA during the first irradiation (see the first 2500 days). As can be seen, during the second and third cycle, the changing worth of the Pu and U from EOB to BOB are of increasing importance.

The figure shows that the worths of both Pu and U decrease from EOB to BOB. Pu decreases due to the decay of ^{241}Pu. U decreases due to the addition of DU, with its negative worth, during reprocessing, temporary storage and fuel fabrication. The MA decreases slightly from EOB to BOB due to buildup of ^{241}Am. The total HM worth from BOB-1 to BOB-2 remains the same even though the worth of MA increases by more than 10% relative to the total fissionability.

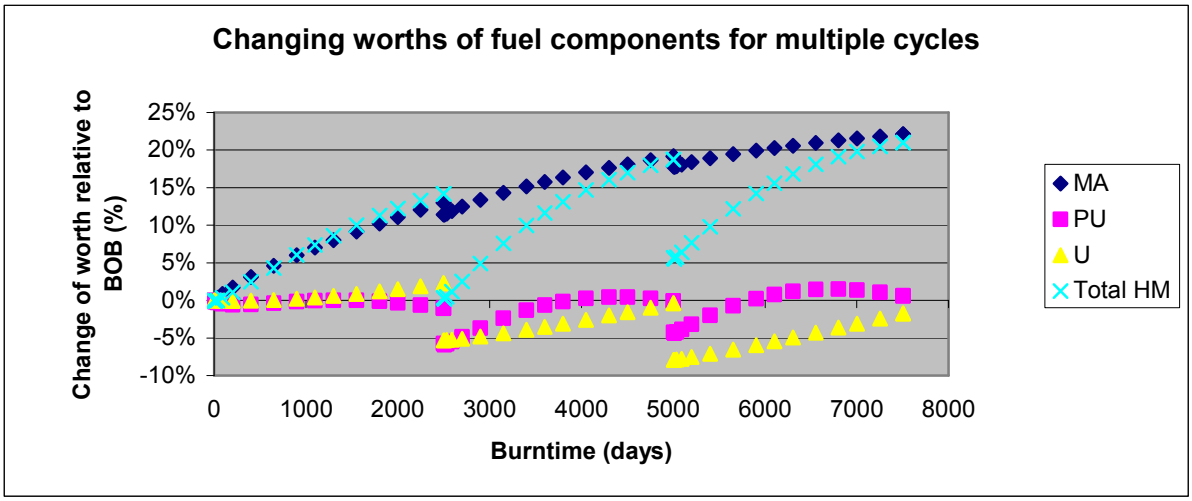

Figure 29: Changing worths of the MA, PU and U components are shown for multiple cycle burnup. The analysis is performed for the recycling strategy adding only DU. The changing worth is relative to fissionability at BOB-1.

Where the worths of the Pu and U vectors change very little during the first irradiation, the worths change considerably during the second and third irradiation. Combined with the MA worth, the HM worth increases for multiple cycles. For example, the HM worth at BOB-3 (~5000 days) is 5% higher compared to the first cycle.

An isotopic analysis has been made of the changes of the Pu vector for multiple cycles (see figure 30). There are three plutonium isotopes (^{238}Pu, ^{239}Pu, ^{241}Pu) that change their contribution to the macroscopic worth considerably from the first burnup to the second and third burnups. After the first burnup, the isotopes are closer to an equilibrium composition. The atomic density of ^{241}Pu decreases during the first burnup, and decreases further during decay. During the next cycles, ^{241}Pu increases during irradiation, and decreases a similar amount during decay. The worth of ^{241}Pu stays virtually constant from BOB-2 to BOB-3.

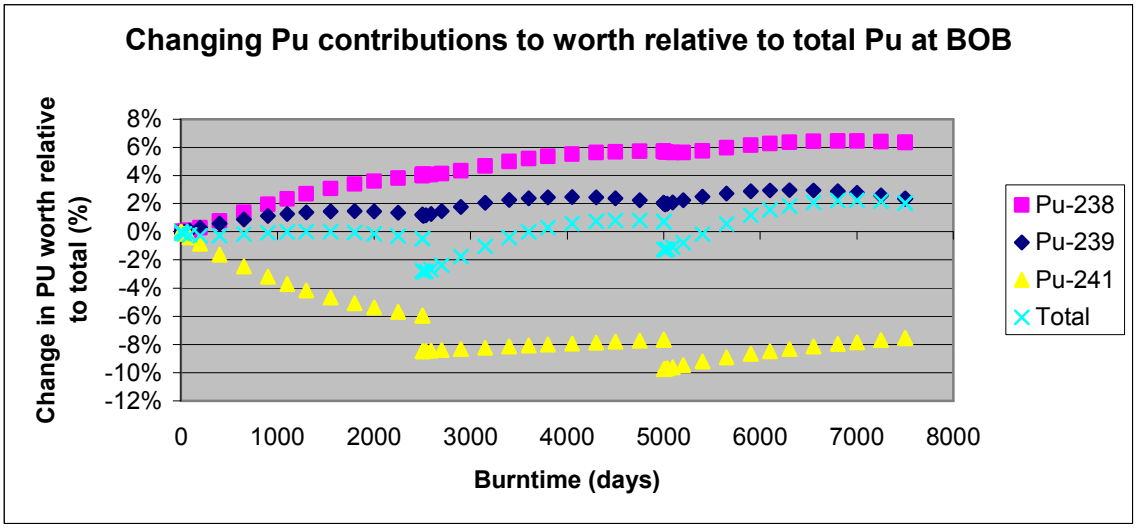

Figure 30: **Changing Plutonium worths during multiple cycle irradiation. Change in Pu relative to the total worth at BOB for the recycling strategy adding only DU. ^{240}Pu shows very little change.**

The isotopic vectors of Pu, MA and U of the first cycle are not at an equilibrium composition. There are significant changes in the isotopic densities from the first cycle to the second cycle. However, the changes of the initial isotopic composition become smaller from the second to the third cycle. The changing isotopic compositions are compared in the table 19.

	Isotope	BOB-1	BOB-2	BOB-3
PU	Pu-238	2.7%	6.4%	6.6%
	Pu-239	56.5%	54.8%	54.4%
	Pu-240	26.1%	28.4%	29.7%
	Pu-241	7.5%	3.3%	2.7%
	Pu-242	7.2%	7.1%	6.6%
U	U-235	0.7%	0.3%	0.2%
	U-238	99.3%	99.7%	99.8%
MA	Np-237	16.5%	15.1%	13.5%
	Am-241	61.7%	56.0%	50.2%
	Am-243	15.3%	16.8%	19.1%
	Cm-243	0.1%	0.2%	0.3%
	Cm-244	5.0%	9.6%	13.4%
	Cm-245	1.2%	1.8%	2.6%
	Cm-246	0.1%	0.4%	0.8%

Table 19: Changing isotopic densities for HM vectors. Relative to total PU / U / MA at BOB. Recycling strategy adding only DU

Logically, the fraction of higher Cm-isotopes in the MA vector increases per cycle. The fraction of ^{241}Am decreases for the first three cycles, while the ^{243}Am density increases. Most Pu-isotopes (including ^{238}Pu, ^{239}Pu and ^{241}Pu) are close to an equilibrium composition. As there is no fissile uranium added to the fuel, the U-vector will reach an equilibrium equal to the DU vector. Increasing the number of cycles would determine the closed cycle fuel composition for the DU recycling strategy.

4.5 Consequences for waste reduction

The reduction of waste produced by the GCFR is possible due to front-end and back-end fuel cycle advantages. In contrast to the open fuel cycle of thermal reactors, the GCFR recycles all of its core inventory. However, small reprocessing losses remain as waste.

At the front-end of the cycle (mining, enrichment), the volume of waste produced of the nuclear fuel cycle is reduced drastically. There are no front-end activities necessary for a closed cycle. All of the fissile material necessary for subsequent irradiations is present in the irradiated fuel. Around 1570 kg depleted uranium is added during the recycling step. The added DU is taken from the existing nuclear stocks (for example from the tails of enrichment facilities).

In this section, the reduction of back-end waste production is quantified, both the volume and the radiotoxicity of HM waste. A comparison is made with the mass and radiotoxicity of waste produced by thermal reactors per unit energy. As both the mass and radiotoxicity of fission products are comparable for fast and thermal reactors, and as the long term radiotoxicity is caused by HM atoms, fission product waste is not discussed. [34]

4.5.1 Volume reduction

The GCFR produces much less waste per unit of energy produced. In table 20, the measure of 'fuel efficiency' is calculated for both the GCFR and a LWR.[35] The efficiency of the GCFR is calculated using the estimated 275 MWe produced by the GCFR 600 MWth.[36] The HM lost per year for the GCFR is equal to 1% of the total HM loading at EOB taken over the entire irradiation period of 2500 days (assumption: 1% reprocessing loss). The specifications of the 3600 MWth LWR are also given in the table.

Comparing waste per unit energy [kg/TWhe]	GCFR	Thermal LWR
Power (MWth)	600	3600
Efficiency (%)	46%	34%
Electric power (Mwe)	275	1230
Loading (ton)	16	130
Energy per year (TWhe)	2.4	11
HM lost per year (kg)	22	30.000
Energy produced per ton waste (kg / TWhe)	9	2700

Table 20: Comparing waste production per unit of energy produced [kg / TWhe]

The calculation in table 20 shows that the GCFR produces a factor 300 less waste compared to the LWR for the same amount of energy produced. The above calculation disregards the time needed to change fuel loading (assumption: 100% load factor).

In addition to the limited amount of waste produced by the GCFR, it has the potential to burn part of the MA produced by the thermal reactor park. The potential to burn the back-end nuclear waste of thermal reactors is greatest when keeping the MA loaded equal to 5% or higher.

For the 1230 MWe (3600 GWth) thermal reactor, 0.10-0.15% of the mass discharged are MA. This is an equivalent of 30 - 45 kg / year. In 2500 days (proposed irradiation period of the GCFR), a thermal PWR would produce around 300 kg of MA.

After GCFR burnup, ~9.6% of the initial 16.4 ton loading is fissioned. Thus 1570 kg of HM must be replaced. When adding MA to increase it from 3.4% MA (EOB – 14.830 kg) to 5% MA (BOB – 16.400 kg), an equivalent of 260 kg of MA must be added. This is equal to an average of 23 kg of MA per irradiation year. The GCFR kept at constant MA % would thus be able to burn just under an equivalent single PWR's worth of MA fuel during its six year cycle.

As a greater number of thermal reactors will run with MOx fuel, the above estimated production of MA by thermal reactors (0.10-0.15%) is most likely on the low side. Although use of MOx decreases the volume of plutonium, there are also increasing number of capture and decay reactions which produce higher actinides. It is likely that the amount of MA produced per reactor will increase. Dedicated burner reactors – or Accelerated Driven Systems (ADS) – will be needed to fully close the fuel cycle for MA.

Thus, the GCFR does have the ability to drastically reduce waste reduction and close its own fuel cycle. However, the 600 MWth reactor is not able to burn the larger amounts of additional MA produced by thermal reactors. It should be remarked that the size, and to a large degree the costs, of a geological disposal site are primarily defined by the total mass of wastes. This can be seen as an additional important cost advantage of the closed fuel cycle. The volume of relatively short-lived fission products, a large part of the waste produced, will not be reduced by closing the nuclear fuel cycle.

4.5.2 Radiotoxicity reduction

The radiotoxicity of a nuclide is a measure for its radiological hazard to humans. The measure accounts for the decay mode of each nuclide (gamma, beta or alpha decay), the biological half life in a human body, and the intake of radionuclides by the human body through inhalation or ingestion.

In this section, the changing radiotoxicity of the different components of the total fuel inventory for different storage times is studied. In addition, the radiotoxicity of waste of the reactor fuel of the GCFR is compared to the waste of the LWR. The study has been performed employing the changing radiotoxicity contributions of the different isotopes and their daughters over a time-span of 10 years to 1 million years.[37]

As the amount of MA in the fuel decreases during burnup, the radiotoxicity of the inventory decreases as well. However, after the first 1000 years of storage, the radiotoxicity of the different original fuel compositions are almost equal to each other (around 1% of the original radiotoxicity). As seen in the table below, the long term radiotoxicity of the inventory is predominantly dependent on Pu-isotopes and ^{241}Am. The ^{244}Cm decays almost fully during the first 100 years.

Radiotoxicity - short and long term storage					
10 years		**2000 years**		**500.000 years**	
Pu-238	43%	Pu-239	29%	Pu-238	59%
Am-241	13%	Pu-240	46%	Pu-242	8%
Cm-244	29%	Am-241	11%	Am-241	13%

Table 21: Main contributors to radiotoxicity for short- and long term storage. Other smaller contributors include: ^{240}Pu, ^{241}Pu, ^{242}Am, ^{242}Cm (10 years), ^{243}Am (2000 years), and ^{237}Np, ^{242}Am, ^{242}Cm (500.000 years).

As is seen in table 21, the ^{238}Pu contributes significantly to the radiotoxicity both during the first years of storage and after a long period of half-a-million years. In the interval, other isotopes contribute more significantly to the radiotoxicity. The behavior of ^{238}Pu is due to the increasing radiotoxic contribution of ^{238}Pu between 1000 and 200.000 years. During this period, the radiotoxicity of a mole of ^{238}Pu increases by a factor 3. The isotopes ^{237}Np and ^{241}Am and ^{242m}Am display similar behavior. The radiotoxicity of all other isotopes, ignoring uranium isotopes, decrease over time.

As discussed in the previous section, the GCFR has the ability to radically decrease the mass of waste produced. An analysis has been made of the radiotoxicity of the HM waste produced by a thermal reactor and the GCFR for the same amount of energy produced. The LWR that is studied implements the open fuel cycle. The composition of the spent fuel of the LWR is shown in table 22. The isotopic densities of Pu and MA are set equal to the recycling vectors of Pu and MA in 2016. It is assumed that the waste of the GCFR is limited to the 1% loss of HM during reprocessing. The composition of the reprocessing losses has been determined using the atomic densities of the spent fuel at EOB.

Composition of LWR spent fuel			
Element	**Weight (%)**	**Isotopic composition**	
Uranium	95.83%	U-235	0.90%
		U-236	0.40%
		U-238	98.70%
Plutonium	1.00%	Pu vector in 2016	
MA	0.17%	MA vector in 2016	
f.p.'s	3.00%		

Table 22: Composition of LWR waste[38]

As shown in figure 31 (next page), after 50.000 years the radiotoxicity of the GCFR fuel becomes equal to the radiotoxicity of the uranium ore. For the LWR, it takes 700.000 years before the radiotoxicity reaches the same reference value.

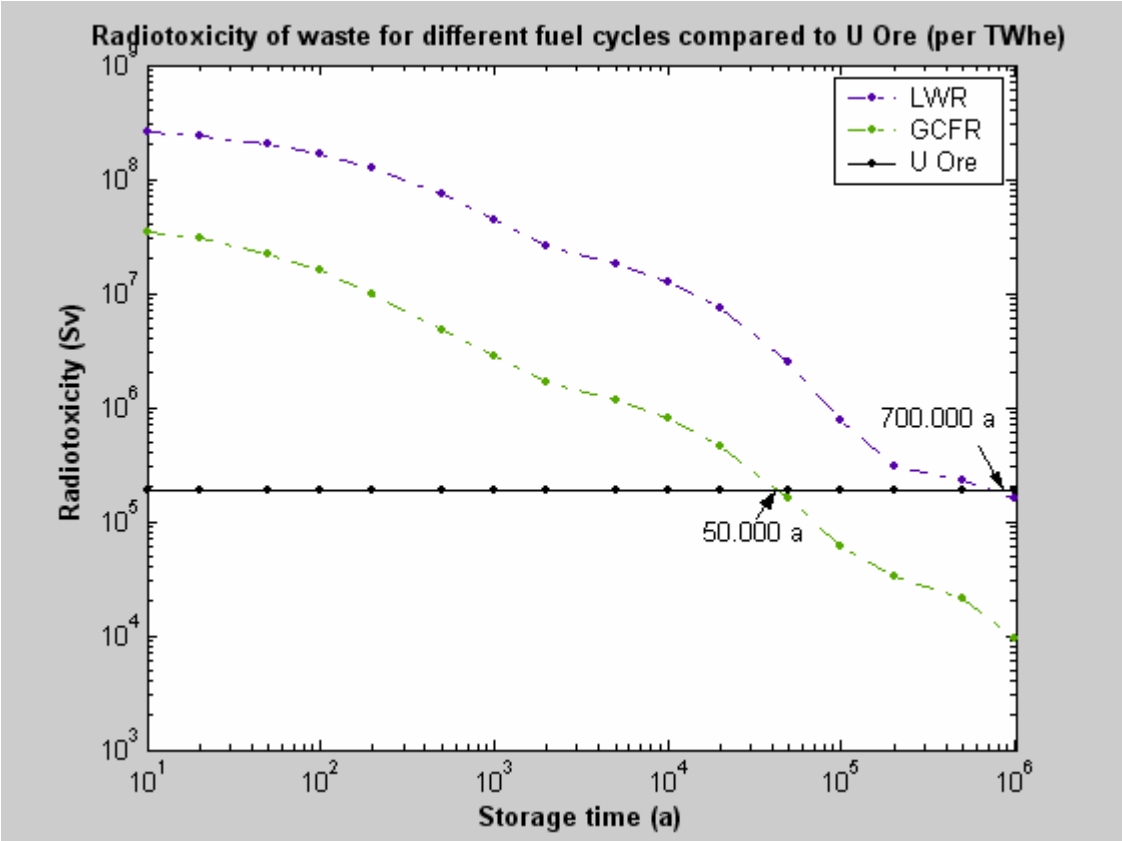

Figure 31: **The radiotoxicity of the waste of the GCFR 600 MWth is compared to that of a typical LWR 3600 MWth per unit energy. It is seen that the waste of the GCFR decays to the radiotoxicity of uranium ore within 50.000 years, while the waste of the LWR takes 700.000 years (factor 14 reduction).**

While the volume of the waste per unit of energy produced in the closed cycle of a GCFR is significantly smaller than the volume of waste of a thermal reactor (factor ~300), the time that the reprocessing losses must be stored before it reaches the reference radiotoxicity of uranium ore reduces by a factor 14.

The above conclusion is dependent on the assumption that 1% of all HM atoms is lost during reprocessing, recycling and fuel fabrication. As continued research improves reprocessing efficiency, the time at which GCFR waste becomes equivalent to uranium ore could be further decreased.

4.6 Conclusions

- The irradiated fuel of the GCFR can be reprocessed and consequently recycled in a closed cycle. The favorable properties that have been shown for a single cycle irradiation in the GCFR (e.g. its small reactivity swing) are also shown in the multiple cycle burnup. In the analysis of multiple cycle burnup, reprocessing losses were disregarded. The theoretical density of the fuel was kept constant.
- It is confirmed that the microscopic worth calculated within a different mixture cannot be accurately implemented to calculate the worth of recycled fuel. An uncertainty of at least 4% of the total worth of the reactor has been shown. As a rough tool, it does give a good indication of the different effects of nuclides on the HM worth (positive or negative) during the irradiation.
- The worth of the fuel decreases during the storage time needed to allow cooling of the spent fuel. The decrease is due to the decay of relatively short-lived fissile ^{241}Pu to ^{241}Am. Increasing the speed of reprocessing and fuel fabrication from 6 years to 3 years increases the fissionability. The ^{241}Am that is produced during decay plays an important role in subsequent cycles by transmuting to fissile fuel after a neutron absorption, limiting the reactivity swing and thus allowing for cycles of zero breeding gain.
- To compensate for the decrease of HM worth during storage, the worth of HM should increase during irradiation to allow for a closed fuel cycle.
- Three different recycling strategies were studied (DU only, constant MA% and constant fissionability). When analyzing the reactivity and fissionability of the fuel mixtures undergoing multiple recycling, DU displays the best ‘closed fuel cycle’ properties. The reactivity stays constant during multiple cycles. However, if reprocessing losses would be greater than 1%, adding extra MA during the recycling step, or increasing theoretical density slightly, could be options.
- The fuel temperature coefficient becomes more negative for multiple cycle burnup, as the percentage of uranium in the fuel increases when recycling with depleted uranium. The void coefficient stays constant for the different recycling strategies for multiple burnups.
- When recycling to keep a constant MA%, a single GCFR can burn 260 kg of MA while a thermal reactor produces 300 kg of MA per irradiation period of 2500 days. The GCFR can contribute to reductions of MA inventory. However, to burn all MA produced by thermal reactors, other dedicated burner reactors would be needed.
- The GCFR can reduce the HM waste produced per unit of energy by a factor ~300. Assuming 1% reprocessing loss, the time that the reprocessing losses must be stored before it reaches the reference radiotoxicity of uranium ore is reduced by a factor 14. The reprocessing losses must be stored for up to 50.000 years before reaching the reference radiotoxicity of uranium ore.

5 Decay Heat Production analysis

Throughout reactor operation, fission- and decay power combined result in the total thermal power rating of the reactor. The decay power is a fraction of the total nominal power of the reactor and dependent on the irradiation history. After the fission reaction has stopped, the spontaneous decay of fission products and minor actinides continues to produce residual heat - so called decay heat.

When the reactor operator shuts down the reactor, the removal of the decay heat poses little challenge for the coolant systems. However, an unexpected shutdown due to malfunctioning of reactor thermalhydraulic systems could make removal of decay heat difficult. Safety studies prior to licensing of the reactor include temperature transients after a loss of coolant accident. Multiple back-up systems are included to make sure that decay heat can be removed in accident situations. Melting of the fuel in the core is thus prevented. An accurate knowledge of the time-dependent Decay Heat Production (DHP) in the GCFR is needed to design the safety systems. Computational models of DHP are used in transient calculations.

In this chapter, results are shown of DHP during the first hours after reactor shutdown. In addition, results of DHP immediately after shutdown at different points in the irradiation cycle are shown. Reasons for the difference in DHP for a thermal reactor and GCFR will be given. Finally, the DHP curves are fitted to an exponential model that can consequently be used in thermalhydraulic codes for transient analysis. The fitting parameters that are determined for the DHP curves of the GCFR can be found in Appendix B.

5.1 Calculations of DHP

Calculations have been performed for first cycle irradiations using different fuel compositions of the GCFR at EOB and at different times during the irradiation. Although it would be expected that the DHP is at its maximum at EOB, since the density of f.p.'s (including short-lived f.p.'s) is at its maximum, research has shown that this is not the case. This is partly due to the different percentage of MA in the fuel.

5.1.1 Breakdown of DHP into fission product and HM contributions

As mentioned, decay of fission products and HM (predominantly minor actinides) are the major contributors to the DHP. Initially, the short-lived fission products contribute most to the DHP. During the first 100 seconds of decay, the contribution of fission products decreases to 50% of the initial value. The contribution of HM decreases much more slowly due to the longer half-lives of the HM (see figure 32).

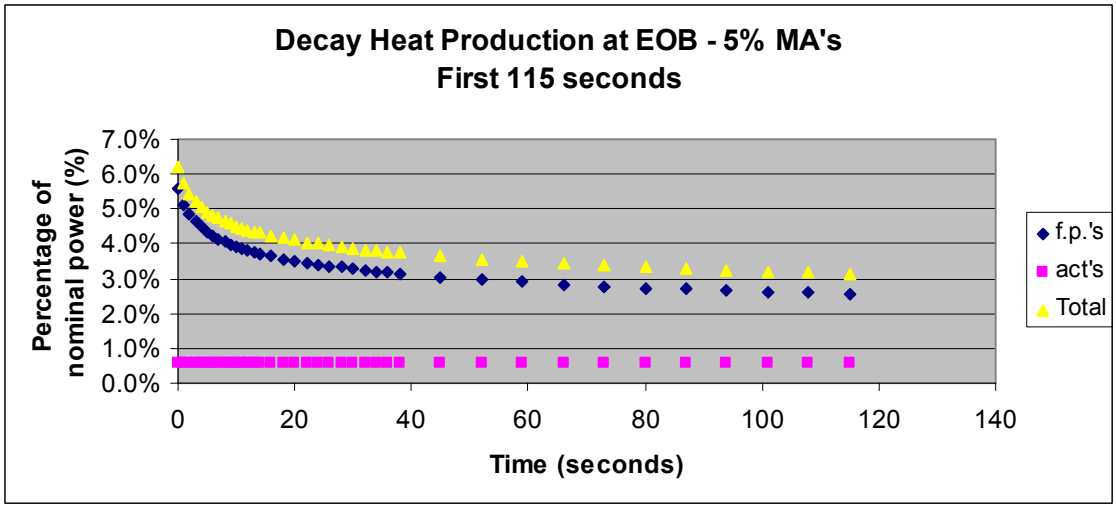

Figure 32: **Decreasing DHP for the first 115 seconds. The rapid decrease of the fission product (f.p.) contribution, as well as the constant HM (act.) contribution are shown. The f.p.'s dominate DHP on short timescales.**

5.1.2 DHP for different initial fuel compositions

The fission products that produce decay heat increase rapidly in concentration after initial GCFR irradiation. After 10 seconds of irradiation, decay heat power is already equal to 6.2% of nominal power for the 10% MA mixture. For different fuel compositions, the amount of DHP due to fission products stays roughly the same throughout the irradiation interval (differences up to 3% for initial MA percentages ranging from 0-10%). Thus, the focus of the research has been on the effect of HM (varying MA%) on DHP.

The total DHP for different compositions is given in figure 33. As can be seen, the power difference between the different loadings is more or less constant during the first hours of decay. The difference is equal to ~0.4% of the nominal power when comparing the initial 0% to the 10% MA loading (difference equals 2.2 MWth at t = 0, 2.4 MWth at t = 3 hours).

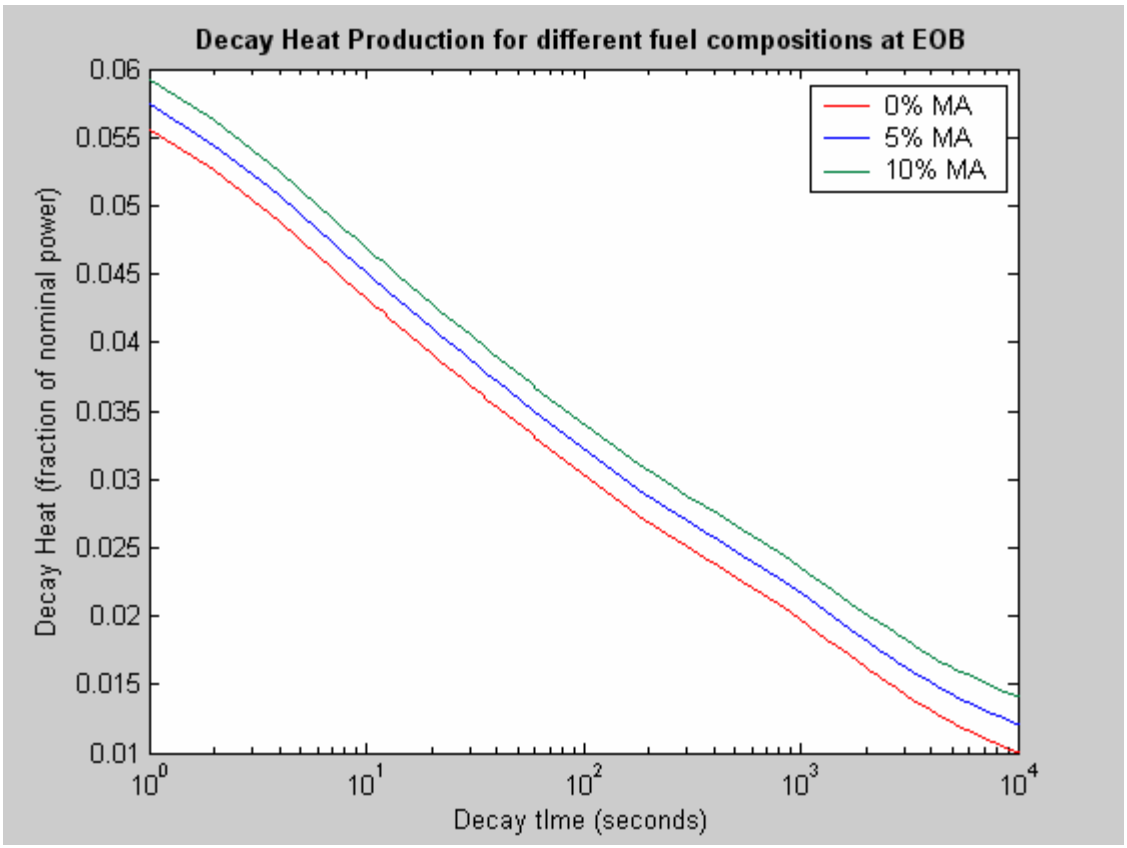

Figure 33: **Varying fuel compositions at EOB result in a difference in DHP. The plot is shown from t = 1 seconds until t = 10^4 seconds (3 hours). At 0 sec (not shown), the DHP is equal to 6.02%, 6.20%, 6.30% for compositions with initial MA loadings of 0%, 5% and 10% respectively.**

Changing the initial MA loading of the fuel influences the immediate DHP very little. However, after the first hour of decay, the difference becomes significant. As is illustrated in the figure 34, total HM DHP after three hours comprises 20% of the total DHP for an initial loading of 0% MA, while for an initial loading of 10% MA, 40% of the DHP is due to HM. In absolute terms, instead of producing 6 MW of DHP after 3 hours, the DHP amounts to 8.4 MW.

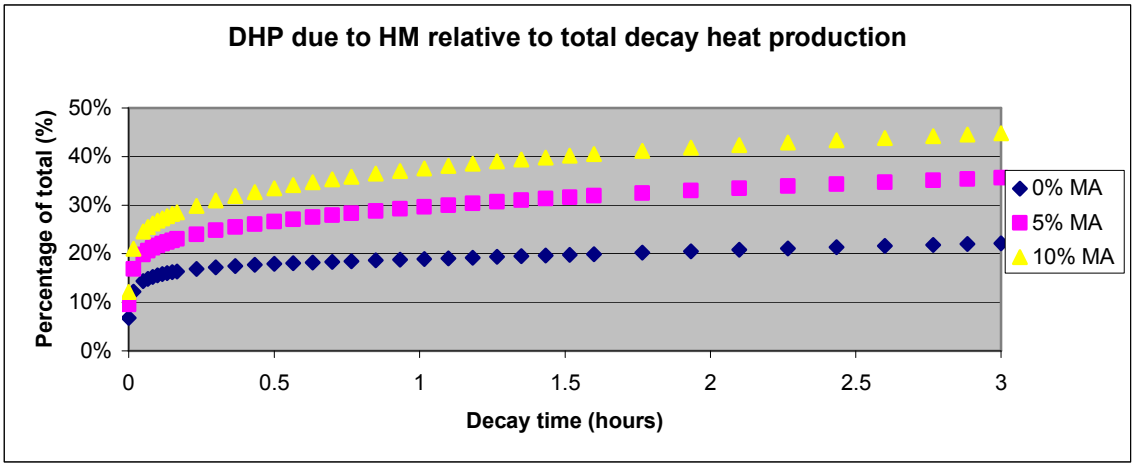

Figure 34: Actinides contribute relatively more to DHP as the timescale increases to hours.

In conclusion, the initial composition of HM and the percentage of MA present in the reactor fuel prior to shutdown is very important for estimations of DHP for longer times after reactor shutdown.

5.1.3 DHP at different times during irradiation immediately after shutdown

The initial DHP varies with the time that the reactor fuel has been irradiated prior to shutdown. During the first 500 days of irradiation, the immediate DHP varies from 6% to 6.8% of the total reactor power. In absolute terms, the difference is 4.8 MWth (changing from 36 to 40.8 MWth). This is shown in figure 35.

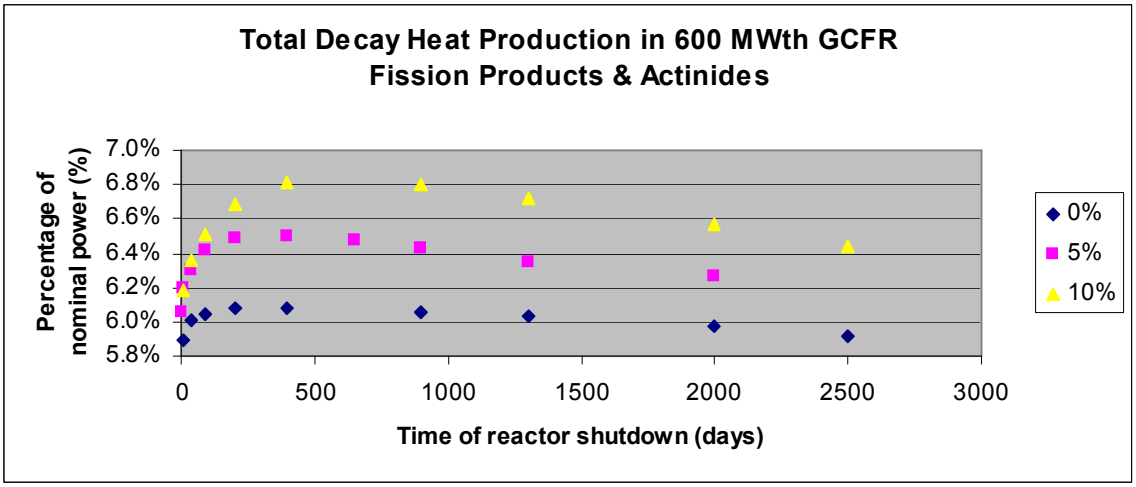

Figure 35: **Total DHP immediately after reactor shutdown is different for different points during the irradiation. The difference is due to short-lived actinides and fission products.**

The fact that the GCFR burns MA explains the decrease of DHP from 500 days to 2500 days. The percentage of MA decreases from 5% to 3.8%, as presented in the previous chapters. However, burning MA does not explain the increase from 6% to higher percentages during the first 500 days of irradiation.

When studying the contributions of both HM and fission products to the DHP, it is seen that both contributions display a similar time-dependent behavior. The effect must be caused by the short-lived nuclides, as it is a 'short-time' phenomena. The most likely reason for this behavior would be a difference in the density of short-lived fission products and HM at different times during the irradiation. There are most likely less short-lived HM (minor actinides) and fission-products at the beginning of burnup. This would explain the increase from 0 to 500 days. If the reactor would shutdown before planned (but well after 500 days), the DHP would be higher compared to EOB due to the higher percentage of MA present in the irradiated fuel.

5.2 Comparing DHP to ANS model

The results of the comparision of the actual DHP of a representative mixture of fissionable nuclides in a fast reactor core is compared to the expected DHP using the ANS model. Recall that in Chapter 2 (figure 8) it was shown that the fission products of ^{235}U contribute more to DHP compared to ^{239}Pu and ^{241}Pu during the first 1000 seconds after reactor shutdown. The difference is largest during the first 100 seconds. See the table 23 (next page) for an overview of the initial DHP of the four different fissioning isotopes.

Initial DHP of fission products for thermal reactors is often quoted as being greater than 6% of nominal power. Due to the change of fissioning isotopes, the DHP of the GCFR is expected to be smaller. In a thermal reactors , predominantly ^{235}U is fissioned. The contribution of ^{239}Pu increases throughout the irradiation. In the GCFR, the percentage of fissions of plutonium isotopes is much greater than the number of fissions of ^{238}U.

A rough estimate of the DHP of fission products of the fissioned isotopes in a thermal and fast reactor (6.4% vs. 6.0%) is shown in table 23. Apparently, the predominance of the plutonium fissions compensates the greater contribution of ^{238}U to the DHP in the GCFR. The net DHP is smaller in the GCFR.

Percentage of DHP after t = 1 sec					
	ANS	**Thermal**	**ANS * Therm**	**Fast**	**ANS * Fast**
U-235	6.50%	90 %	5.9%	0%	0.0%
U-238	7.80%	0 %	0.0%	20%	1.6%
Pu-239	5.10%	10 %	0.5%	40%	2.0%
Pu-241	6.00%	0 %	0.0%	40%	2.4%
			6.4%		6.0%

Table 23: Decay Heat Production according to the ANS model

The decay heat source of the GCFR is estimated by a mixture with 20% fast fissions in ^{238}U, 40% fissions in ^{239}Pu and 40% fissions in ^{241}Pu.[39] Research performed shows that the DHP of the GCFR is higher than is predicted by the ANS model.

5.2.1 Parameters of fast reactor DHP

The decay heat curves calculated using ORIGEN-S were fitted to an exponential model. The number of exponentials used in the model allows it to be used by the thermalhydraulic code CATHARE. The following equation has been used for the fit:

$$DHP = \sum_{i=1}^{11} \alpha_i \exp(-\lambda_i t) \qquad \textbf{5. 1}$$

The parameters describe the curve up to 10^4 seconds (first hours after shutdown) for different initial compositions at EOB (2500 days irradiation), and can be found in Appendix B. The largest value of the exponent λ describe the DHP after short decay times. In contrast, the smallest value of λ gives the greatest contribution to the DHP after long decay times. The value of α weighs each exponent. When the α's are summed at t = 0, the total decay heat as a fraction of nominal power directly after the reactor is shutdown is given.

Figure 36 shows the three DHP curves, including the fit of the 0% MA DHP curve.

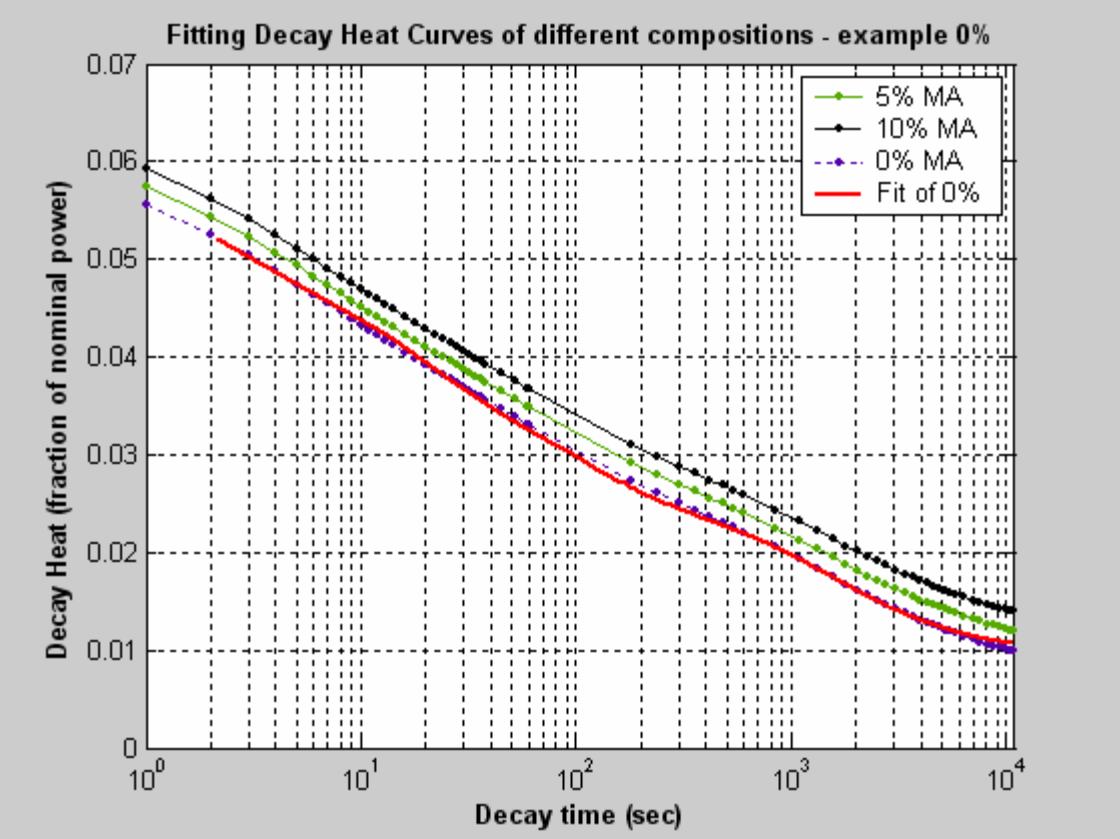

Figure 36: **The three actual decay heat curves for the different mixtures at EOB are shown. The intercept of the fitted curve at t = 0 equals 6.017% while the actual intercept equals 6.018%. The fits for 5% and 10% are shown in Appendix B.**

5.2.2 Comparison of GCFR theoretical mixture to actual DHP

When the fissioning fractions of isotopes in the theoretical GCFR mixture (given in table 23) are used, and the decay heat curves of the four isotopes of the ANS 5.1 model, the actual production of decay heat for all MA mixtures and almost all decay times is underestimated (see figure 37, next page). The DHP is overestimated for the 5% mixture during the first 20 seconds of decay. For the 0% mixture, the overestimation lasts for less than a minute.

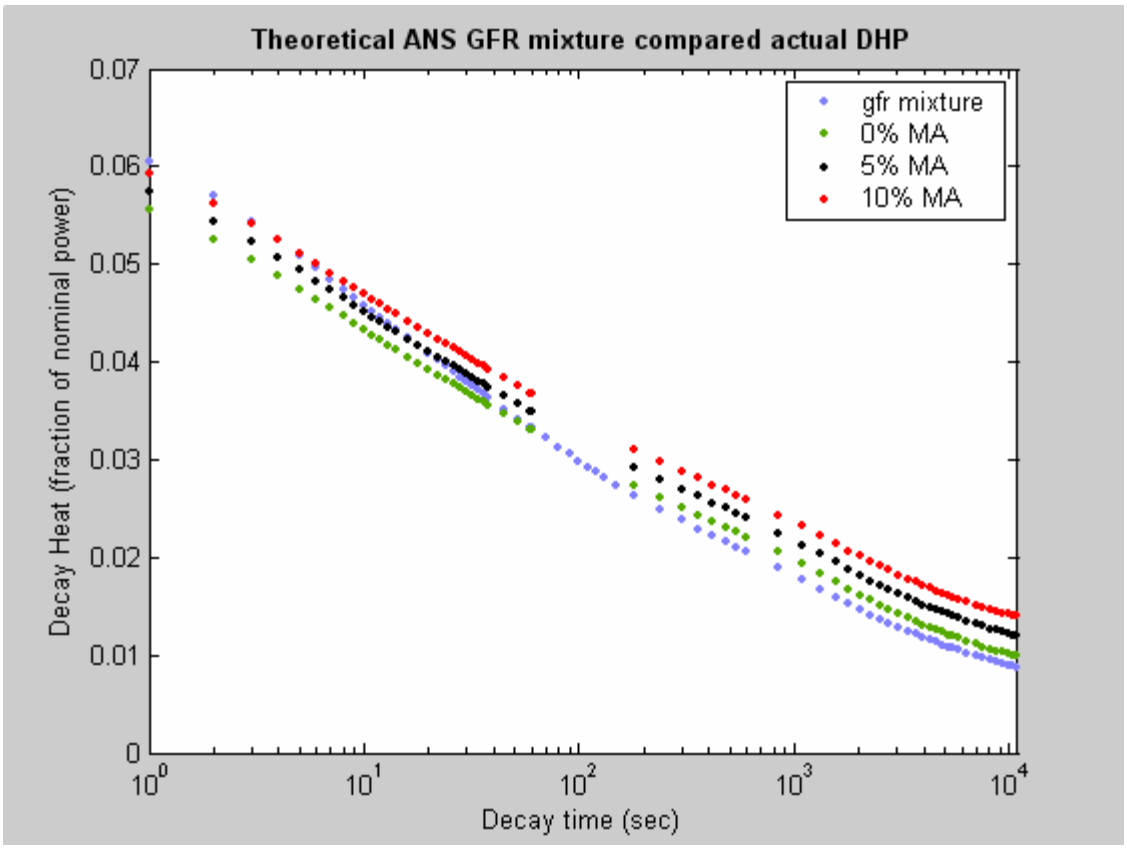

Figure 37: **The theoretical GFR mixture underestimates the actual DHP for all mixtures for times greater than one minute. For very short times, the mixture overestimates the DHP.**

The underestimation of the actual DHP initially loaded with 5% MA increases to 35% of the ANS standard at 10^4 seconds.

Note: $\text{Percentage Difference (\%)} = \frac{\text{Actual-ANSmodel}}{\text{ANSmodel}}$

5.3 Increasing the usability and flexibility of the new parameters

The parameters that are calculated from the ORIGEN-S curve of each composition are more relevant for the GCFR than the thermal reactor parameters and estimated fissioning mixture needed of the ANS model. In this secton, the usability and flexibility of the new parameters are discussed.

The fit is performed for the first three hours of decay (10^4 seconds) as this range is most relevant for transient analysis after reactor shutdown. In order to use the DHP exponential model for other applications, such as temporary storage of spent fuel after irradiation, a new set of parameters should be created that takes into consideration the DHP calculated by ORIGEN-S for longer decay times.

The fitted parameters are specifically valid for the GCFR after 2500 days burnup when initially 0%, 5% or 10% MA is added to the fuel. Using the parameters for different compositions would introduce an uncertainty in the fit. The percentage of MA present in the fuel varies throughout the irradiation. For example, if the reactor is shutdown after 1300 days of irradiation, the percentage of MA is larger than after 2500 days. The DHP at 1300 days due to MA would be greater, resulting in a higher total DHP.

To increase the flexibility of the fit, a correction can be made to the fitting function to compensate for the dependency on the percentage of MA in the fuel. Since the DHP of the fission products does not change for different MA compositions, a single fit could be made of the fission product DHP. As can be seen in figure 36, the difference between the DHP curves remains constant throughout the calculated decay period. The difference between the curves is dependent on the difference of the MA present in the fuel at the end of irradiation. When a functional relationship is determined relating the percentage of MA in the fuel to the DHP of the MA, the following fit would apply to a fuel mixture without the earlier stringent restrictions:

$$f(t) = (\sum_{k=1}^{K} a_k \exp(-\lambda_k t)) + b(MA) \qquad \textbf{5. 2}$$

Where: $b(MA)$ = functional relationship of DHP dependent on MA%

5.4 Conclusions

- The contribution of fission products to the decay heat changes little for different fuel compositions. The magnitude of the DHP increases for increasing amounts of MA present in the fuel.
- The DHP immediately after shutdown is not the same at different points in the irradiation. The maximum DHP is produced if the reactor is stopped after 500 days of irradiation. The decrease of the DHP after 500 days irradiation is due to burning of MA.
- The parameters for the decaying exponential model, calculated for each HM composition, can be used in thermalhydraulic codes to calculate the transient effects of DHP for the first 10^4 seconds. The exponential model with the new parameters is more accurate for the specific reactor fuel than the ANS model. However, the parameters are specifically valid at the EOB of a specific composition of the fast reactor fuel.
- The ANS model underestimates the DHP of the fast reactor.
- For a more general application, a separate exponential model could fit both the fission product and HM DHP separately. The fit for the fission product DHP would be the same for all fuel compositions. An additional term that indicates the HM DHP (as a function of the MA percentage in the fuel) would provide for more flexibility.

6 Conclusions

The goal of the thesis was to determine the fuel composition of the Gas Cooled Fast Reactor (GCFR) with power 600 MWth that realizes zero breeding gain, thus breeding exactly enough fissile fuel, to be able to close its own nuclear fuel cycle. All the stages of the nuclear fuel cycle, including irradiation, reprocessing, recycling and fuel fabrication, are taken into consideration. All of the original HM in the fuel that is not fissioned must remain in the closed cycle. A zero breeding gain is achieved when the fissionability of the HM fuel iterates to the same value at a similar point in the fuel cycle.

To obtain zero breeding gain in the GCFR, it is necessary to mix a small percentage of MA to the fuel. The following volume percentages of HM achieve zero breeding gain for the fuel design of the GCFR: (U,Pu,MA)C – (79%,16%,5%)C. Research confirms that when there are no losses of HM during reprocessing, only DU can be used during the recycling step. For the different recycling strategies (assuming no reprocessing loss), the fissionability increases for each subsequent irradiation cycle. If there are substantial (>1%) HM losses during reprocessing, additional MA can be added to compensate for fissile losses.

It is seen that implementation of this closed fuel cycle offers many advantages. In the following overview, disadvantages, technological challenges and theoretical points of interest are indicated as well.

Advantages

- The GCFR has the potential to burn MA. Higher initial loadings result in greater MA burning potential. When recycling to keep a constant MA%, a single GCFR can burn 260 kg of MA while a thermal reactor produces 300 kg of MA per irradiation period of 2500 days. To burn all MA produced by thermal reactors, other dedicated burner reactors will be needed.
- The initial excess positive reactivity necessary to achieve long periods of irradiation is small (around \$4). For MA loading greater than 6%, the reactivity swing becomes positive. Addition of ~5% of MA increases the burnup potential of the fuel from 40 to 90 MWd / kg. This is due to the transmutation of ^{237}Np to fissionable ^{238}Pu and ^{241}Am to fissionable ^{242}Am.
- The fuel temperature coefficient is negative, ranging varying between -0.91 to -0.80 pcm / K for a mixture without MA, and -0.37 to -0.34 pcm / K for an initial mix with 10% MA.
- The void- and fuel temperature coefficients do not deteriorate for multiple cycle burnup.
- The GCFR can reduce the HM waste produced per unit of energy by a factor ~300.

Disadvantages

- Mixing MA negatively affects safety parameters by decreasing the delayed neutron fraction. In addition, β_{eff} decreases with increasing irradiation times. However, the magnitude of β_{eff} is comparable to existing fast reactors.
- Voiding of the coolant introduces positive reactivity. Around \$0.50 is inserted for 50% voiding.

Technological challenges

- Addition of MA significantly influences the build-up of fission gas during fuel burnup and storage. The production of helium through α-decay is much greater than the production of the fission gas krypton and xenon. Increasing the loading of MA to 10% could increase the internal pressure of the fission gas in the fuel by a factor 5.
- Assuming 1% reprocessing loss, the time that the waste of the GCFR must be stored before it reaches the reference radiotoxicity of uranium ore is reduced by a factor 14 (50.000 years from 700.000 years). Improving reprocessing efficiencies will further decrease the radiotoxic inventory of the reprocessed waste.

Theoretical points of interest

- The change of the fissionability during irradiation closely follows the change of reactivity.
- Increasing the MA loading in the fuel decreases initial fissionability. The fissionability of compositions with high MA loading increases during burnup.
- The worth of the fuel decreases during the storage time needed to allow for cooling of the spent fuel and fuel fabrication. The decrease of the worth is due to the decay of relatively short-lived fissile ^{241}Pu to ^{241}Am.
- To achieve a closed fuel cycle, the HM worth must increase during irradiation to compensate for the decreasing HM worth during storage.
- The DHP immediately after shutdown is not the same at different points in the irradiation. The maximum DHP is produced if the reactor is stopped after 500 days of irradiation. After 500 days, the DHP immediately after shutdown decreases. The decrease is due to burning of MA.
- The parameters for the decaying exponential model, calculated for each HM composition, can be used in thermalhydraulic codes to calculate the transient effects of DHP for the first 10^4 seconds. The exponential model with the new parameters is more accurate for the specific reactor fuel than the ANS model. However, the parameters are specifically valid at the EOB of a specific composition of the fast reactor fuel.
- The ANS model underestimates the DHP of the fast reactor.

7 Discussions & Recommendations

The research has focused on the nuclear fuel cycle, safety parameters and decay heat production of the 600 MWth GCFR. Recommendations are given for follow-up investigations to further improve the understanding of the safety, economics, and sustainability of the GCFR. The decision of the research partners within the international community to focus further research on the 2400 MWth reactor will be discussed.

7.1 Recommendations for follow-up investigations

Investigating safety

- As the atomic density of the fission gas and helium increases when MA is added to the fuel, an investigation of the pressure build-up in the cavities of the carbide fuel should be initiated. The relationship between pressure build-up and the theoretical density of the fuel is of interest. Higher pressures could cause greater fission gas leakage from the fuel. The design of the fuel could be changed in such a way as to limit pressure build-up.
- A study of the coupling between the void- and temperature reactivity feedback mechanisms is needed to determine the equilibrium flux, power, and maximum fuel temperature after a temperature excursion. Voiding of the coolant inserts a positive reactivity which will result in an increased flux, increasing reactor power and fuel temperature. After an increase of the temperature, the negative fuel temperature coefficient introduces a prompt negative reactivity feedback.
- The rate of flow of the coolant through the channels is varied over the diameter of the core to keep the overall fuel temperature over the core more or less constant. The coupling between thermalhydraulics and neutronics could be studied (e.g. determining the 'hot spots' or the rate of temperature increase in the core after flow perturbations).
- The effect of multiple cycle burnup on β_{eff} should be investigated.
- From a theoretical perspective, it would be interesting to determine which fission products with a short lifetime cause the increase in the initial DHP during the first 500 days of irradiation.
- An additional set of exponential decay parameters could be created for DHP times longer than 10^4 seconds. Knowledge of this time range would allow for an analysis of DHP during the storage of spent fuel.
- For a more general application of DHP fits, a separate exponential model could fit both the fission product and HM DHP separately. The fit for the fission product DHP would be the same for all fuel compositions. An additional term that indicates the HM DHP (as a function of the MA percentage in the fuel) would provide for more flexibility. However, the extra functional relationship could only be introduced in the transient simulations if the thermalhydraulic codes are altered to allow for this extra term.
- The accuracy of neutron (temperature dependent) cross section data, particularly data in the unresolved resonance regions of the minor actinides, is limited. International research research is being performed to increase the accuracy of these cross sections.[40]

Investigating closed fuel cycle economics

- The financial consequences of closing the fuel cycle, including savings at the front-end and back-end, could be analyzed. As is well-known from the literature, implementing fast reactor technology will stay more expensive than LWR technology as long as the price of uranium fuel does not increase. If the extra cost of closing the fuel cycle is known, the 'sustainable nuclear' cost can be compared to costs of other sustainable energy technologies. The decision to built fast reactors is then based on both engineering fundamentals and economic common sense.
- Research on the costs of safety measures, needed to shield and cool the irradiated fuel with larger quantities of MA during reprocessing and fabrication, is needed.

Investigating sustainability

- The effect of improved reprocessing efficiencies on the radiotoxicity should be further researched. For example, if plutonium and uranium losses would be limited to 0.1% and MA to 1%, the long-term radiotoxicity of reprocessing wastes would further decrease. Better knowledge of the effects of improvements could help prioritize reprocessing research.
- While refraining from the use of fertile blankets, a heterogeneous loading with special burner assemblies for minor actinides may be able to destroy a greater percentage of MA compared to a homogeneous loading.

7.2 Discussing advantages of the 2400 MWth GCFR

Within the Generation IV Forum, consensus has been reached that the unit power of the GCFR should be increased. The main reasons that are given for this increase are: an increased economy of scale and a realistic fuel design.[41] Research will focus on a power reactor of 2400 MWth designed. In addition, research will also take the indirect power conversion cycle into account.[42] See table 24 for a comparison of the 2400 MWth and 600 MWth GCFR's for a number of specific parameters.

Increased economy of scale

The same fuel and sub-assembly design as utilized in the direct cycle can be implemented for the 2400 MWth GCFR. There are economy of scale when producing specific high reactor cost components, such as the pressurized reactor vessel. Fixed costs that are made to operate the reactor are kept constant for both small and large GCFR's. However, the initial cost of capital to build a large GCFR will be greater. Other advantages of the larger power system include that it is more adaptable to large base load operation, and it can utilize the current VHTR reactor pressure vessel size.[43]

In the indirect power conversion cycle, at least three decay heat removal loops are needed. One or two loop options is not feasible due to the limited power that can be transferred per Intermediate Heat Exhanger (IHX). An additional advantage of a greater number of IHX is the creation of redundancy within the main heat removal system. However, implementing a four loop system would simply result in 4 x 600MWth plant secondary systems. This would negatively affect the economy of scale.

Comparing GCFR's	2400 MWth	600 MWth
Structures / Helium / Fuel	10 / 40 / 50	10 / 55 / 35
(U,Pu,MA)C - SiC	(50 / 50)	(70/30)
Dimensions Height; Diameter (m)	1.55; 4.44	1.95; 1.95
H / D	0.35	1.00
Core ΔP (bar)	0.62	0.52

Table 24: Comparing 2400 MWth to 600 MWth GCFR

Realistic fuel design

The power density remains the same for both reactor designs. Thus, increasing unit power results in an increased volume of the reactor core. The larger size gives increased margins for the neutronics.[44] In general, increasing the core volume decreases leakage. Thus, self-sustainability can be achieved with less challenging fuels. The amount of structural material (inert matrix) in the fuel can be increased from 30% to 50%. The percentage of helium coolant in the core decreases from 55% to 40%. Thus, the volume percentage of fuel in the core stays more or less equal.

If the height to diamter ratio (H/D ratio) is kept equal to one, two safety parameters would be negatively affected [45]:
- in general, larger cores have a greater void reactivity effect. Decreasing H/D decreases the positive void effect;
- the core pressure drop for the 2400 MWth would increase. Decreasing H/D decreases the pressure drop below 1 bar (~0.62 bar).

To keep the void reactivity effect and the core pressure drop at acceptable levels, the H/D ratio is decreased to ~0.35.

Appendix A: Benchmark comparison 1D- and 3D codes

CIRTEN (Consorzio InterUniversitario per la Ricerca Tecnologica) and TUD have analyzed the GCFR within a benchmark exercise of the GCFR Specific Targeted Research Project (STREP) sponsored by the European Commission via its 6th Framework Programme (FP6). Goal of the benchmark exercise was to compare results of the probabilistic burnup script MONTEBURNS [46,47] and the burnup script BURN1D using the deterministic SCALE system (TUD). It was confirmed that the codes and cross section data deliver similar results. Both institutes can be confident that the research that has been done within the STREP using the benchmarked codes and cross section data can be compared. This is a summary of the report that was sent to the European STREP partners in December 2006.

A1: Description of SCALE system

The internal workflow of the BURN1D script, necessary to calculate the k-effective and the atomic densities during burnup, is controlled by the SCALE, CSAS and ORIGEN-S systems. Calculations utilize the multi-energy-group cross sections from standardized JEFF3 data. The SCALE system, developed at Oak Ridge National Laboratory (ORNL), computes the flux-weighted cross sections simulating conditions within any given reactor fuel assembly, and converts the data into a library that can be input to ORIGEN-S. Time-dependent libraries may be produced, reflecting fuel composition variations during irradiation.

In the SCALE system, general microscopic cross section data is made problem-dependent with the modules NITAWL-II and XSDRNPM for the particular symmetric array of slabs and fuel mixtures. Then the COUPLE module updates the ORIGEN-S cross section libraries with the neutron flux-averaged constants from XSDRNPM. Thus, the SCALE system provides the capability of executing ORIGEN-S with data that have been rigorously processed for a particular fuel assembly.

The Criticality Safety Analysis Sequences (CSAS) were developed within the SCALE code system. CSAS allows for automated, problem dependent cross section calculations followed by the calculation of the neutron multiplication factor. Below, the different functional modules of CSAS and ORIGEN-S are described.

BONAMI and NITAWL

The cross sections in the master library for each isotope are known for many energy groups. However, cross sections of isotopes are assumed to be in a homogeneous environment. Cross sections in a fuel mixture must be corrected for unit cell effects, including self shielding and rod shadowing. BONAMI[48]and NITAWL[49] correct for these self-shielding effects.

BONAMI is a module of the SCALE system which is used to perform Bondarenko calculations for resonance self-shielding. Cross sections and Bondarenko factor data are input from a master library.

NITAWL-II is a module to produce a working cross section library that can be used for transport calculations (XSDRNPM). The module provides the Nordheim Integral Treatment for resonance self-shielding.

XSDRNPM
XSDRNPM is a discrete-ordinates code that solves the one-dimensional transport equation, determining the eigenvalue. The function of XSDRNPM is twofold:
- perform a 1D calculation in the slab geometry to determine the k-infinity of the system;
- use the fluxes determined from its spectral calculation to collapse input cross sections and write these into different formats. A variety of weighting options are allowed, including zone and cell.

ORIGEN-S
ORIGEN-S is a functional module in the SCALE system and is one of the modules invoked in within CSAS. The ORIGEN-S system takes the flux and averaged cross sections, after which it solves for the depletion equation.

A2: Parameters of GCFR and input for SCALE 4.4

Much of the design specifications of the GCFR have been shown in Chapter 1 of this thesis. The following additional input is given to the SCALE 4.4 code system:
- geometry of the unit cells and the the reactor zones
- initial atomic densities using the material information processor
- reactor type
- burnup steps

Geometry of the unit cell and the reactor zones
The configuration of the unit cell is determined by the type of lattice specified by the user. The configuration SYMMSLABCELL, a symmetric array of slabs, is implemented for the fuel zones of the GCFR. Given the volume ratio of fuel / cladding / coolant (35 / 10 / 55), the dimensions for the unit cell are specified in table A1:

	Abbreviation	**Dimension (cm)**
Outside diameter of the fuel	fuelod	0.471
Sum of the thickness of the fuel, gap and clad	cladod	0.6066
Centre-to-centre spacing between fuel lumps	pitch	1.348

Table A1: Unit cell dimensions for GCFR in BURN1D code

Geometry of reactor zones
Three fuel zones and one reflector zone were specified in the BURN1D code. The following information is presented in table A2 per zone:
- number of sub-assemblies
- volume of fissile fuel and total zone volume
- radii corresponding to the volume of the number of S/A's in the different zones.

	Fissile S/A's	**Fissile volume (m^3)**	**Total Volume (m^3)**	**Outer radius (cm)**
Zone 1	37	0.6713	1.921	56.00
Zone 2	38	0.6894	1.973	79.73
Zone 3	37	0.6713	1.921	97.43
Zone 4 *	234	-	12.1	171.24

Table A2: Dimensions of the subassemblies per zone

Initial atomic densities using the material information processor
The MIP of the SCALE 5.0 system is used to calculate the initial atomic densities, which are consequently used as starting-point for the burnup program. The output of each burnup step includes the new atomic densities. The MIP uses basic information such as the volume ratios of fuel, cladding and coolant, as well as the isotopic vectors of different elements (see Chapter 1). The MIP can calculate the densities of the fuel mixture when uranium, depleted uranium, or 5% minor actinides are included in the initial composition.

Reactor type
It is necessary to indicate the type of reactor (e.g. a fast reactor) for which the burnup calculation is performed. The Liquid Metal Fast Breeder Reactor (LMFBR) option in the SCALE system is used for a calculation of the GCFR. Indication of the type of reactor influences the fission yield cross sections of the ORIGEN library. It is also used as an indication which nuclides are important to your calculation. There are usually only five nuclides per library of which all fission yield data is known. The LMFBR has all information on ^{238}U, ^{239}Pu, ^{240}Pu, ^{241}Pu, and ^{242}Pu.

Burnup steps
In the benchmark exercise, the total irradiation time of 1323 days is split into 10-12 steps. The period varies between 20-100 days, as shown in table A3. The fuel composition is evaluated at each step.

Burntime in GCFR benchmark calculation					
Cycle	TUD	CIRTEN		TUD	CIRTEN
1	23	21	7	884	756
2	128	126	8	1010	882
3	317	315	9	1199	903
4	443	441	10	1325	1008
5	569	462	11		1197
6	758	567	12		1323

Table A3: Burnup steps used in MONTEBURNS and BURN1D

A3: Comparing k-effective and nuclide mass

In the section, the CIRTEN results[50] are compared to the TUD simulation for k-effective, nuclide mass and reactor safety parameters. The results have been presented to the GCFR STREP in December 2005 in Knutsford, United Kingdom. The results fulfill task 4 in the frame of GCFR Work Package 1.1

Comparing k-effective

The benchmark shows that the value of k-effective is very close to one, decreasing slowly during the burnup. At the end-of-burnup, the k-effective dips below one. It decreases due to the build-up of fission products and the small decrease of the fissionable nuclide density. CIRTEN consistently has a higher k-effective than TUD. As CIRTEN models the axial reflector with the MONTEBURNS code system, this could be the cause of the difference.

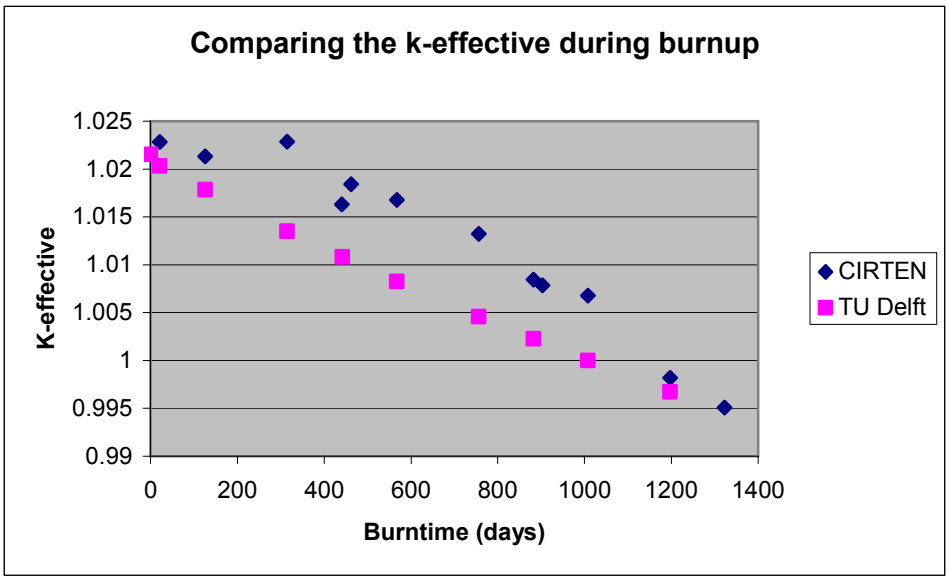

Figure A1: K-effective of TUD and CIRTEN during burnup

The k-effective can be increased by increasing the Heavy Mass (HM) fuel inventory. When the theoretical density of the fuel is increased slightly above 85%, the subcriticality of the GCFR is prevented.

Comparing nuclide mass

The absolute and relative differences between the isotopes expressed in nuclide mass and atomic density have been calculated. Figure A2 (next page) compares the mass of ^{238}U during burnup. It is seen that the mass calculated in the burnup codes compare well. The kink in figure A2 is caused by the small number of significant digits used by CIRTEN. Three significant digits were given in the results of the MONTEBURNS burnup.

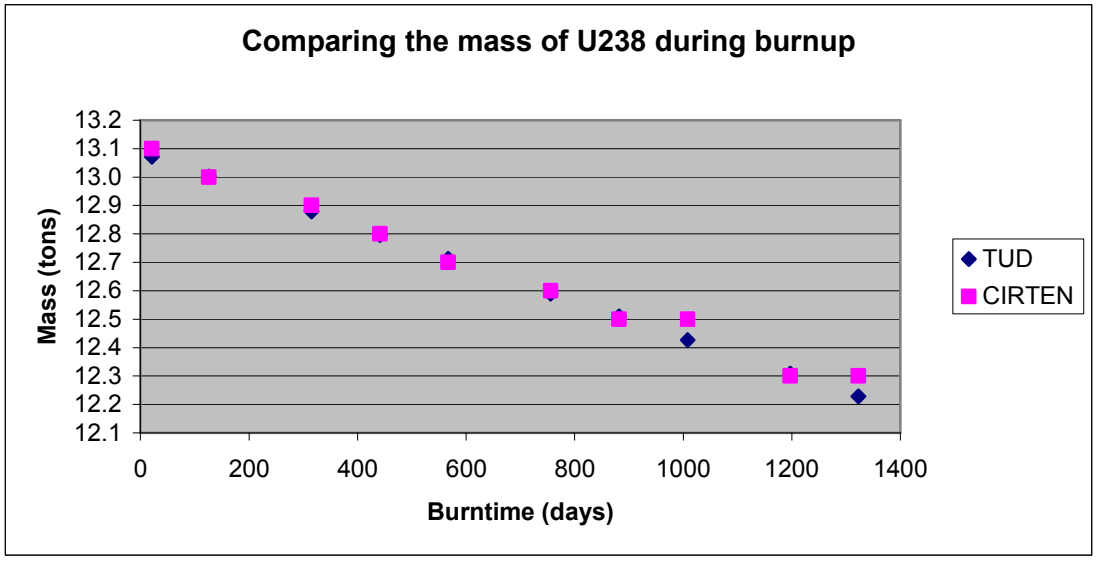

Figure A2: Burnup of ^{238}U in GCFR

Similarly, the buildup of ^{239}Pu and ^{240}Pu is very similar. The mass of fissile ^{239}Pu increases by 60 kg during burnup. In addition, 60% of the plutonium at the end of burnup is ^{239}Pu.

Initial Pu mass	2490 kg
Final Pu mass	2520 kg
Change Pu mass	**30 kg**
Initial ^{239}Pu mass	1400 kg
Final ^{239}Pu mass	1460 kg
Change ^{239}Pu	**60 kg**

Table A4: Total Pu and ^{239}Pu mass at beginning- and end-of -burnup

The relative difference (RD) of the results of TUD and CIRTEN is defined as:

$$RD = \frac{m_{TUD} - m_{CIRTEN}}{m_{TUD}} (\%)$$

Figure A3 illustrates the small relative difference in the mass of ^{239}Pu and ^{240}Pu. Note that a six year decay time has been included.

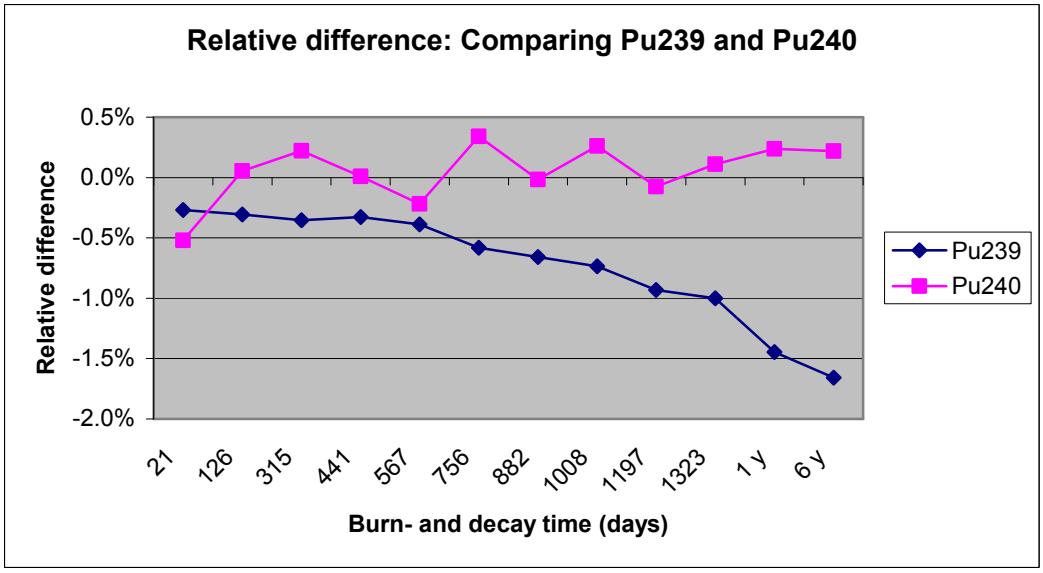

Figure A3: Relative difference of ^{239}Pu and ^{240}Pu during burnup and decay. Note: the decay time is indicated in years.

The relative differences of the curium and americium isotopes are quite high. It is likely that CIRTEN and TUD used somewhat different half-lives for the higher actinides. The difference in decay constants is most obvious when looking at ^{242}Cm with $T_{1/2}$=163 days (see figure A4, next page). The relative differences increases substantially during the cool-down of the irradiated fuel. The half-lives TUD has used for these actinides during burnup and decay calculations are shown in the Table A5.

Half-life of minor actinides			
Curium	*[years]*	*Americium*	*[years]*
Cm-242	0.45	Am-241	434.13
Cm-243	30.01	Am-242m	141.01
Cm-244	18.09	Am-243	7351.64
Cm-245	8492.41		
Cm-246	4721.53		

Table A5: Half-life of curium and americium isotopes

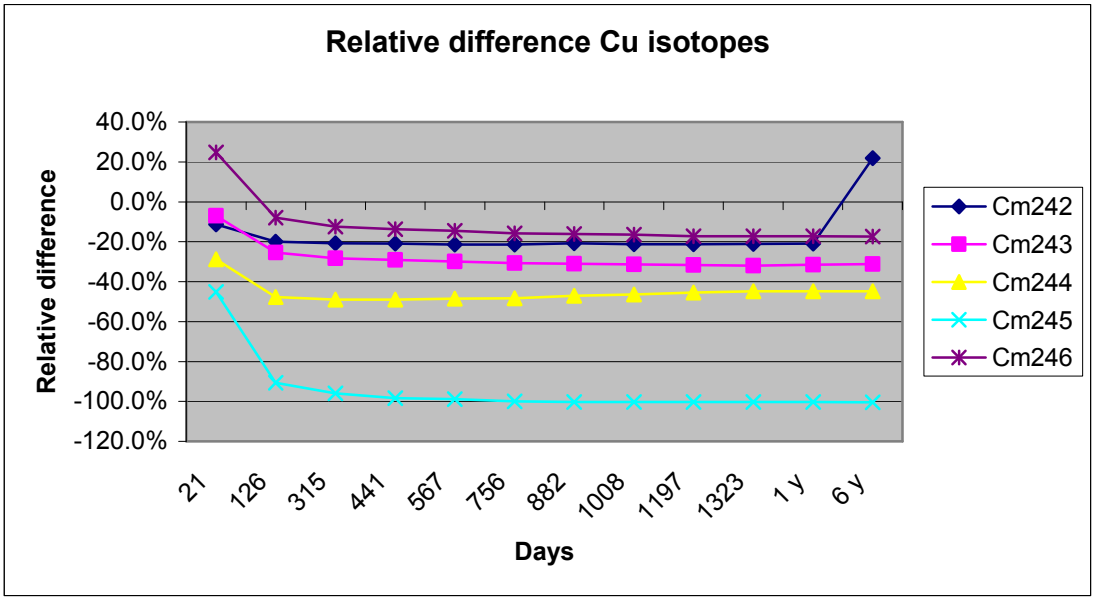

Figure A4: Relative difference of Curium isotopes.
Note: the decay time is indicated in years

A4: Comparing safety parameters: VC and FTC

The void coefficient (VC) and fuel temperature coefficient (FTC) have presented in Chapter 2. The probabilistic character of the CIRTEN calculation is seen in the results of the safety parameter calculation. As can be seen in figure A5 and A6, the MONTEBURNS code calculates a less positive VC and a more negative FTC.

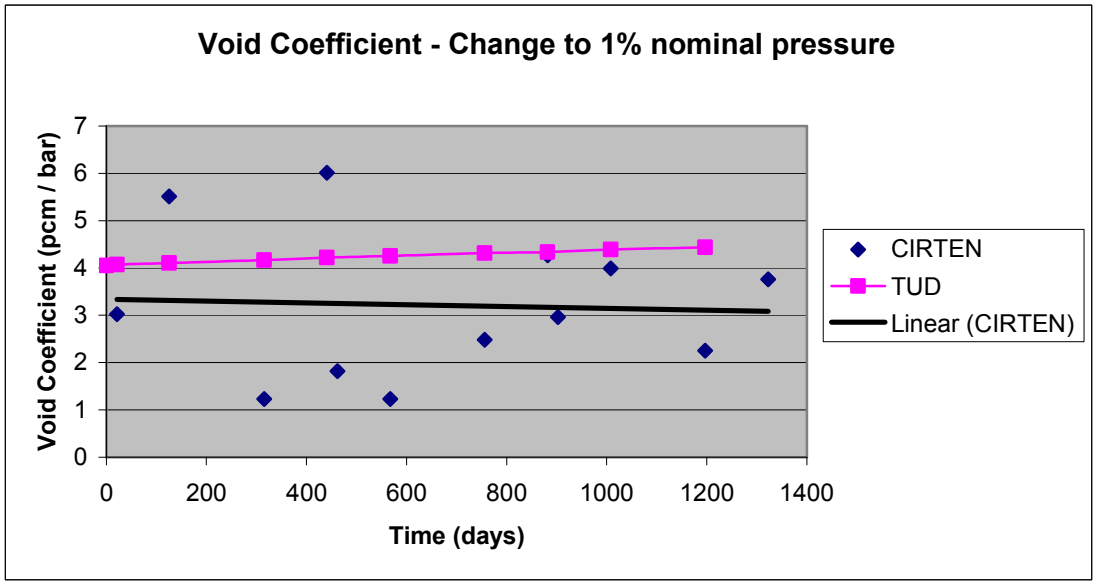

Figure A5: Void Coefficient – comparison of results CIRTEN and TUD

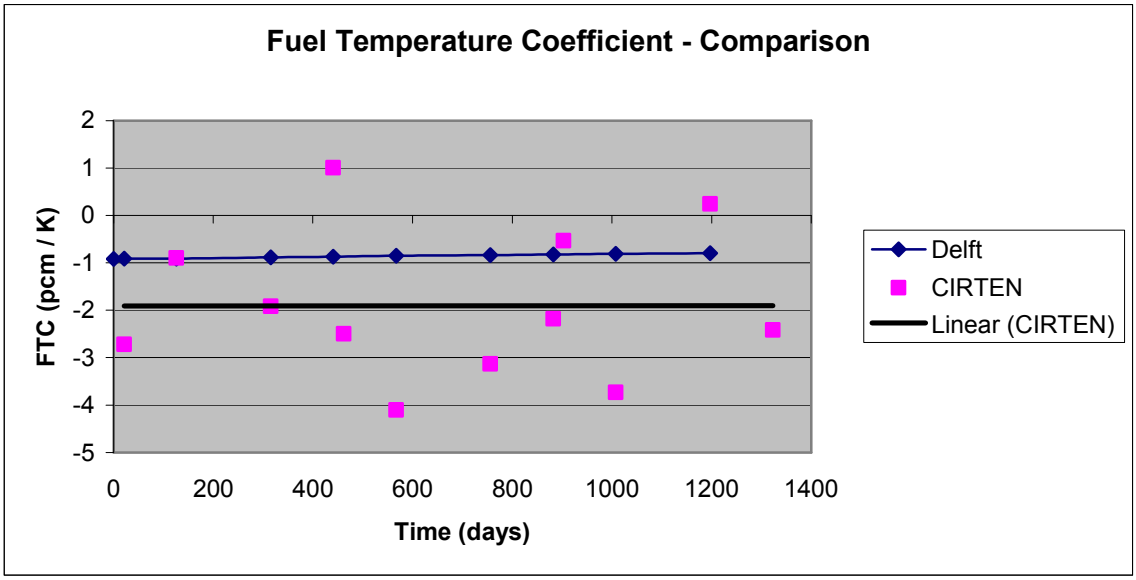

Figure A6: Fuel Temperature Coefficient – comparison of results CIRTEN and TUD

A5: Conclusions

The results of the benchmark exercise give the institutes involved confidence that the research that has been done within the STREP with the benchmarked codes MONTEBURNS and BURN1D and the cross section data can be compared. The nuclide mass comparison is very similar for most Heavy Metal atoms. The difference between decay constants of the higher actinides is most apparent when looking at the changing densities of these actinides during fuel storage. Finally, the differences in the calculated k-effective, void coefficient and fuel temperature coefficient are explained in part by the probabilistic nature of MONTEBURNS.

Appendix B: Fitting parameters for the DHP of the GCFR

Fitting parameters have been calculated for the Decay Heat Production (DHP) curves for the three different initial fuel compositions composed of uranium, plutonium and minor actinides. See Chapter 1 for a detailed discussion of the fuel composition.

The DHP curves have been fit to the following model:

$$DHP = \sum_{i=1}^{11} \alpha_i \exp(-\lambda_i t)$$

The parameters allow a more accurate prediction of the DHP compared to implementation of the ANS model using estimated power fractions. Eleven exponentials are modelled as the thermalhydraulic code CATHARE allows for eleven exponentials, with two parameters per exponential, to be given as an input. The restrictions to the use of the parameters are mentioned below.

B1: Parameters for DHP of different compositions

The parameters in table B1 describe the DHP curve up to 10^4 seconds (first hours) after shutdown for different initial compositions at EOB (2500 days irradiation).

Table: Parameters for DHP estimation for different initial MA mixtures							
	0%	5%	10%		0%	5%	10%
α_1	3.095E-05	2.364E-03	3.303E-05	λ_1	1.877E+00	1.197E+00	1.901E+00
α_2	9.243E-03	6.344E-03	9.259E-03	λ_2	4.971E-01	4.009E-01	4.957E-01
α_3	1.365E-02	1.253E-02	1.382E-02	λ_3	6.183E-02	8.393E-02	6.121E-02
α_4	9.290E-03	1.224E-02	9.250E-03	λ_4	8.911E-03	9.349E-03	8.545E-03
α_5	1.124E-02	1.171E-02	1.108E-02	λ_5	9.800E-04	7.582E-04	9.721E-04
α_6	5.798E-03	5.738E-03	5.808E-03	λ_6	9.289E-05	7.839E-05	7.642E-05
α_7	3.484E-03	6.675E-03	3.746E-03	λ_7	1.731E-04	2.810E-05	1.639E-04
α_8	1.856E-03	1.585E-03	2.257E-03	λ_8	5.828E-06	1.383E-07	5.321E-06
α_9	1.873E-03	1.671E-03	2.273E-03	λ_9	3.567E-07	5.060E-07	4.260E-07
α_{10}	1.852E-03	1.562E-03	2.253E-03	λ_{10}	7.365E-06	3.706E-08	6.842E-06
α_{11}	1.850E-03	1.553E-03	2.252E-03	λ_{11}	7.926E-06	9.676E-10	7.403E-06

Table B1: Fitting parameters α and λ for different compositions. Describing the DHP for the first hours after reactor shutdown.

The two graphs in figure B2 show the fit of the 5% and 10% curves. The fit of the 0% curve has been shown in Chapter 5. As can be seen, the fit follows the DHP as calculated by ORIGEN-S. The statistical accuracy is given in section B2.

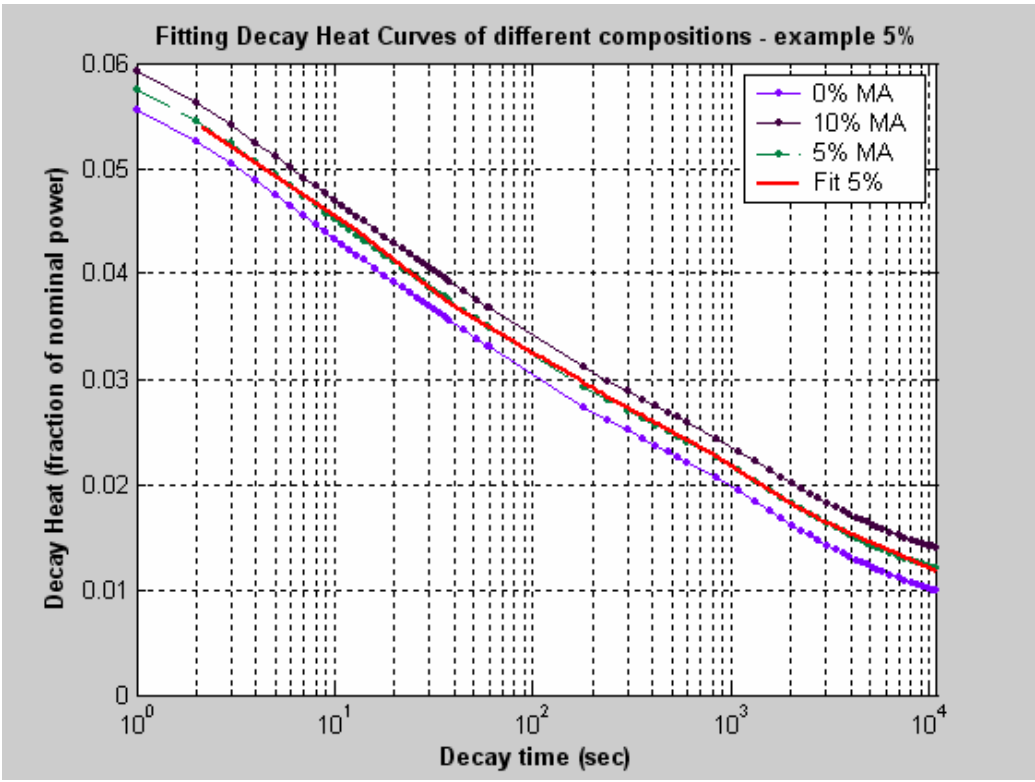

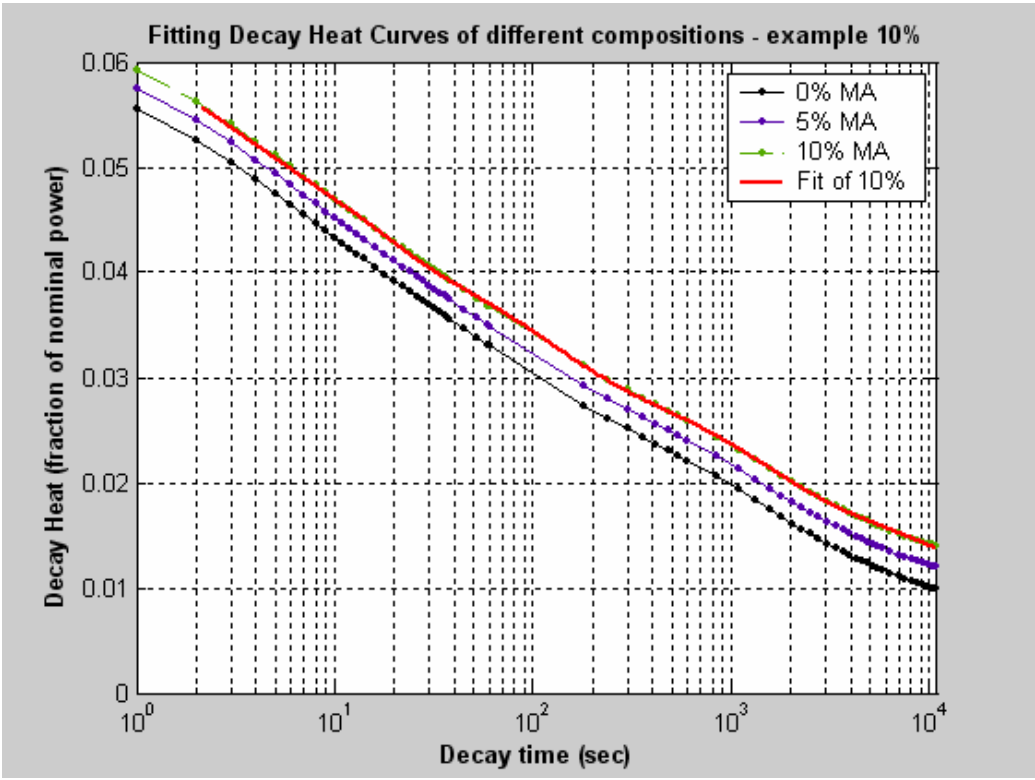

Figure B2: Fits of both the DHP curves for initial compositions of 5% and 10% MA are shown. At t = 0, both curves intersect at the decay heat that is calculated by ORIGEN-S (~0.1%).

As an example, the contributions of each exponential to the total DHP fit is shown in figure B2 for the mixture originally containing 0% MA for decay times ranging from 10^1, 10^2, 10^3 and 10^4 seconds using the above parameters. The contributions to the DHP are shown as a percentage of the total DHP at that point in time. It is seen that the exponents 8-11 contribute relatively more to the total DHP after longer decay times.

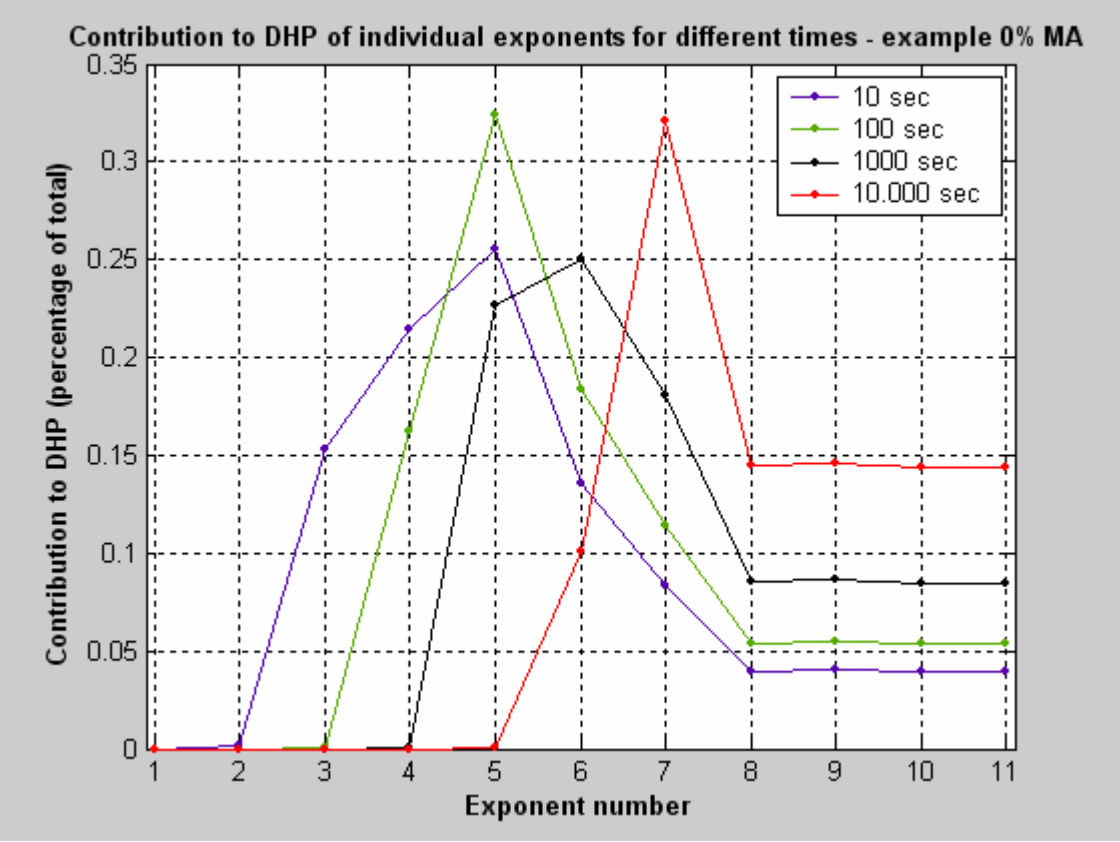

Figure B2: The following figure shows the percentage contribution of each exponential term to the total DHP for the 0% mixture. For example, it is seen that the 8-11 exponential term contributes progressively more to DHP after longer times. After longer times, the fission products and actinides with a short decay period (simulated by exponents 2, 3 and 4) do not contribute to the DHP. The contribution at 100 sec is dominated by the 5^{th} exponent, which contributes almost 35% to the DHP.

B2: Statistical accuracy of the fit of the DHP curves

In this section, the accuracy of the fits are analyzed. A graphical analysis of the residual is given for the DHP curve fitted for the 0% MA composition. The results of the numerical analysis are given for all fits of the DHP curves.

Graphical comparison using the residual

The residuals from a fitted model are defined as the differences between the data and the fit to the data at each point in time:

$$Residual = data - fit$$

In the figure below, the residual is given as a function of decay time. The residual increases to 0.02% of the decay heat at $t = 10^4$ seconds. At this point, the residual is at its maximum and the fraction of decay heat at its minimum. It can be stated that throughout the period of decay, the residual is smaller than 0.02%.

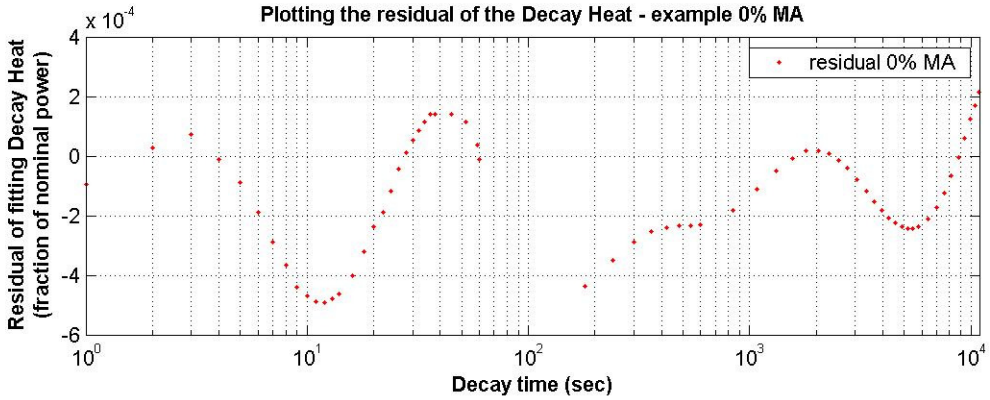

Figure B3: The residual comparing the actual DHP to the fit of the DHP curve is plotted for all times. The residual is at its maximum after 10^4 seconds.

Numerical comparison

In the table B2, the sum of squares due to error (SSE) and the root mean squared error (RMSE) for the parametric model using the eleven exponentials (2 parameters per exponential) are given.

Statistical accuracy of fits to DHP curves			
Measure	0%	5%	10%
SSE	3.841e-006	3.719e-006	7.33e-007
RMSE	0.0002889	0.0002843	0.0001223

Table B2: Accuracy of fits to the DHP curves

Sum of Squares Due to Error[51]
This statistic measures the total deviation of the data from the fit to the data. It is also called the summed square of residuals and is usually labeled as SSE.

$$SSE = \sum_{i=1}^{n} w_i (y_i - \hat{y}_i)^2$$

A value closer to 0 indicates that the fit will be more useful for prediction.

Root Mean Squared Error[52]
This statistic is also known as the fit standard error and the standard error of the regression. It is an estimate of the standard deviation of the random component in the data, and is defined as

$$RMSE = s = \sqrt{MSE}$$

where MSE is the mean square error or the residual mean square

$$MSE = \frac{SSE}{\upsilon}$$

υ = number of data points

Just as with SSE, an MSE value closer to 0 indicates a fit that is more useful for prediction.

List of symbols

Abbreviations

ABWR	Advanced Boiling Water Reactor
BOB-x	Beginning of Burnup - x_{th} cycle
CEA	Commisariat à l'Energie Atomique
EOB	End of Burnup
EOD	End of Decay
EPR	European Pressurized water Reactor
eV	Electronvolt
FIMA	Fissions per Initial Metal Atom
FTC	Fuel Temperature Coefficient
GCFR	Gas Cooled Fast Reactor
HM	Heavy Metal, i.e. uranium and all heavier metals
HTR	High Temperature Reactor
IHX	Intermediate Heat Exchanger
LWR	Light Water Reactor
MA	Minor Actinides
MWe	Megawatt electric
MWth	Megawatt thermal
PUREX	Plutonium Uranium REduction and eXtraction
PWR	Pressurized Water Reactor

Nuclear quantities

α	Capture to fission ratio
β	Delayed neutron fraction
$\chi(E)$	Fission spectrum
η	Average number of new neutrons per absorption - reproduction factor
Ω	Spatial angle / direction
ν	Average number of new neutrons per fission
φ	Neutron flux
ρ	Reactivity
σ_a, Σ_a	Absorption cross section (microscopic, macroscopic)
σ_c, Σ_c	Capture cross section (microscopic, macroscopic)
σ_f, Σ_f	Fission cross section (microscopic, macroscopic)
σ_s, Σ_s	Scatter cross section (microscopic, macroscopic)
σ_t, Σ_t	Total cross section (microscopic, macroscopic)
σ_i	Microscopic cross section of isotope 'i'
C_i	Delayed neutron precursor concentration
B_g	Geometrical buckling
BG	Breeding Gain
BR	Breeding Ratio

E	Energy
E_{rel}	Average energy release per fission
f_j	Fraction of fissions in isotope 'j' for decay heat calculation
$f(t)$	Decay heat impulse response
fiss	Fissionability
k_{eff}	Effective multiplication factor
k_{inf}	Infinite medium multiplication factor
m	Mass
N	Nuclide density
n	Neutron
p	Proton
S	Independent source (neutrons)
r	Space location
v	Velocity
w_i	Microscopic worth of an isotope
W_i	Macroscopic worth of an isotope
y	yield

NOTES

[1] "A Technology Roadmap for Generation IV Nuclear Energy Systems", U.S. DOE Nuclear Energy Research Advisory Committee and the Generation IV International Forum, December 2002.
[2] See ref. 1.
[3] G. Rimpault, J. C. Bosq, H. B. Choi, J.C. Garnier, "A feasibility study on a 600 MWth Gas-Cooled Fast Reactor Core", Commissariat à l'Energie Atomique (CEA) Cadarache, Global New Orleans, 2003.
[4] Lecture notes Jan Leen, including comparison thermal and fast reactors, Doppler, presentation Defense in Depth.
[5] See ref. 4.
[6] A.E. Waltar and A.B. Reynolds. Fast breeder reactors. Pergamon Press, 1981.
[7] See ref. 3.
[8] Garnier, J.C., Chauvin, N., Francois, G., Wei, T.Y.C., Taiwo, T., Meyer, M., "Feasibility of an advanced GFR – Design trends and safety options – Status of France & US studies", CEA Cadarache, Framatome ANP, Argonne National Laboratory, Global New Orleans, 2003.
[9] See ref 8.
[10] See ref. 3.
[11] Conti, A., Bosq J. C. – "01/2004 - 600 MWth GFR cores containing plates CERCER – characteristics", CEA Cadarache, December 2004.
[12] See ref. 8.
[13] See ref. 3.
[14]See ref. 11.
[15] See ref. 3.
[16] J.J. Duderstadt and L.J. Hamilton. Nuclear reactor analysis. John Wiley & Sons, Inc., 1976.
[17] Dam, van, H., Hagen, van der, T.H.J.J., Hoogenboom, J.E., "Nuclear Reactor Physics, lecture notes AP3341", June 2004.
[18] See ref. 16.
[19] Keepin, G.R., "Physics of Nuclear Reactors", p.99, Addison-Wesley Publishing Co., Reading, Massachusetts, 1965.
[20] Graves, H. W. , "Nuclear Fuel Mangement", Jr. John Wiley & Sons, 1979.
[21] "SCALE: A Modular Code System for Performing Standardized Computer Analyses for Licensing Evaluations, ORNL/TM-2005/39, Version 5, Vols. I–III", April 2005. Available from Radiation Safety Information Computational Center at Oak Ridge National Laboratory as CCC-725.
[22] Hoogenboom, J.E., Kloosterman, J.L., "Generation and validation of ORIGEN-S libraries for depletion and transmutation calculations based on JEF2.2 and EAF3 basic data", Nuclear engineering and design, 1997.
[23] Gauld, I.C., Hermann, O.W., Westfall, R.M., "ORIGEN-S: SCALE system module to calculate fuel depletion, actinide transmutation, fission product buildup and decay, and associated radiation source terms", ORNL, April 2005.
[24] Salvatores, M., "Handbook of Nuclear Reactor Calculations", volume III, chapter "Fast Reactor Calculations", pages 263-363. CRC Press, 1986.
[25] "American National Standard for Decay Heat Power in Light Water Reactors", ANS, 1979.
[26] ANSI/ANS-5.1-1994, 2004.
[27] Rooijen, van, W.F.G, "Improving fuel cycle design and safety characteristics of a Gas Cooled Fast Reactor", IOS Press – The Netherlands - 2006.
[28] Broeders, C.H.M., Kiefhaber, E., WieseBurning, H.W., Burning transuranium isotopes in thermal and fast reactors, Nuclear Engineering and Design 202 (2000) 157–172

[29] Yamaoka, M., Wakabayashi, T., "Study on super-long-life cores loaded with minor actinide fuel", O-arai Engineering Center, Power Reactor and Nuclear Fuel Development Corp., 4002 Narita, O-arai-machi, Higashi-ibaraki-gun, lbaraki 311-13, Japan, Nuclear Engineering and Design 154 (1995) 239 - 250.
[30] Kloosterman, J.L, Kuijper, J.C., "VAREX, A Code for Variational Analysis of Reactivity Effects: Description and Examples", M&C 2001 Salt Lake City, Utah, USA, September 2001.
[31] See ref. 27.
[32] See ref. 27.
[33] "Trends in the Nuclear Fuel Cycle – Economical, Environmental and Social Aspects", Nuclear Energy Agency (NEA), OECD, 2001.
[34] Kloosterman, J.L., http://wwwtest.iri.tudelft.nl/~klooster/covra_20050603.php
[35] See ref. 17, lecture notes AP3341, Chapter 7.
[36] Poette, C., "FP6 GCFR STREP- Summary of basic design options for GFR design tasks", March 2005.
[37] Salvatores, M., "Nuclear fuel cycle strategies including Partitioning and Transmutation", Nuclear Engineering and Design 235 (2005) 805–816.
[38] Source: **http://wwwtest.iri.tudelft.nl/~klooster/covra_20050603.php**
[39] See ref. 27.
[40] See http://www.physor2004.anl.gov/PlenarySessions_files/HusseinKhalil.pdf
[41] Poette, C., "Unit power switch from 600 to 2400 MWth", Technical Meeting, WP 1.1 GFR Design, CEA Cadarache, June 20 - 22, 2006
[42] Garnier, J.C., Bassi, C., Blanc, M., Bosq, J.C., Chauvin, N., Dumaz, P., Malo, J.Y., Mathieu, B., Nicolas, L., "Contribution to GFR Design Option Selection", CEA.
[43] Weaver, K.D., "Interim Status Report on the Design of the Gas-Cooled Fast Reactor (GFR)", INL, January, 2005. p.7.
[44] See ref. 27.
[45] Lecture notes: http://134.208.3.6/twocw/mit/NR/rdonlyres/Nuclear-Engineering/22-39Fall-2005/4B29B47B-71E6-4C90-9994-97BAAE9122A9/0/lec7_ph.pdf
[46] Poston, D. I., Trellue, H. R., "User's manual, Version 2.0 for MONTEBURNS Version 1.0 - LA-UR-99-4999 PSR-0455/01", September 1999.
[47] Lomonaco, G., "MONTEBURNS code description", presentation at STREP meeting, Knutsford, England, December 2005.
[48]Greene, N.M., "BONAMI Resonance Shielding by the Bondarenko Method", March 2000.
[49] Greene, N.M. et. al., "NITAWL-II: SCALE System Module for Performing Resonance Shielding and Working Library Production", March 2000.
[50] Cerullo, N., Lomonaco, G. Bomboni, E. "GFR-STREP Work Package 1.1, Results of reference calculation – Task 4", CIRTEN – University of Pisa, November 2005.
[51] Helpdesk of MATLAB – Curve Fitting Toolbox
http://www.mathworks.com/access/helpdesk/help/toolbox/curvefit/index.html?/access/helpdesk/help/toolbox/curvefit/exampleindex.html&http://www.mathworks.com/access/helpdesk/help/toolbox/curvefit/curvefit_product_page.html
[52] See ref. 51.